

ISSN 1881-7815 Online ISSN 1881-7823

BST

BioScience Trends

Volume 8, Number 4
August, 2014



www.biosciencetrends.com

BST

BioScience Trends



ISSN: 1881-7815
Online ISSN: 1881-7823
CODEN: BTIRCZ
Issues/Year: 6
Language: English
Publisher: IACMHR Co., Ltd.

BioScience Trends is one of a series of peer-reviewed journals of the International Research and Cooperation Association for Bio & Socio-Sciences Advancement (IRCA-BSSA) Group and is published bimonthly by the International Advancement Center for Medicine & Health Research Co., Ltd. (IACMHR Co., Ltd.) and supported by the IRCA-BSSA and Shandong University China-Japan Cooperation Center for Drug Discovery & Screening (SDU-DDSC).

BioScience Trends devotes to publishing the latest and most exciting advances in scientific research. Articles cover fields of life science such as biochemistry, molecular biology, clinical research, public health, medical care system, and social science in order to encourage cooperation and exchange among scientists and clinical researchers.

BioScience Trends publishes Original Articles, Brief Reports, Reviews, Policy Forum articles, Case Reports, News, and Letters on all aspects of the field of life science. All contributions should seek to promote international collaboration.

Editorial Board

Editor-in-Chief:

Masatoshi MAKUUCHI
Japanese Red Cross Medical Center, Tokyo, Japan

Co-Editors-in-Chief:

Xue-Tao CAO
Chinese Academy of Medical Sciences, Beijing, China
Rajendra PRASAD
University of Delhi, Delhi, India
Arthur D. RIGGS
Beckman Research Institute of the City of Hope, Duarte, CA, USA

Chief Director & Executive Editor:

Wei TANG
The University of Tokyo, Tokyo, Japan

Managing Editor:

Munehiro NAKATA
Tokai University, Hiratsuka, Japan

Senior Editors:

Xunjia CHENG
Fudan University, Shanghai, China
Yoko FUJITA-YAMAGUCHI
Tokai University, Hiratsuka, Japan
Na HE
Fudan University, Shanghai, China
Kiyoshi KITAMURA
The University of Tokyo, Tokyo, Japan

Misao MATSUSHITA
Tokai University, Hiratsuka, Japan
Takashi SEKINE
The University of Tokyo, Tokyo, Japan
Yasuhiko SUGAWARA
The University of Tokyo, Tokyo, Japan

Web Editor:

Yu CHEN
The University of Tokyo, Tokyo, Japan

Proofreaders:

Curtis BENTLEY
Roswell, GA, USA
Christopher HOLMES
The University of Tokyo, Tokyo, Japan
Thomas R. LEBON
Los Angeles Trade Technical College, Los Angeles, CA, USA

Editorial Office

Pearl City Koishikawa 603,
2-4-5 Kasuga, Bunkyo-ku,
Tokyo 112-0003, Japan
Tel: +81-3-5840-8764
Fax: +81-3-5840-8765
E-mail: office@biosciencetrends.com

BioScience Trends

Editorial and Head Office

Pearl City Koishikawa 603, 2-4-5 Kasuga, Bunkyo-ku,
Tokyo 112-0003, Japan

Tel: +81-3-5840-8764, Fax: +81-3-5840-8765
E-mail: office@biosciencetrends.com
URL: www.biosciencetrends.com

Editorial Board Members

Girdhar G. AGARWAL (Lucknow, India)	Takahiro HIGASHI (Tokyo, Japan)	Mark MEUTH (Sheffield, UK)	Koji TANAKA (Tsu, Japan)
Hirotsugu AIGA (Geneva, Switzerland)	De-Xing HOU (Kagoshima, Japan)	Satoko NAGATA (Tokyo, Japan)	John TERMINI (Duarte, CA, USA)
Hidechika AKASHI (Tokyo, Japan)	Sheng-Tao HOU (Ottawa, Canada)	Miho OBA (Odawara, Japan)	Usa C. THISYAKORN (Bangkok, Thailand)
Moazzam ALI (Geneva, Switzerland)	Yong HUANG (Ji'ning, China)	Xianjun QU (Ji'nan, China)	Toshifumi TSUKAHARA (Nomi, Japan)
Ping AO (Shanghai, China)	Hirofumi INAGAKI (Tokyo, Japan)	John J. ROSSI (Duarte, CA, USA)	Kohjiro UEKI (Tokyo, Japan)
Hisao ASAMURA (Tokyo, Japan)	Masamine JIMBA (Tokyo, Japan)	Carlos SAINZ-FERNANDEZ (Santander, Spain)	Masahiro UMEZAKI (Tokyo, Japan)
Michael E. BARISH (Duarte, CA, USA)	Kimitaka KAGA (Tokyo, Japan)	Yoshihiro SAKAMOTO (Tokyo, Japan)	Junming WANG (Jackson, MS, USA)
Boon-Huat BAY (Singapore, Singapore)	Ichiro KAI (Tokyo, Japan)	Erin SATO (Shizuoka, Japan)	Ling WANG (Shanghai, China)
Yasumasa BESSHO (Nara, Japan)	Kazuhiro KAKIMOTO (Osaka, Japan)	Takehito SATO (Isehara, Japan)	Xiang-Dong Wang (Boston, MA, USA)
Generoso BEVILACQUA (Pisa, Italy)	Kiyoko KAMIBEPPU (Tokyo, Japan)	Akihito SHIMAZU (Tokyo, Japan)	Hisashi WATANABE (Tokyo, Japan)
Shiuan CHEN (Duarte, CA, USA)	Haidong KAN (Shanghai, China)	Zhifeng SHAO (Shanghai, China)	Lingzhong XU (Ji'nan, China)
Yuan CHEN (Duarte, CA, USA)	Bok-Luel LEE (Busan, Korea)	Ri SHO (Yamagata, Japan)	Masatake YAMAUCHI (Chiba, Japan)
Naoshi DOHMAE (Wako, Japan)	Mingjie LI (St. Louis, MO, USA)	Judith SINGER-SAM (Duarte, CA, USA)	Aitian YIN (Ji'nan, China)
Zhen FAN (Houston, TX, USA)	Shixue LI (Ji'nan, China)	Raj K. SINGH (Dehradun, India)	George W-C. YIP (Singapore, Singapore)
Ding-Zhi FANG (Chengdu, China)	Ren-Jang LIN (Duarte, CA, USA)	Junko SUGAMA (Kanazawa, Japan)	Xue-Jie YU (Galveston, TX, USA)
Yoshiharu FUKUDA (Ube, Japan)	Daru LU (Shanghai, China)	Hiroshi TACHIBANA (Isehara, Japan)	Benny C-Y ZEE (Hong Kong, China)
Rajiv GARG (Lucknow, India)	Hongzhou LU (Shanghai, China)	Tomoko TAKAMURA (Tokyo, Japan)	Yong ZENG (Chengdu, China)
Ravindra K. GARG (Lucknow, India)	Duan MA (Shanghai, China)	Tadatoshi TAKAYAMA (Tokyo, Japan)	Xiaomei ZHU (Seattle, WA, USA)
Makoto GOTO (Tokyo, Japan)	Francesco MAROTTA (Milano, Italy)	Shin'ichi TAKEDA (Tokyo, Japan)	
Demin HAN (Beijing, China)	Yutaka MATSUYAMA (Tokyo, Japan)	Sumihito TAMURA (Tokyo, Japan)	
David M. HELFMAN (Daejeon, Korea)	Qingyue MENG (Beijing, China)	Puay Hoon TAN (Singapore, Singapore)	

(as of August 2014)

Review

- 192 - 201 **Semantic Web technologies for the big data in life sciences.**
Hongyan Wu, Atsuko Yamaguchi

Brief Report

- 202 - 205 **A novel EGFP-expressing nude mice with complete loss of lymphocytes and NK cells to study tumor-host interactions.**
Kumiko Gotoh, Ryusho Kariya, Kouki Matsuda, Shinichiro Hattori, Kulthida Vaeteewoottacharn, Seiji Okada

Original Articles

- 206 - 211 **Pathological changes in primary cilia: A novel mechanism of graft cholangiopathy caused by prolonged cold preservation in a rat model of orthotopic liver transplantation.**
Hongwei Lu, Jiahong Dong, Yafei Zhang, Chonghui Li, Qiang Yu, Wei Tang
- 212 - 216 **Migration of breast cancer cells into reconstituted type I collagen gels assessed via a combination of frozen sectioning and azan staining.**
Kyohei Fukuda, Yo Kamoshida, Taisuke Kurokawa, Mito Yoshida, Yoko Fujita-Yamaguchi, Munehiro Nakata
- 217 - 226 **Ferulic acid combined with astragaloside IV protects against vascular endothelial dysfunction in diabetic rats.**
Yonghui Yin, Fanghua Qi, Zhenhua Song, Bo Zhang, Jialin Teng
- 227 - 234 **A simple, rapid, economical, and practical method for the determination of efavirenz in plasma of Chinese AIDS patients by reverse phase high-performance liquid chromatography with ultraviolet detector.**
Kang Yin, Xianmin Meng, Ping Dong, Tianran Ding, Li Shen, Li Zhang, Renfang Zhang, Weimin Cai, Hongzhou Lu

CONTENTS

(Continued)

Case Report

- 235 - 239 **A case of advanced lung cancer with malignant pericardial effusion treated by intrapericardial Cinobufacini injection instillation.**
Tao Sun, Yuhua Zhang, Yang Shen, Kaiwen Hu, Minghuan Zuo

Letter

- 240 - 241 **Japan's emerging challenge for child abuse: System coordination for early prevention of child abuse is needed**
Kenzo Takahashi, Hideyuki Kanda, Nagisa Sugaya

Guide for Authors

Copyright

Semantic Web technologies for the big data in life sciences

Hongyan Wu*, Atsuko Yamaguchi*

Database Center for Life Science, Research Organization of Information and Systems, Japan.

Summary

The life sciences field is entering an era of big data with the breakthroughs of science and technology. More and more big data-related projects and activities are being performed in the world. Life sciences data generated by new technologies are continuing to grow in not only size but also variety and complexity, with great speed. To ensure that big data has a major influence in the life sciences, comprehensive data analysis across multiple data sources and even across disciplines is indispensable. The increasing volume of data and the heterogeneous, complex varieties of data are two principal issues mainly discussed in life science informatics. The ever-evolving next-generation Web, characterized as the Semantic Web, is an extension of the current Web, aiming to provide information for not only humans but also computers to semantically process large-scale data. The paper presents a survey of big data in life sciences, big data related projects and Semantic Web technologies. The paper introduces the main Semantic Web technologies and their current situation, and provides a detailed analysis of how Semantic Web technologies address the heterogeneous variety of life sciences big data. The paper helps to understand the role of Semantic Web technologies in the big data era and how they provide a promising solution for the big data in life sciences.

Keywords: Big data, Semantic Web technologies, life-science databases

1. Introduction

Data deluge in the life sciences The life sciences field is entering an era of big data with the breakthroughs of science and technology. Moore's law shows that computers double in speed and halve in size every 18 months (1). A similar trend is observed for hard disks (2) and networks (3). The exponential growth of scientific instruments has resulted in an exponentially growing amount of scientific data (4). Until recent years, Moore's law kept outpacing the generation of biological sequence data by its growth in storage and processing capacity. This trend has remained true for approximately 40 years and was not broken until the completion of the Human Genome Project in 2003. From 2005, the sequencing output doubling rate decreased to 5 months because of the development of Next-Generation Sequencing technologies (NGS) (5). Since 2008, genomics data are

outpacing Moore's Law by a factor of 4 (6). The 1,000 Genomes Project (7), which involves sequencing and cataloging human genetic variations, has deposited 2 times more raw data into GenBank (<http://www.ncbi.nlm.nih.gov/genbank/>) at National Center for Biotechnology Information (NCBI) during its first 6 months than all the previous sequences deposited in the last 30 years (5). In the last five years, more scientific data have been generated than in the entire history of mankind (8). Figure 1 illustrates the GenBank and Whole Genome Shotgun (WGS) statistics up to February 2014. Human DNA comprises approximately 3 billion base pairs with a personal genome representing approximately 100 gigabyte (GB) of data (6). Two nanopore sequencing platforms (GridION™ and MinION™) (9), reported in February 2012, are capable of delivering ultra-long sequencing reads (~100 kb) with additionally higher throughput and much lower cost. Sequencing a human genome has decreased in cost from \$10,000 in 2007 to \$1,000 in 2012 (10) and is likely to drop below \$100 per genome in the next decade (11). In the third decade of the 21st century, it has been estimated that 1 billion people will be sequenced and that approximately 3,000 petabyte (PB) (1 PB is approximately equivalent to 10⁶ GB) of storage will be needed. Grossman *et al.* predicated that

*Address correspondence to:

Dr. Hongyan Wu and Dr. Atsuko Yamaguchi, DBCLS, Univ. of Tokyo Kashiwa-no-ha Campus Station Satellite 6F, 178-4-4 Wakashiba, Kashiwa-shi, Chiba 277-0871, Japan.

E-mail: wu@dbcls.rois.ac.jp (Wu HY)

atsuko@dbcls.rois.ac.jp (Yamaguchi A)

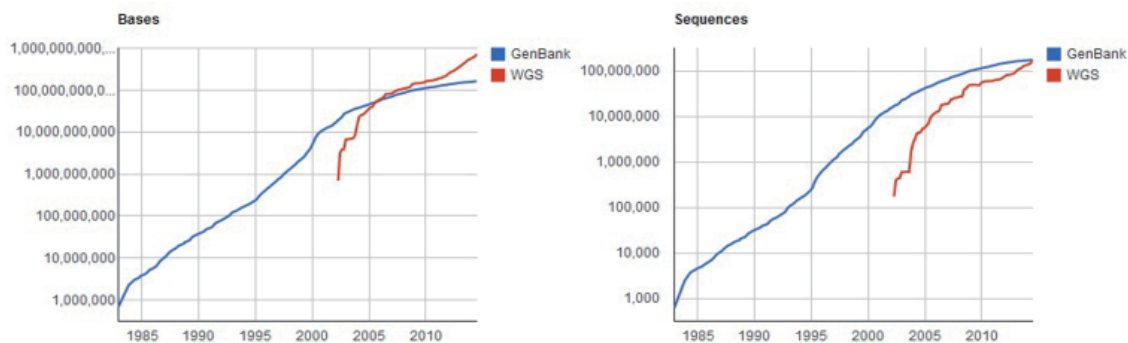


Figure 1. Growth of GenBank and WGS. NCBI GenBank ([Internet] [cited July 18, 2014]. Available from <http://www.ncbi.nlm.nih.gov/genbank/statistics>).

we would be in an era of ubiquitous sequencing within a few years, in which genome sequencing would become routine for both research and clinical applications (11).

Many other kinds of life science big data are being produced at high speed as well as genomics data. Functional magnetic resonance imaging or functional MRI (fMRI) is a functional neuroimaging procedure using MRI technology that measures brain activity by detecting associated changes in blood flow. This technique generates complex data sets: ~100,000 locations, measured simultaneously hundreds of times, resulting in billions of pairwise relations, collected in multiple experimental conditions, and from dozens of participants per study (12). Other data, including Computerized Tomography (CT) Scan data, epidemic data, Electronic Health Records (EHR) system data, patient behavior and sentiment data *etc.*, are also being generated and gathered at a fast pace.

Big data-related projects and activities More and more big data-related projects and activities are being performed in the world. The Genome 10K project (<http://www.genome10k.org>) aims to assemble a genomic zoo, which will be a collection of DNA sequences representing the genomes of 10,000 vertebrate species, approximately one for every vertebrate genus. The 1001 Genomes Project (<http://www.1001genomes.org>), launched at the beginning of 2008, has the goal of discovering the whole-genome sequence variation in 1,001 strains of the reference plant *Arabidopsis thaliana*. The 1K Insect Transcriptome Evolution (1KITE) Project (<http://www.1kite.org>) aims to study the transcriptomes of more than 1,000 insect species encompassing all recognized insect orders. The ENCyclopedia of DNA Elements (ENCODE) project (<http://www.genome.gov/10005107>) aims to identify all functional elements in the human genome sequence. ENCODE generated more than 15 terabyte (TB) of raw data, and the data analysis consumed the equivalent of more than 300 years of computing time. The Cancer Genome Atlas (TCGA) (<http://cancergenome.nih.gov/>) began as a three-year pilot in 2006 with an investment of \$50 million each from the National Cancer Institute (NCI) and National Human Genome Research Institute (NHGRI), confirming

that an atlas of changes could be created for specific cancer types. The European life-science infrastructure for biological information (ELIXIR) (<http://www.elixir-europe.org/>) unites Europe's leading life science organizations in managing and safeguarding the massive amounts of data being generated every day by publicly funded research. ELIXIR aims to provide the facilities necessary for life science researchers, from bench biologists to cheminformaticians, to make the most of the rapidly growing store of information about living systems. Tohoku University Tohoku Medical Megabank Organization (<http://www.megabank.tohoku.ac.jp/english/>) was founded to establish an advanced medical system to foster the reconstruction from the Great East Japan Earthquake. The organization will develop a biobank that combines medical and genome information during the process of rebuilding the community medical system and supporting health and welfare in the Tohoku area. Approximately 60 PB of data representing 1.5 million genomic and medical pieces of information is predicted to be acquired. In China, Beijing Genomics Institute (BGI) and their publishing partner BioMed Central, a leader in scientific data sharing, announced the launch of a new journal, GigaScience, which publishes large-scale biological research in a unique format (http://www.genomics.cn/en/news/show_news?nid=99134).

Big data issues Life sciences data are continuing to grow in not only size but also variety and complexity with great speed. The role of genome sequencing in the life sciences is the tip of the iceberg. To investigate the complex systematic effects of drugs and other chemical compounds on biological systems and to validate a hypothesis in drug discovery, we require the data on diseases, compounds, genes, targets, side effects, and metabolic pathways, as well as from the clinic and other sources (13). These data reside in a number of different data sources, such as GenBank (14), Genome Sequence DataBase (GSDB) (15), SWISS-PROT (16), European Molecular Biology Laboratory (EMBL), Online Mendelian Inheritance in Man (OMIM) (17), and many others (18). Data sources can store different data types in different formats (19); for example, flat file (*e.g.*, tab-delimited file), sequence file (*e.g.*, FASTA), structure file

(e.g., Protein Structure File (PSF)), Extensible Markup Language (XML) file (e.g., KGML- Kyoto Encyclopedia of Genes and Genomes (KEGG) Markup Language for describing graph objects), and database management systems (DBMSs). Even for the same data type, data formats in different sources are often incompatible. In addition, new data formats are being invented along with the development of new technologies (20), such as Sequence Alignment/Map (SAM) (21) and Genome Variation Format (GVF) (22).

To ensure that big data has a major influence in the life sciences, comprehensive data analysis across multiple data sources and even across disciplines is indispensable. For example, research on the neurodegenerative disease Alzheimer's disease (AD) spans the disciplines of psychiatry, neurology, microscopic anatomy, neuronal physiology, biochemistry, genetics, molecular biology, and bioinformatics (23). A series of combination and integration problems such as data, terminologies, knowledge, and service integration must be solved first (24). Eliminating the inconsistency of data and terms as well as finding and meaningfully combining information in the vast majority of data all require knowing the exact semantics of the data (25).

The increasing volume of data generated by new technologies at an unprecedented rate and the heterogeneous complex varieties of data are two principal issues mainly discussed in life science informatics (26). In the remainder of this paper, we provide insight into how the Semantic Web technologies address the heterogeneous variety of life sciences big data. We also present a survey of the state-of-the-art development of every technology and some related projects. Finally, we summarize the challenges and problems that we have to face now and in the future.

2. Semantic Web technologies

The ever-evolving next-generation Web, characterized as the Semantic Web (27), is an extension of the current Web, aiming to provide information for not only humans but also computers to semantically process data. Berners-Lee *et al.* (27) believed that this form of Web content that was meaningful to computers would unleash a revolution of new possibilities. The following introduces a series of the Semantic Web technologies.

2.1. Resource Description Framework (RDF)

The RDF (28) is a model for representing information about resources on the World Wide Web. The RDF model identifies items with Web identifiers (called Uniform Resource Identifiers, or URIs) and encodes data in the form of subject, predicate, and object (with the whole usually referred to as a "triple"). The subject is a URI or blank node. The object is a URI or string literal. The predicate specifies the relationship between

the subject and object and is also represented by a URI. For example, in the KEGG database the breast cancer gene hsa:675 encodes the *Homo sapiens protein* with the number 119395734 in NCBI Protein database. This gene is the same as gene ENSG00000139618 in Ensemble database. This could be expressed as two triples: "<hsa:675> <encodes> <protein:119395734>." "<hsa:675> <owl:sameAs> <ENSG00000139618>". The relationship among these three resources: hsa:675, protein:119395734, and ENSG00000139618, in three databases is established. Similar to how any document expressed in HyperText Markup Language (HTML) can be linked to any other document expressed in HTML, the information expressed in RDF can be connected to any other information expressed in RDF (26). However, with respect to HTML, a linked resource must be a whole document, whereas with RDF, any information defined as a resource can be linked together.

RDF is expressive with the simple triple format. The Semantic Web integrates not only resources that are themselves built or represented using RDF but also those resources that can be mapped to RDF (29).

2.2. SPARQL Protocol and RDF Query Language (SPARQL)

SPARQL is an RDF query language (30). A SPARQL endpoint is a conformant SPARQL protocol service as defined in the SPROT (SPARQL Protocol for RDF) specification. A SPARQL endpoint enables users (human or other) to query a knowledge base *via* the SPARQL language. SPARQL 1.1 specification, produced by the SPARQL Working Group on 21 March 2013, defines the syntax and semantics of the SERVICE extension, which allows a query author to direct a portion of a query to a particular SPARQL endpoint. The results are returned to the federated query processor and are combined with results from the rest of the query (31). The growing number of SPARQL query services offer data consumers an opportunity to merge data distributed across the Web. However, SPARQL query is still in its infancy, and its service provider tends to change its endpoint in the development stage. The site (32) monitors the availability of some SPARQL endpoints. Table 1 summarizes the main current available SPARQL endpoints in the life sciences.

2.3. Ontology

Semantic heterogeneities arise at the entry level where different terms are used for the same things or the same terms are used for different things. *Ontology* describes the types of entities in the world and how they are related. The RDF model enables a link between two resources. Ontology strengthens and implements the link by specifying the semantics of terminology systems in a well-defined and unambiguous manner (33,

Table 1. List of some available biomedical SPARQL endpoints

-
- Allie: <http://allie.dbcls.jp/>
 - Bio2RDF:
 - HGNC: <http://hgnc.bio2rdf.org/sparql>
 - GO: <http://go.bio2rdf.org/sparql>
 - PharmGKB: <http://cu.pharmgkb.bio2rdf.org/sparql>
 - Pubmed: <http://pubmed.bio2rdf.org/sparql>
 - BioGateway: <http://www.semantic-systems-biology.org/biogateway/querying>
 - Cell Cycle Ontology: <http://www.semantic-systems-biology.org/cco/queryingcco/sparql>
 - HDP: <http://healthdata.tw.rpi.edu/sparql>
 - Linked Food: <http://www.linkedfood.org:8890/sparql/>
 - Linked Life Data: <http://linkedlifedata.com/sparql>
 - myExperiment: <http://rdf.myexperiment.org/sparql>
 - NCBO: <http://sparql.bioontology.org/>
 - Neuroscience Information Framework: <http://rdf-stage.neuinfo.org/>
 - The EBI RDF platform:
 - BioModels :<http://www.ebi.ac.uk/rdf/services/biomodels/sparql>
 - BioSamples: <http://www.ebi.ac.uk/rdf/services/biosamples/sparql>
 - ChEMBL: <http://www.ebi.ac.uk/rdf/services/chembl/sparql>
 - Expression Atlas: <http://www.ebi.ac.uk/rdf/services/atlas/sparql>
 - Reactome: <http://www.ebi.ac.uk/rdf/services/reactome/sparql>
 - UniProt: <http://beta.sparql.uniprot.org/>
-

34). Ontology provides a shared understanding of data, services and processes and has thus far played a role in the semantic integration of databases (35).

The OWL Web Ontology Language (*OWL*) (36) is designed for use by applications that need to process the content of information instead of just presenting information to humans. By providing additional vocabulary along with formal semantics, OWL facilitates a greater machine interpretability of Web content than that supported by XML and RDF. Consider the following simple example (37): (i) frog and Amphibian are two classes, and both have an *is-a* property; (ii) there is a restriction in which Frog is a subclass of Amphibian; and (iii) Herry is one example of a Frog class. We can simplify the model as "<Frog> <rdfs:subClassOf> <Amphibian>" and "<Herry> <is-a> <Frog>", and then we can infer that "<Herry> <is-a> <Amphibian>". By including descriptions of classes, properties and their examples, the OWL formal semantics specifies how to derive its logical consequences, *i.e.*, facts not literally present in the ontology but *entailed* by the semantics. These entailments may be based on a single document or multiple distributed documents that have been combined using defined OWL mechanisms (<http://www.w3.org/TR/owl-guide/>). In this way, RDF enables the data publisher to explicitly state the nature of the connection (38). In contrast, HTML links typically only indicate that two documents are related in some way without showing the nature of the relationship. Together with RDF Schema (39), which provides a data-modeling vocabulary for RDF data, OWL offers a standard, machine-processable means of describing relationships between RDF statements, *e.g.*, that one property is an `rdfs:subPropertyOf` of another.

The life sciences are flourishing with ontologies to enable the data in distributed sources to be shared and analyzed. The Open Biological and Biomedical

Ontologies (OBO) Foundry (<http://www.obofoundry.org/>) is a collaborative experiment involving developers of science-based ontologies who are establishing a set of principles for ontology development, with the goal of creating a suite of orthogonal interoperable reference ontologies in the biomedical domain. The ontologies developed by them include biological process, cellular component, chemical entities of biological interest, molecular function ontology and so on. The Ontology Working Group of the Health Care and Life Sciences (HCLS) is to facilitate creation, evaluation and maintenance of "core vocabularies and ontologies to support cross-community data integration and collaborative efforts". The Gene Ontology (GO) project (<http://www.geneontology.org/>) is a collaborative effort of Gene Ontology Consortium, to address the need for consistent descriptions of gene products in different databases. The Micro Array Gene Expression Data (MGED) Ontology (40) describes Microarray data and experiments. Biological Pathway Exchange (BioPAX) is an ontology for biological pathway data. National Center for Biomedical Ontology's (NCBO) BioPortal (<https://biportal.bioontology.org/>) contains URIs for concepts from almost 300 biomedical ontologies and reference terminologies. BioPortal is a convenient tool that can be used to identify public ontologies that best map to the entities in biomedical and clinical data sets. Ontobee (<http://www.ontobee.org/>) aims to facilitate ontology data sharing, visualization, query, integration, and analysis. Several web services have been developed to efficiently use the existing ontologies. The Ontology Lookup Service (OLS, <http://www.ebi.ac.uk/ontology-lookup/>) provides a web service interface to query multiple ontologies from a single location with a unified output format. To support ontology production based on existing resources, the OntoFinder/OntoFactory system (<http://ontofinder.dbcls.jp/>) aims to provide

non-computer experts with an easy interface to assist ontology selection and term selection from BioPortal, until a user produces his/her seed ontology. Ontologies have been widely applied and play an important role in the life science field. Gene Set Enrichment Analysis (GSEA) (41) utilizes GO to determine whether an a priori defined set of genes shows significant, concordant differences between two biological states. Great efforts have been paid on how to design a good ontology system and use it in data integration and automated reasoning. The pathway data sharing in the BioPAX community standard (42) and cross-product extensions of the Gene Ontology (43) use ontology to verify the consistency of a data model. Multiple ontologies have been integrated (44). Formal approaches to ontology research and their potential impact on biomedical applications and analyses have been summarized (45).

2.4. Linked data

Similar to how the idea to add, search, and automatically discover documents in the world stimulated the Web's explosive growth, the same principles of linking, and therefore ease of discovery, can be applied to data on the Web (38). Different from a key word search, linked data make automated reasoning about data possible by using semantic technologies. We are moving from the era of "data on the web" to an era of "web of data (linked data)" (46). Linked data try to create the Web into a giant global database. The term *Linked Data* refers to a set of best practices for publishing and interlinking structured data on the Web. Tim Berners-Lee in his Design Issues

introduced four *Linked Data* principles (47): (i) Use URIs as names for things. (ii) Use HTTP URIs to allow people to look up those names. (iii) When an individual looks up a URI, provide useful information using recommended standards (e.g., RDF and SPARQL). (iv) Include links to other URIs so that more things can be discovered.

Hypertext Transfer Protocol (HTTP) URIs provide a simple way to create globally unique names and a means to access information describing the identified entity. The RDF model enables the establishment of RDF links between data. A SPARQL query facilitates the retrieval of the data of interest across the distributed sources.

Linked Data has gained significant uptake in the life sciences. The HCLS group works on the Linking Open Drug Data (LODD) project (<http://www.w3.org/wiki/HCLSIG/LODD>), which provides linked RDF data exported from several data sources such as ClinicalTrials.gov, DrugBank (<http://www.drugbank.ca/>), and DailyMed (<http://dailymed.nlm.nih.gov/dailymed/about.cfm>). In particular, the Bio2RDF project has interlinked more than 30 widely used data sets (48), including the Universal Protein Resource (UniProt), KEGG, the Chemical Abstracts Service (CAS), PubMed, and Gene Ontology. Linking Open Data (<http://www.w3.org/wiki/SweoIG/TaskForces/CommunityProjects/LinkingOpenData>), a W3C Semantic Web Education and Outreach (SWEO) community project, aims to publish existing open license datasets as Linked Data on the Web to interlink things between different data sources. In Figure 2 the pink corner shows the life science data of the Linking Open Data (LOD) Project Cloud Diagram.

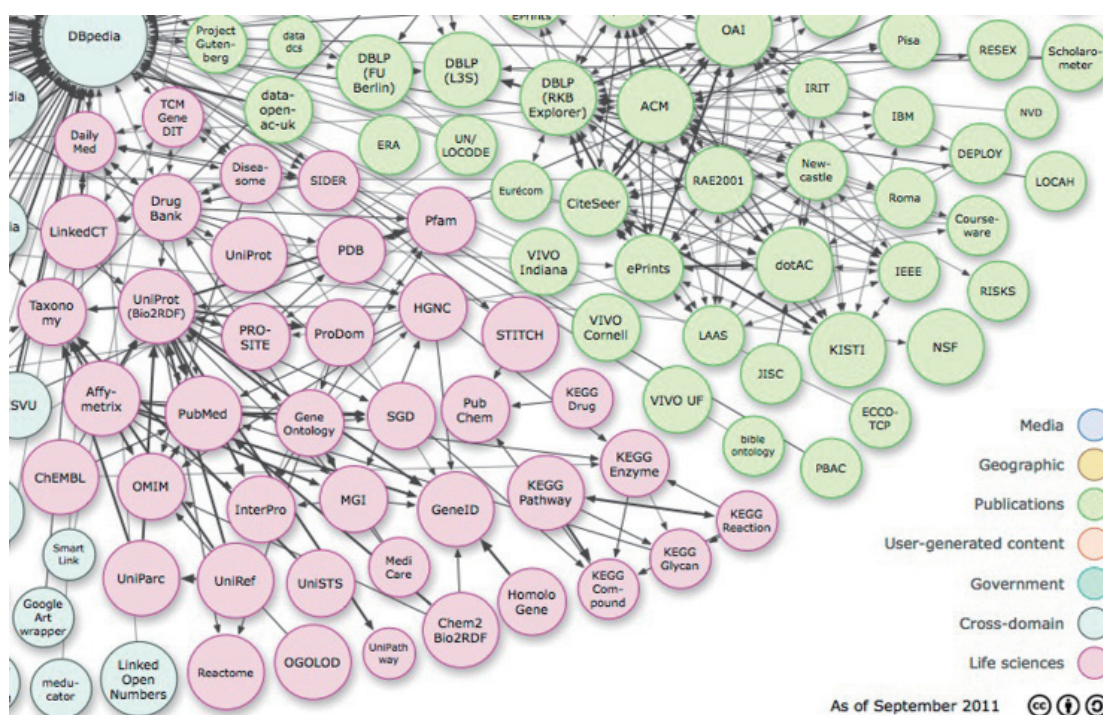


Figure 2. The lower right corner of the Linking Open Data cloud diagram ([Internet] [cited July 18, 2014], Linking Open Data cloud diagram, by Richard Cyganiak and Anja Jentzsch. Available from <http://lod-cloud.net/>). The pink part illustrates the life sciences data.

Table 2. Popular triple stores

Name	Language	Cluster	Inference	Available at
4store	C	Yes	No	http://www.4store.org/
Bigdata	Java	Yes	RDFS and limited OWL inference	http://www.bigdata.com/
Mulgara	Java	Yes	RDFS and limited OWL	http://www.mulgara.org/
OWLIM	Java	Yes	RDFS, OWL 2 RL and OWL 2 QL	http://www.ontotext.com/owlim
Virtuoso	C	Yes	limited RDFS and OWL	http://virtuoso.openlinksw.com/dataspace/doc/dav/wiki/Main/
AllegroGraph	Common Lisp	Yes	RDFS and limited OWL	http://franz.com/agraph/allegrograph/
Apache Jena	Java	Yes	RDFS, OWL	http://jena.apache.org/
RDF-3X	C++	No	No	https://www.mpi-inf.mpg.de/~neumann/rdf3x/
Sesame	Java	Yes	RDFS	http://www.openrdf.org/

Life science has 40 datasets with more than 3 billion triples, accounting for 9.60% of all data.

2.5. Triple store

Life and health science communities have made remarkable progress as early adopters of Semantic Web technologies. A triple store is a database for the storage and retrieval of triples. The UniProt knowledge base (49) connects more than 150 molecular biology and cheminformatics databases and integrates, interprets, and standardizes data from numerous resources to achieve the most comprehensive catalog of protein sequences and functional annotations. As another example, the Protein Data Bank Japan (PDBj) (50) accepts and processes PDB entries that are deposited mainly from Asian and Oceanic researchers and maintains a centralized archive of macromolecular structures in collaboration with other Worldwide Protein Data Bank (wwPDB) members, including the Research Collaboratory for Structural Bioinformatics (RCSB) PDB (51), the Biological Magnetic Resonance Bank (BMRB) (52) in the US, and the Protein Data Bank Europe (PDBe) (53) in Europe. DNA Data Bank of Japan (DDBJ) (54) contains approximately 8 billion triples, a number that will likely increase. Whether RDF stores can meet the needs of a biological database provider, such as loading, querying, and scaling the data efficiently, will be a major concern.

The triple store benchmark is a benchmark for evaluating the performance of storage systems, such as load cost, query performance and scalability. The Benchmark can be classified into a synthetic data benchmark and a real data benchmark. The Lehigh University Benchmark (LUBM) (55) and the Berlin SPARQL Benchmark (BSBM) (56) are two often-used general benchmarks, and they use a data generator to produce synthetic e-commerce knowledge data. Cell Cycle Ontology (57) and BioBenchmark Toyama 2012 (58) uses real biological data. BioBenchmark Toyama evaluated five triple stores, 4store (59), Bigdata (60), Mulgara (61), Virtuoso (62), and OWLIM-SE (63), with five biological data sets, Cell Cycle Ontology, Abbreviation/Long Form Search in Life Sciences (Allie), PDBj, UniProt, and DDBJ, ranging in size

from approximately 10 million to 8 billion triples. Table 2 lists some popular triple stores according to their implemented language, inference ability and the presence of support for running in clusters. 4store was used in cell cycle ontology. Mulgara was used as an internal triple store in DDBJ. OWLIM-SE has been applied as a UniProt triple store. Virtuoso shows good performance in BSBM and DBpedia SPARQL Benchmark. Bigdata is a complete free open source triple that performs averagely well in BSBM, supports most inference functions and runs in both single node and cluster modes and could be a potentially good candidate to customize one's own triple store.

2.6. Triple store in the cloud

To address such large-scale data management and analysis, Semantic Web services necessitate the adoption of advances in high performance computing (64), such as cloud computing (65,66). Cloud computing has been proposed as a promising technology to solve both the economic and efficiency problems caused by the data explosion. Users do not need to purchase and install their own local expensive servers, and cloud computing vendors prepare all the computing resources and infrastructures as on-demand services. Users need only to pay the rental fee for the resources they have used in the cloud, which saves much money as the users pay by use instead of provisioning for peak (high-end sources purchased only for dealing with tough but few tasks). The most important benefit is that cloud computing greatly facilitates the sharing of analysis pipelines and data between researchers. According to the level of resources to be shared, cloud computing can be divided into four categories (67): Data as a Service (DaaS), Software as a Service (SaaS), Platform as a Service (PaaS), and Infrastructure as a Service (IaaS). DaaS provides on-demand access to up-to-date public data that can be accessed and used through the Internet. SaaS provides online software services in publicly accessible servers. PaaS provides a platform that enables users to develop, test and deploy their applications in the cloud. IaaS provides virtualized resources, including hardware and software, through the Internet. Cloud computing

provides big data in the life sciences field with good storage space, web services and development platforms.

The ability to address big data studies on cloud-based triple stores is drawing more attention. Apache Cassandra (68) is a cloud database with linear scalability. CumulusRDF (69) is an RDF store on a cloud-based architecture, licensed under the GNU Affero General Public License. The current version uses Apache Cassandra as a storage backend. CumulusRDF supports a SPARQL1.1 endpoint and allows for fast queries of 1 billion triples on 16 nodes (70). Apache HBase is an open source, horizontally scalable, row consistent, low latency, random access data store. HBase has a proven track-record for scaling out to clusters containing approximately 1,000 nodes. It has been implemented as two versions: Jena-HBase (71), using Jena as the SPARQL query engine, and Hive+HBase, a SQL-like data warehousing tool that allows for querying using MapReduce (72). MapReduce is a programming model and an associated implementation for processing and generating large data sets. MapReduce is highly fault tolerant and scalable and can run on clusters with thousands of machines, facilitating its wide use as a cloud programming framework in bioinformatics (67). The projects (72-76) focused on developing large-scale RDF stores using the MapReduce paradigm. Fensel *et al.* (77) focused on web-scale data analysis and reasoning. Stratustore (78) is an RDF store that uses Amazon's SimpleDB as an RDF store back-end in combination with Jena's API. It is an open source project. The results show that its performance is not competitive with other RDF stores such as Virtuoso when using 20 simultaneous Stratustore instances. The throughput of the system also increases as the number of Stratustore instances grows. Bugiotti *et al.* used SimpleDB to store RDF files in the Amazon Simple Storage Service (S3) and used Amazon SimpleDB to store the index (79). Dydra (80) relied on the Amazon EC2 infrastructure, providing a SPARQL endpoint to query the data stored. SHARD (81), a Berkeley Software Distribution (BSD) licensed open source project, is a proof-of-concept high-performance, low-cost distributed computing technology to develop a highly scalable triple-store built on Hadoop and Hadoop Distributed File System (HDFS). Accumulo (82) is an open-source, distributed, column-oriented store model. Rya (83) uses Accumulo as a storage backend. The evaluation (83) showed that, in most cases, Rya outperforms existing distributed RDF solutions.

3. Challenge

Semantic Web technologies were not born for big data. As the basis for Semantic Web technologies, RDF was originally designed as a metadata data model in 1997, providing interoperability between applications that exchange machine-understandable information on the

Web. Six joint documents (Primer, Concepts, Syntax, Semantics, Vocabulary, and Test Cases) superseded the W3C RDF Recommendation and described updates to the syntax and a more detailed model in 2004. In 2014 RDF Schema 1.1, as well as more representation formats such as JSON-LD, was introduced. The introduction of vocabulary, semantics, formal syntax, and rich representation formats made RDF evolve into a general-purpose language for representing information on the Web. The introduction of vocabulary and semantics (such as RDF Schema (RDFS), OWL, *etc.*) laid a foundation for dealing with the *variety* problem of big data in life sciences. Take wwPDB as an example.

wwPDB is a collection of the experimentally determined 3D structures of biopolymers and their complexes. Metadata such as *Functional Keywords*, *Biological source* and *Total molecular weight* of an entry are encoded into RDF data directly, while the corresponding detailed structure information of the entry is encoded into URI links as a resource. Therefore the detailed information, such as atom model, can be retrieved from the linked file, "<PDBo:link_to_pdbml_extatom rdf:resource='ftp://ftp.wwpdb.org/pub/pdb/data/structures/all/XML-extatom/1gof-extatom.xml.gz'>" for the entry 1GOF in the PDBj database. Compared with relational database systems, RDF is more flexible for defining metadata with the current vocabulary. In the following statements, owl:DatatypeProperty defines a data type property instance metadata "datablockName". rdfs:domain indicates that the subjects of such property must belong to a "datablock" class, and the property itself should be a "string" Class.

```
<owl:DatatypeProperty xmlns:xsd="http://www.w3.org/2001/
XMLSchema" rdf:ID="datablockName">
<rdfs:domain rdf:resource="#datablock"/>
<rdfs:range rdf:resource="http://www.w3.org/2001/
XMLSchema#string"/>
</owl:DatatypeProperty>
```

According to the priority or importance of the data, one can choose to encode the information into the RDF model to do further analysis or act as search tags, or only include the detailed information into a linked file. By temporarily omitting the data file and concentrating on the metadata, the search or analysis can be reduced to a more effective space. Likewise Semantic web technologies can effectively manage the metadata of various kinds of data, such as videos and images, thus providing a good solution for the famous *variety* problem of big data.

On the other hand, the other two Vs, velocity and volume, are still posing a big challenge for Semantic Web technologies. SPARQL 1.1, proposed in 2013, facilitates the distributed RDF data query, and is promising for enabling a global big database. However, some kinds of practical problems are hindering the

query efficiency, such as some SPARQL endpoints do not support SPARQL 1.1 yet; no Vocabulary of Interlinked Datasets (VoID) for Semantic Web Integrator and Query Engine (SemWIQ) (84), Web of Data Query Analyzer (WoDQA) (85), and SPARQL Endpoint Federation Exploiting VOID Descriptions (Splendid) framework (86); no service description for DARQ system (87) and so on. Specifications and guidance about what artifacts a SPARQL endpoint is obliged to offer are needed to make a federated query responsive. A lot of effort has also been put into the research of triple store. Wu *et al.* in the BioBenchmark (58) show that a single Virtuoso 6.4 and OWLIM-SE 5.1 node can deal with 8 billion triples well. BSBM V3.1 also proves that Virtuoso 7 can handle 150 billion triples with 8 machines. At the same time distributed RDF systems based on Hadoop and other cloud platforms, as mentioned in Section 2.6, are also being developed rapidly. It still needs a great effort to effectively manage petabyte and even bigger data.

Data integration is a typical application of Semantic Web technologies in life sciences. TogoTable uses database identifiers (IDs) in the table as a query key for searching. Because TogoTable (88) uses RDF, it can integrate annotations from not only the reference database to which the IDs originally belong, but also externally linked databases *via* the LOD network. TogoGenome (<http://togogenome.org/>) is a Semantic Web-based genome database collection. Neurocommons project (89) uses Semantic Web technology for assembling and querying biomedical knowledge from multiple sources and disciplines.

However, the concept of big data, especially big data in the life sciences, is still in its infancy. Personal data, such as a personal genome, personalized medicine, and clinical data (*e.g.*, electronic health records), are mostly still in an embryonic stage and located in the local data warehouses of their specific organizations. Effective-enough data processing platforms are needed to provide enough incentives for biological organizations to publish and share their data. More importantly, the platform or systems must ensure data security in a collaborative environment and not risk medical privacy (24). S3QL provides a permission control mechanism that allows the users to protect their data by specifying contextual minutia (90). Cloud security solutions include the use of better security systems with advanced encryption algorithms and proper signing of Service level agreements (91). Private and hybrid clouds are being built to ensure data safety (92). Similar problems exist in the LOD project. In addition, maintaining semantics links in a dynamic big data era is another difficult problem for LOD.

Big data in the life sciences requires a high level of knowledge of both biology and computer science. Big data technologies, such as cloud-based applications, are based on parallel processing. Until now, few

bioinformatics tools have been designed to run in parallel (6), a process that requires a high level of computational know-how. By contrast, ontology design, data analysis, hypothesis building and validation, and many other problems need specialized biological knowledge.

Despite these difficulties the flexibility on metadata, the development of distributed and cloud-based triple store systems, and the improvement of federated query systems facilitate Semantic Web technologies as a promising solution for the big data in life sciences, with great efforts and collaboration from the computer and biological community.

4. Conclusions

Big data poses a great challenge for the life sciences. To address the heterogeneous variety of life scientific big data, a series of Semantic Web technologies provides a promising solution. RDF, SPARQL, triple store and ontology facilitate the integration and analysis of heterogeneous multi-disciplinary data. Linked data turns the Web into a giant global database. Triple store in the cloud takes full advantage of cloud services to address the exponential growth of biological data. Although still in its infancy, the whole scientific community is making efforts to develop new technologies and tools to ensure that big data is accessible, analyzable and applicable to the field of life sciences.

Acknowledgements

This work has been supported by the National Bioscience Database Center (NBDC) of the Japan Science and Technology Agency (JST).

References

1. Moore GE. Cramming more components onto integrated circuits. Proc IEEE. 1998; 86:82-85.
2. Walter C. Kryder's law. Sci Am. 2005; 293:32-33.
3. Reynolds C. As we may communicate. ACM SIGCHI Bulletin. 1998; 30:40-44.
4. Szalay A, Gray J. 2020 computing: Science in an exponential world. Nature. 2006; 440:413-414.
5. Stein LD. The case for cloud computing in genome informatics. Genome Biol. 2010; 11:207.
6. O'Driscoll A, Daugelaite J, Sleator RD. 'Big data', Hadoop and cloud computing in genomics. J Biomed Inform. 2013; 46:774-781.
7. Mathe C, Sagot MF, Schiex T, Rouze P. Current methods of gene prediction, their strengths and weaknesses. Nucleic Acids Res. 2002; 30:4103-4117.
8. Harvard School of Public Health. The promise of 'big data'. 2012. <http://www.hsph.harvard.edu/news/magazine/spr12-big-data-tb-health-costs/> (accessed August 4, 2014).
9. Eisenstein M. Oxford Nanopore announcement sets sequencing sector abuzz. Nat Biotech. 2012; 30:295-296.

10. Davies K. The \$1,000 genome: the revolution in DNA sequencing and the new era of personalized medicine. *Am J Hum Genet.* 2010; 87:742.
11. Grossman RL, White KP. A vision for a biomedical cloud. *J Intern Med.* 2012; 271:122-130.
12. Turk-Browne NB. Functional interactions as big data in the human brain. *Science.* 2013; 342:580-584.
13. Wild DJ, Ding Y, Sheth AP, Harland L, Gifford EM, Lajiness MS. Systems chemical biology and the Semantic Web: what they mean for the future of drug discovery research. *Drug Discov Today.* 2012; 17:469-474.
14. NCBI. GenBank. <http://www.ncbi.nlm.nih.gov/genbank/> (accessed August 4, 2014).
15. Harger C, Skupski M, Bingham J, *et al.* The genome sequence database (GSDB): improving data quality and data access. *Nucleic Acids Res.* 1998; 26:21-26.
16. UniProt. <http://www.uniprot.org/> (accessed August 4, 2014).
17. OMIM-Online Mendelian Inheritance in Man. <http://www.omim.org/> (accessed August 4, 2014).
18. Davidson SB, Overton C, Buneman P. Challenges in integrating biological data sources. *J Comput Biol.* 1995; 2:557-572.
19. Li A. Facing the challenges of data integration in biosciences. *Eng Lett.* 2006; 13:327.
20. Zhang Z, Bajic VB, Yu J, Cheung KH, Townsend JP. Data integration in bioinformatics: current efforts and challenges. In: *Bioinformatics – Trends and Methodologies.* 2011. DOI: 10.5772/21654.
21. Li H, Handsaker B, Wysoker A, Fennell T, Ruan J, Homer N, Marth G, Abecasis G, Durbin R, 1000 Genome Project Data Processing Subgroup. The sequence alignment/map format and samtools. *Bioinformatics.* 2009; 25:2078-2079.
22. Reese MG, Moore B, Batchelor C, Salas F, Cunningham F, Marth GT, Stein L, Flicek P, Yandell M, Eilbeck K. A standard variation file format for human genome sequences. *Genome Biol.* 2010; 11:R88.
23. Ruttenberg A, Clark T, Bug W *et al.* Advancing translational research with the Semantic Web. *BMC Bioinformatics.* 2007; 8(Suppl 3):S2.
24. Chen H, Yu T, Chen JY. Semantic web meets integrative biology: A survey. *Brief Bioinform.* 2013; 14:109-125.
25. Bizer C, Boncz P, Brodie ML, Erling O. The meaningful use of big data: four perspectives - four challenges. *Sigmod Rec.* 2011; 40:56-60.
26. Neumann EK, Miller E, Wilbanks J. What the semantic web could do for the life sciences. *Drug Discov Today Biosilico.* 2004; 2:228-236.
27. Berners-Lee T, Hendler J, Lassila O. The semantic web. *Sci Am.* 2001; 284:34-43.
28. W3C. RDF Primer. <http://www.w3.org/TR/2004/REC-rdf-primer-20040210/> (accessed August 4, 2014).
29. W3C. The Self-Describing Web. <http://www.w3.org/2001/tag/doc/selfDescribingDocuments#RDFSection> (accessed August 4, 2014).
30. W3C. SPARQL Query Language for RDF. <http://www.w3.org/TR/rdf-sparql-query/> (accessed August 4, 2014).
31. W3C. SPARQL 1.1 Federated Query. <http://www.w3.org/TR/sparql11-federated-query/> (accessed August 4, 2014).
32. AVAILABILITY. <http://sparql.es.okfn.org/availability> (accessed August 4, 2014).
33. Gruber TR. A translation approach to portable ontology specifications. *Knowledge Acquisition.* 1993; 5:199-220.
34. Guarino N. Formal Ontology and Information Systems. 1998. <http://citeseerx.ist.psu.edu/viewdoc/summary?doi=10.1.1.29.1776> (accessed August 4, 2014).
35. Smith B, Kohler J, Kumar A. On the application of formal principles to life science data: A case study in the gene ontology. In: *Data Integration in the Life Sciences* (Lambrix P, Kemp G). Berlin Heidelberg, Springer, 2004; 2994:79-94.
36. W3C. OWL Web Ontology Language Overview. <http://www.w3.org/TR/owl-features/> (accessed August 4, 2014).
37. Suntisrivaraporn B. Empirical evaluation of reasoning in lightweight DLs on life science ontologies. 2009; <http://www.citeulike.org/user/cjm/article/6332859> (accessed August 4, 2014).
38. Bizer C, Heath T. Linked data: evolving the web into a global data space. 2011; <http://linkeddatabook.com/editions/1.0/> (accessed August 4, 2014).
39. W3C. RDF Schema 1.1. <http://www.w3.org/TR/rdf-schema/> (accessed August 4, 2014).
40. Whetzel PL, Parkinson H, Causton HC, Fan L, Fostel J, Frago G, Game L, Heiskanen M, Morrison N, Rocca-Serra P, Sansone SA, Taylor C, White J, Stoeckert CJ Jr. The MGED ontology: A resource for semantics-based description of microarray experiments. *Bioinformatics.* 2006; 22:866-873.
41. Subramanian A, Tamayo P, Mootha VK, Mukherjee S, Ebert BL, Gillette MA, Paulovich A, Pomeroy SL, Golub TR, Lander ES, Mesirov JP. Gene set enrichment analysis: A knowledge-based approach for interpreting genome-wide expression profiles. *Proc Natl Acad Sci U S A.* 2005; 102:15545-15550.
42. Demir E, Cary MP, Paley S, *et al.* The BioPAX community standard for pathway data sharing. *Nature Biotechnol.* 2010; 28:935-942.
43. Mungall CJ, Bada M, Berardini TZ, Deegan J, Ireland A, Harris MA, Hill DP, Lomax J. Cross-product extensions of the Gene Ontology. *J Biomed Inform.* 2011; 44:80-86.
44. Hoehndorf R, Dumontier M, Gennari JH, *et al.* Integrating systems biology models and biomedical ontologies. *BMC Syst Biol.* 2011; 5:124.
45. Hoehndorf R, Dumontier M, Gkoutos GV. Evaluation of research in biomedical ontologies. *Brief Bioinform.* 2013; 14:696-712.
46. Bauer F, Kaltenböck M. Linked open data: the essentials. 2011. <http://www.semantic-web.at/LOD-TheEssentials.pdf> (accessed August 4, 2014).
47. Bizer C, Heath T, Berners-Lee T. Linked data - the story so far. *IJSWIS.* <http://tomheath.com/papers/bizer-heath-berners-lee-ijswis-linked-data.pdf> (accessed August 4, 2014).
48. Bizer C. Interlinking scientific data on a global scale. *Data Science Journal.* 2013; 12.
49. Consortium U. Update on activities at the Universal Protein Resource (UniProt) in 2013. *Nucleic Acids Res.* 2013; 41(D1):D43-D47.
50. Kinjo AR, Suzuki H, Yamashita R, Ikegawa Y, Kudou T, Igarashi R, Kengaku Y, Cho H, Standley DM, Nakagawa A. Protein Data Bank Japan (PDBj): Maintaining a structural data archive and resource description framework format. *Nucleic Acids Res.* 2012; 40(D1):D453-D460.
51. Rose PW, Bi C, Bluhm WF, Christie CH, Dimitropoulos D, Dutta S, Green RK, Goodsell DS, Prlić A, Quesada M. The RCSB Protein Data Bank: new resources for research and education. *Nucleic Acids Res.* 2013;

- 41(D1):D475-D482.
52. Ulrich E L, Akutsu H, Doreleijers JF, Harano Y, Ioannidis YE, Lin J, Livny M, Mading S, Maziuk D, Miller Z. BioMagResBank. *Nucleic Acids Res.* 2008; 36(suppl 1):D402-D408.
 53. Velankar S, Best C, Beuth B, *et al.* PDBe: Protein data bank in Europe. *Nucleic Acids Res.* 2010; 38(suppl 1):D308-D317.
 54. Kodama Y, Mashima J, Kaminuma E, Gojobori T, Ogasawara O, Takagi T, Okubo K, Nakamura Y. The DNA DATA BANK of Japan launches a new resource, the DDBJ Omics Archive of functional genomics experiments. *Nucleic Acids Res.* 2012; 40(D1):D38-D42.
 55. Guo Y, Pan Z, Heflin J. LUBM: A benchmark for OWL knowledge base systems. *Web Semantics: Science, Services and Agents on the World Wide Web.* 2005; 3: 158-182.
 56. Bizer C, Schultz A. The Berlin sparql benchmark. *Int J Semant Web Inf.* 2009; 5:1-24.
 57. Mironov V, Seethappan N, Blondé W, Antezana E, Lindi B, Kuiper M. Benchmarking triple stores with biological data. SWAT4LS. 2010.
 58. Wu H, Fujiwara T, Yamamoto Y, Bolleman J, Yamaguchi A. BioBenchmark Toyama 2012: An evaluation of the performance of triple stores on biological data. *J Biomed Semant.* 2014; 5:32.
 59. 4store. <http://4store.org/> (accessed August 4, 2014).
 60. Bigdata. <http://www.sysstap.com/bigdata.htm> (accessed August 4, 2014).
 61. Mulgara. SEMANTIC STORE. <http://www.mulgara.org/> (accessed August 4, 2014).
 62. OPENLINK SOFTWARE. Virtuoso Universal Server. <http://virtuoso.openlinksw.com/> (accessed August 4, 2014).
 63. ontotext. OWLIM. <http://www.ontotext.com/owlim> (accessed August 4, 2014).
 64. Schadt EE, Linderman MD, Sorenson J, Lee L, Nolan GP. Computational solutions to large-scale data management and analysis. *Nat Rev Genet.* 2010; 11:647-657.
 65. Bateman A, Wood M. Cloud computing. *Bioinformatics.* 2009; 25:1475-1475.
 66. Stein LD. The case for cloud computing in genome informatics. *Genome Biol.* 2010; 11:207.
 67. Zhou S, Liao R, Guan J. When cloud computing meets bioinformatics: A review. *J Bioinform Comput Biol.* 2013; 11:1330002.
 68. Cassandra. <http://cassandra.apache.org/> (accessed August 4, 2014).
 69. Harth G, Ladwig A. CumulusRDF: linked data management on nested key-value stores. ISWC 2011.
 70. Cudré-Mauroux P, Enchev I, Fundatureanu S, Groth P, Haque A, Harth A, Keppmann F, Miranker D, Sequeda J, Wylot M. NoSQL databases for RDF: an empirical evaluation. ISWC 2013.
 71. Vaibhav K, Hadilkar MK, Bhavani Thuraisingham, Castagna P. Jena-HBase: a distributed, scalable and efficient RDF triple store. ISWC 2012.
 72. Dean J, Ghemawat S. MapReduce: Simplified data processing on large clusters. *Comm ACM.* 2008; 51:107-113.
 73. Mika P, Tummarello G. Web semantics in the clouds. *Ieee Intell Syst.* 2008; 23:82-87.
 74. Husain M, Khan L, Kantarcioglu M, Thuraisingham B. Data intensive query processing for large rdf graphs using cloud computing tools. IEEE CLOUD 2010.
 75. Myung J, Yeon J, Lee Sg. SPARQL basic graph pattern processing with iterative MapReduce. MDAC 2010.
 76. Schatzle A, Przyjaciel-Zablocki M, Lausen G. PigSPARQL: Mapping SPARQL to Pig Latin. SIGMOD/PODS 2011.
 77. Fensel D, van Harmelen F, Andersson B, Brennan P, Cunningham H, Della Valle E, Fischer F, Huang Z, Kiryakov A, Lee TI. Towards LarKC: A platform for web-scale reasoning. ICSC 2008.
 78. Stein R, Zacharias V. RDF on cloud number nine. SIGMOD/PODS 2012.
 79. Bugiotti F, Goasdoue F, Kaoudi Z, Manolescu I. RDF data management in the Amazon cloud. EDBT/ICDT Workshops 2012.
 80. DYDRA. <http://dydra.com/> (accessed August 4, 2014).
 81. Rohloff K. Cloud computing for scalability: the SHARD triple-Store. DIDC 2011.
 82. Accumulo. <http://wiki.apache.org/incubator/accumulo/propose> (accessed August 4, 2014).
 83. Punnoose R, Crainiceanu A, Rapp D. Rya: A scalable RDF triple store for the clouds. Cloud-I 2012.
 84. Langedger A, Wöß W, Blöchl M. SemWIQ-semantic web integrator and query engine. INFORMATIK 2008.
 85. Akar Z, Halaç TG, Ekinci EE, Dikenelli O. Querying the web of interlinked datasets using void descriptions. LDOW 2012.
 86. Görlitz O, Staab S. SPLENDID: SPARQL endpoint federation exploiting void descriptions. COLD 2011.
 87. Quilitz B, Leser U. Querying distributed RDF data sources with SPARQL. ESWC 2008.
 88. Kawano S, Watanabe T, Mizuguchi S, Araki N, Katayama T, Yamaguchi A. TogoTable: cross-database annotation system using the Resource Description Framework (RDF) data model. *Nucleic Acids Res.* 2014. doi: 10.1093/nar/gku403.
 89. Rutenberg A, Rees JA, Samwald M, Marshall MS. Life sciences on the Semantic Web: the Neurocommons and beyond. *Brief bioinform.* 2009;10:193-204.
 90. Deus H, Correa M, Stanislaus R, Miragaia M, Maass W, Lencastre H, Fox R, Almeida J. S3QL: A distributed domain specific language for controlled semantic integration of life sciences data. *BMC Bioinformatics.* 2011; 12:1-15.
 91. Nemade P, Kharche H. Big data in bioinformatics & the era of cloud computing. IOSR-JCE. 2013; 14:53-56.
 92. Qiu J, Ekanayake J, Gunarathne T, Choi JY, Bae SH, Li H, Zhang B, Wu TL, Ruan Y, Ekanayake S. Hybrid cloud and cluster computing paradigms for life science applications. *BMC bioinformatics.* 2010; 11(Suppl 12):S3.

(Received April 7, 2014; Revised July 18, 2014; Re-revised August 4, 2014; Accepted August 12, 2014)

A novel EGFP-expressing nude mice with complete loss of lymphocytes and NK cells to study tumor-host interactions

Kumiko Gotoh, Ryusho Kariya, Kouki Matsuda, Shinichiro Hattori, Kulthida Vaeteewoottacharn, Seiji Okada*

Division of Hematopoiesis, Center for AIDS Research, Kumamoto University, Kumamoto, Japan.

Summary Enhanced green fluorescent protein (EGFP) expressing Balb/c nude mice strain with Rag-2 and Jak3 double mutants (Nude-R/J-EGFP mice) was established to improve the take rate of human tumors and to distinguish tumor and host cells. EGFP was ubiquitously expressed in all organs including the brain, lung, liver, heart, kidney, spleen, and gastrointestinal tract in Nude-R/J-EGFP mice. The mice showed complete loss of T lymphocytes, B lymphocytes, and NK cells, indicating a higher take rate of human tumor xenograft. M213-mCherry, an mCherry expressing the cholangiocarcinoma cell line, was successfully detected and tumor vessels derived from the host were clearly identified with fluorescence imager. Thus, dual-color fluorescence imaging visualizes the tumor-host interaction by non-invasive *in vivo* fluorescent imaging in Nude-R/J-EGFP mice. These finding suggests that Nude-R/J-EGFP mice are becoming a powerful tool to investigate human tumor-host interactions.

Keywords: Enhanced green fluorescence protein (EGFP), nude mice, NK cells, fluorescence imaging, xenotransplantation

1. Introduction

Human cancer xenograft models of immunodeficient mice are widely used in oncology research (1). Athymic nude mice, Scid mice, and NOD/Scid mice have been used for this purpose. Since nude mice lack T cells but retain functional B cells and NK cells, they show limited growth of human tumors and tumor cell lines (2,3). However, they are still commonly used because their lack of fur facilitates tumor implantation and assessment (4,5). In particular, recent advances of *in vivo* fluorescent technologies enable us to detect fluorescence-expressing tumor cells inside mice without fur. In addition, several fluorescence protein-expressing transgenic mice have been established to distinguish tumor cells from host cells (6-9). Thus, fluorescence protein-expressing severe immunodeficient mice without fur are optimized for *in vivo* imaging.

Recent approaches have involved the use of severe

immunodeficient mice with NK defective genetically modified mice (10-13), which markedly improved the efficiency of xenotransplantation. We have previously generated Rag-2/Jak3 double-deficient mice with a Balb/c genetic background (Balb/c R/J mice) (14). These mice showed a lack of mature T and B lymphocytes and NK cells, and showed high efficiency of human hematopoietic stem cell (HSC) and peripheral blood mononuclear cell (PBMC) transplantation, and human tumor xenograft (15). Based on these findings, we established an enhanced green fluorescent protein (EGFP) -expressing Balb/c nude mice strain with Rag-2 and Jak3 double mutants (Nude-R/J-EGFP mice) and evaluated them for use in fluorescence bio-imaging.

2. Materials and Methods

2.1. Mice

Transgenic C57/BL6-EGFP mice were obtained from Prof. Masaru Okabe (Osaka University, Osaka, Japan). C57/BL6-EGFP mice express EGFP under the control of chicken β -actin promoter and cytomegalovirus enhancer (16). Balb/c-EGFP mice were established by crossing C57/BL6-EGFP mice with the Balb/c strain

*Address correspondence to:

Dr. Seiji Okada, Division of Hematopoiesis, Center for AIDS Research, Kumamoto University, Japan 2-2-1 Honjo, Kumamoto, 860-0811, Japan.
E-mail: okadas@kumamoto-u.ac.jp

for 10 generations. Balb/c-EGFP Rag-2^{-/-}Jak3^{-/-} mice were then established by crossing Balb/c Rag-2^{-/-}Jak3^{-/-} mice (14) and Balb/c-EGFP mice. Finally, Balb/c-EGFP nude Rag-2^{-/-}Jak3^{-/-} mice (referred to as Nude-R/J-EGFP mice) were established by crossing Balb/c-EGFP Rag-2^{-/-}Jak3^{-/-} mice and Balb/c nude mice, and were housed and monitored in our animal research facility according to institutional guidelines. The mice were maintained by mating nu/nu males with nu/+ females as nu/nu females cannot feed infants (17). The nude (18), Rag-2 (19) and Jak3 (20) mutations were genotyped using a previously described PCR method using genomic DNA extracted from tail tissue. EGFP mice were detected with Ultra violet lamp. All experimental procedures and protocols were approved by the Institutional Animal Care and Use Committee of Kumamoto University.

2.2. Cell lines

The human cholangiocarcinoma cell line, KKU-M213, was cultured in Dulbecco's modified Eagle's medium (DMEM; Wako Pure Chemical, Osaka, Japan) supplemented with 10% (v/v) heat-inactivated fetal bovine serum (JRH Bioscience, Lenexa, KS, USA), 100 u/mL penicillin and 100 µg/mL streptomycin (21). mCherry-transfected KKU-M213 (M213-mCherry) was established with pmCherry-N1 Vector (Clontech, Mountain View, CA, USA) and the transfection reagent Lipofectamine 2000 (Invitrogen, Carlsbad, CA, USA) according to the manufacturer's instructions. Transfected cells were selected in medium containing neomycin (G418; Carbiochem, Darmstadt, Germany), followed by limiting dilution to isolate stable clones.

2.3. Flow cytometry

Mouse spleen cells were stained with DX5-APC (pan NK marker), mCD122 (IL-2Rβ)-PE, mCD19-PE, and mCD3-Pacific Blue (eBiosciences, San Diego, CA, USA), and analyzed using LSR II (BD Biosciences, San Diego, CA, USA) to detect murine lymphocytes (14). Data were analyzed with FlowJo (Tree Star, San Carlos, CA, USA).

2.4. Xenograft mouse model

Eight-ten-week-old Nude-R/J-EGFP mice were subcutaneously inoculated with M213-mCherry (6×10^6 cells) suspended in 100 µL phosphate-buffered saline (PBS) in both flanks. On day 16, xenotransplanted mice were euthanized and imaged with an *in vivo* imaging system.

2.5. Image acquisition

We confirmed that organs and cells obtained from nude-R/J-EGFP mice could be visualized fluorescently.

In brief, after euthanizing Nude-R/J-EGFP mice, internal organs were placed on a tray and imaged using an Maestro *in vivo* fluorescence imaging system (Cambridge Research & Instrumentation, MA, USA). For M213-mCherry inoculated mice, euthanized nude-R/J-EGFP mice were placed on a tray and imaged using a Nuance multispectral imaging system (Cambridge Research & Instrumentation).

3. Results and Discussion

In the present study, we developed and characterized nude mice with ubiquitously expressed EGFP and complete loss of lymphocytes and NK cells on a Balb/c background (Nude-R/J-EGFP mice). The generated Nude-R/J-EGFP mice survived and bred well under specific pathogen-free conditions. Green fluorescence expression can be readily detected by the naked eye under fluorescent light in nude-R/J-EGFP and clearly detected in Nude-R/J-EGFP using a hand-held UV lamp (Figure 1A). Almost all internal organs showed green fluorescence under the imaging instrument (Figure 1B). The expression of EGFP in spleen cells was confirmed with flow cytometry (Figure 2A). To confirm the predicted immunophenotype of Nude-R/J-EGFP mice, single-cell suspensions from spleen cells were labeled with fluorescent antibodies against mouse DX-5 (pan NK marker), CD122 (IL-2Rβ), CD3 (T cell marker) and CD19 (B cell marker). In contrast to wild-type mice, no B (CD19 positive) and T (CD3 positive) lymphocytes or NK cells (DX-5 and CD122 double-positive cells) were detected in Nude-R/J-EGFP mice as expected (14) (Figure 2B).

The fluorescence of Nude-R/J-EGFP mice (green) and subcutaneously transplanted M213-mCherry

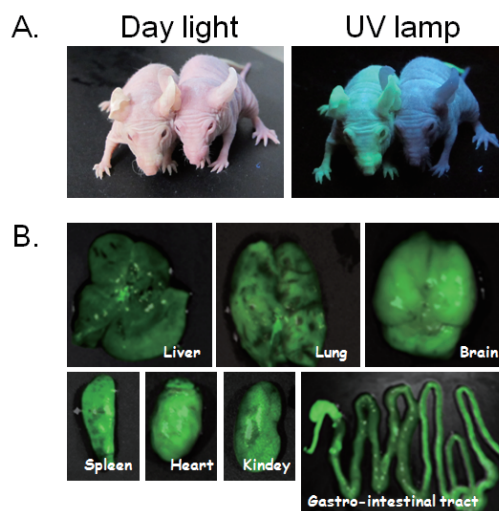


Figure 1. EGFP expression of the Nude-R/J-EGFP mice. (A) Nude-R/J-EGFP mice visualized in daylight or using a handheld UV lamp (left: Nude-R/J-EGFP mice, right: Nude mice). (B) Internal organs showing strong EGFP expression in the heart, lung, kidney, liver, brain, spleen, and gastrointestinal tract using a fluorescence imaging system.

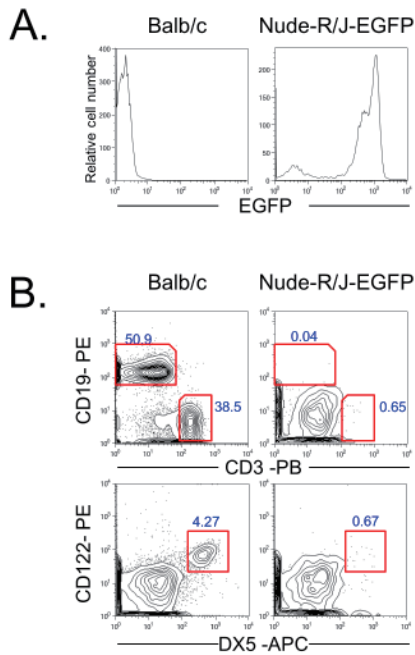


Figure 2. Flowcytometric analysis of EGFP and lineage markers of the Nude-R/J-EGFP mice spleen cells. (A) Strong expression of EGFP in spleen cells of Nude-R/J-EGFP mice. **(B)** Lack of mature lymphocytes and NK cells in Nude-R/J-EGFP mice. Spleen cells from Balb/c wild-type mice and Nude-R/J-EGFP mice were stained with DX5-APC (pan NK marker) and mCD122 (IL-2R β)-PE, or mCD19-PE and mCD3-Pacific Blue, and analyzed with flow cytometry. No T and B lymphocytes or NK cells were observed in the spleen of Nude-R/J-EGFP mice.

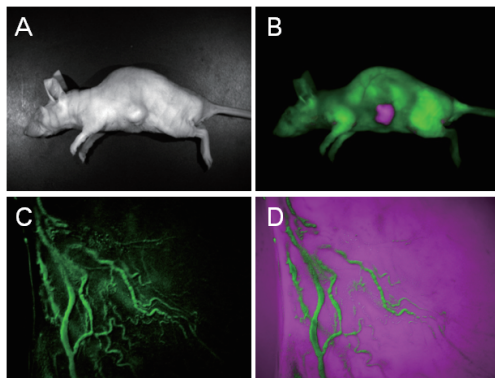


Figure 3. Visualization of mCherry expressing tumor in Nude-R/J-EGFP mice. (A and B) Direct fluorescence of M231-mCherry tumor grown in the subcutaneous region of Nude-R/J-EGFP mice and visualized using a non-invasive fluorescence imaging system. **(C)** Direct green fluorescence of tumor vessels in the M213-mCherry tumor visualized using a multispectral imaging system (Nuance). **(D)** Merged with tumor red fluorescence.

(red) was successfully detected with a Maestro *in vivo* fluorescence imaging system (Figure 3). The tumor vessels inside M213-mCherry were further detected with a Nuance multispectral imaging system.

Nude mice are used as recipients of human tumor xenotransplantation, since the lack of a hair phenotype enables easy measurement of subcutaneous tumors and makes them suitable for fluorescence detection of tumors. However, only 25-35% of human tumors

obtained from patients have been successfully transplanted into nude mice, because nude mice lack mature T cells, but retain B cells and NK cells. To overcome this weakness, several attempts have been made to develop more immunodeficient mice such as beige-nude, CBA/N nude and hairless scid mice (22,23). However, significant NK activity remains in these mice. Recent advances in developmental engineering have enabled to develop immunodeficient mice with complete loss of NK cells, such as NOD/Scid/common γ ^{-/-} (NOG and NSG) mice (24), NOD/Scid/Jak3^{-/-} mice (13), Balb/c Rag-2^{-/-}common γ ^{-/-} mice (11), Balb/c Rag^{-/-}-Jak3^{-/-} mice (14), which markedly improved the efficiency of xenotransplantation. In addition, several immunodeficient mice expressing fluorescence protein have been developed to optimize *in vivo* imaging (7,9). These mice are very useful to distinguish host cells and transplanted human tumor cells (25). However, the level of immunodeficiency is not sufficient for transplantation of human cells in nude based mice (7). NOD/Scid based mice are sufficient for human cell transplantation; however, their fur prevented precise assessment of tumor size and detection of fluorescence subcutaneously and within the body (9). Newly generated Nude-R/J-EGFP mice have favorable attributes for *in vivo* bio-imaging, *i.e.* high immunodeficiency with NK deficiency, being hairless, and expressing EGFP, indicating that Nude-R/J-EGFP mice are optimized for human cancer xenotransplantation and detection using a Nuance multispectral imaging system.

In summary, we established an EGFP-expressing Balb/c nude mice strain with Rag-2 and Jak3 double mutants (Nude-R/J-EGFP mice) and showed that Nude-R/J-EGFP mice are optimal for human tumor engraftment and non-invasive *in vivo* fluorescent imaging.

Acknowledgements

We thank I. Suzu and S. Fujikawa for providing technical assistance and K. Tokunaga and Y. Endo for secretarial assistance. This work was supported in part by a Health and Labour Science Research Grant from the Ministry of Health, Labour and Welfare of Japan (H25-AIDS-I-002), an A-STEP grant from Japan Science and Technology Agency (No. 221Z00712), and Grants-in-Aid for Science Research (No. 21107522 and 21591209) from the Ministry of Education, Science, Sports, and Culture of Japan.

References

1. Sausville EA, Burger AM. Contributions of human tumor xenografts to anticancer drug development. *Cancer Res.* 2006; 66:3351-3354, discussion 3354.
2. Taghian A, Budach W, Zietman A, Freeman J, Gioioso D,

- Ruka W, Suit HD. Quantitative comparison between the transplantability of human and murine tumors into the subcutaneous tissue of NCr/Sed-nu/nu nude and severe combined immunodeficient mice. *Cancer Res.* 1993; 53:5012-5017.
3. Carreno BM, Garbow JR, Kolar GR, Jackson EN, Engelbach JA, Becker-Hapak M, Carayannopoulos LN, Piwnicka-Worms D, Linette GP. Immunodeficient mouse strains display marked variability in growth of human melanoma lung metastases. *Clin Cancer Res.* 2009; 15:3277-3286.
 4. Kelland LR. Of mice and men: Values and liabilities of the athymic nude mouse model in anticancer drug development. *Eur J Cancer.* 2004; 40:827-836.
 5. Bellet RE, Danna V, Mastrangelo MJ, Berd D. Evaluation of a "nude" mouse-human tumor panel as a predictive secondary screen for cancer chemotherapeutic agents. *J Natl Cancer Inst.* 1979; 63:1185-1188.
 6. Yang M, Reynoso J, Bouvet M, Hoffman RM. A transgenic red fluorescent protein-expressing nude mouse for color-coded imaging of the tumor microenvironment. *J Cell Biochem.* 2009; 106:279-284.
 7. Yang M, Reynoso J, Jiang P, Li L, Moossa AR, Hoffman RM. Transgenic nude mouse with ubiquitous green fluorescent protein expression as a host for human tumors. *Cancer Res.* 2004; 64:8651-8656.
 8. Shima K, Mizuma M, Hayashi H, et al. Potential utility of eGFP-expressing NOG mice (NOG-EGFP) as a high purity cancer sampling system. *J Exp Clin Cancer Res.* 2012; 31:55.
 9. Niclou SP, Danzeisen C, Eikesdal HP, Wiig H, Brons NH, Poli AM, Svendsen A, Torsvik A, Enger PO, Terzis JA, Bjerkvig R. A novel eGFP-expressing immunodeficient mouse model to study tumor-host interactions. *FASEB J.* 2008; 22:3120-3128.
 10. Yahata T, Ando K, Nakamura Y, Ueyama Y, Shimamura K, Tamaoki N, Kato S, Hotta T. Functional human T lymphocyte development from cord blood CD34+ cells in nonobese diabetic/Shi-scid, IL-2 receptor gamma null mice. *J Immunol.* 2002; 169:204-209.
 11. Traggiai E, Chicha L, Mazzucchelli L, Bronz L, Piffaretti JC, Lanzavecchia A, Manz MG. Development of a human adaptive immune system in cord blood cell-transplanted mice. *Science.* 2004; 304:104-107.
 12. Ishikawa F, Yasukawa M, Lyons B, Yoshida S, Miyamoto T, Yoshimoto G, Watanabe T, Akashi K, Shultz LD, Harada M. Development of functional human blood and immune systems in NOD/SCID/IL2 receptor {gamma} chain(null) mice. *Blood.* 2005; 106:1565-1573.
 13. Okada S, Harada H, Ito T, Saito T, Suzu S. Early development of human hematopoietic and acquired immune systems in new born NOD/Scid/Jak3(null) mice intrahepatic engrafted with cord blood-derived CD34 (+) cells. *Int J Hematol.* 2008; 88:476-482.
 14. Ono A, Hattori S, Kariya R, Iwanaga S, Taura M, Harada H, Suzu S, Okada S. Comparative study of human hematopoietic cell engraftment into BALB/c and C57BL/6 strain of rag-2/jak3 double-deficient mice. *J Biomed Biotechnol.* 2011; 2011:539748.
 15. Phimsen S, Kuwahara K, Nakaya T, Ohta K, Suda T, Rezano A, Kitabatake M, Vaeteewoottacharn K, Okada S, Tone S, Sakaguchi N. Selective cell death of p53-insufficient cancer cells is induced by knockdown of the mRNA export molecule GANP. *Apoptosis.* 2012; 17:679-690.
 16. Okabe M, Ikawa M, Kominami K, Nakanishi T, Nishimune Y. 'Green mice' as a source of ubiquitous green cells. *FEBS Lett.* 1997; 407:313-319.
 17. Flanagan SP. 'Nude', a new hairless gene with pleiotropic effects in the mouse. *Genet Res.* 1966; 8:295-309.
 18. Hirasawa T, Yamashita H, Makino S. Genetic typing of the mouse and rat nude mutations by PCR and restriction enzyme analysis. *Exp Anim.* 1998; 47:63-67.
 19. Shinkai Y, Rathbun G, Lam KP, Oltz EM, Stewart V, Mendelsohn M, Charron J, Datta M, Young F, Stall AM, Alt FW. RAG-2-deficient mice lack mature lymphocytes owing to inability to initiate V(D)J rearrangement. *Cell.* 1992; 68:855-867.
 20. Park SY, Saijo K, Takahashi T, Osawa M, Arase H, Hirayama N, Miyake K, Nakauchi H, Shirasawa T, Saito T. Developmental defects of lymphoid cells in Jak3 kinase-deficient mice. *Immunity.* 1995; 3:771-782.
 21. Seubwai W, Wongkham C, Puapairoj A, Okada S, Wongkham S. 22-oxa-1,25-dihydroxyvitamin D3 efficiently inhibits tumor growth in inoculated mice and primary histoculture of cholangiocarcinoma. *Cancer.* 2010; 116:5535-5543.
 22. Maruo K, Shimamura K, Hioki K, Itoh M, Ueyama Y, Tamaoki N. Role of x-linked immunodeficiency (xid) and NK activity in rejection of human tumor xenotransplants in nude mice. *APMIS.* 1993; 101:345-352.
 23. Clarke R. Human breast cancer cell line xenografts as models of breast cancer. The immunobiologies of recipient mice and the characteristics of several tumorigenic cell lines. *Breast Cancer Res Treat.* 1996; 39:69-86.
 24. Shultz LD, Ishikawa F, Greiner DL. Humanized mice in translational biomedical research. *Nat Rev Immunol.* 2007; 7:118-130.
 25. Yang M, Li L, Jiang P, Moossa AR, Penman S, Hoffman RM. Dual-color fluorescence imaging distinguishes tumor cells from induced host angiogenic vessels and stromal cells. *Proc Natl Acad Sci U S A.* 2003; 100:14259-14262.

(Received April 9, 2014; Revised July 10, 2014; Re-revised August 1, 2014; Accepted August 2, 2014)

Pathological changes in primary cilia: A novel mechanism of graft cholangiopathy caused by prolonged cold preservation in a rat model of orthotopic liver transplantation

Hongwei Lu^{1,2}, Jiahong Dong^{2,*}, Yafei Zhang¹, Chonghui Li², Qiang Yu², Wei Tang³

¹ Department of General Surgery, Second Affiliated Hospital, Xi'an Jiaotong University, Xi'an, Shanxi, China;

² Department of Hepatobiliary Surgery, Chinese PLA General Hospital, Beijing, China;

³ Hepato-Biliary-Pancreatic Surgery Division, Artificial Organ and Transplantation Division, Department of Surgery, Graduate School of Medicine, The University of Tokyo, Tokyo, Japan.

Summary

To study the impairment of cholangiocyte primary cilia caused by prolonged cold preservation and its correlation with graft cholangiopathy after orthotopic liver transplantation (OLT). Subjects were 60 male Wistar rats that were divided into 2 groups: a control group ($n = 30$) receiving a donor liver preserved for 1 h and a study group ($n = 30$) receiving a donor liver preserved for 12 h. A two-cuff method was used to establish the OLT model, and the hepatic artery and bile ducts were reconstructed using stents. Samples were collected 2, 8, and 16 weeks after surgery, and 5 samples were collected from each group at each time point. Serum biochemical indicators were measured, morphological changes in intrahepatic bile ducts and cholangiocyte primary cilia were observed using an optical microscope and scanning electronic microscope, respectively, and the ciliary marker (α -tubulin) and membrane proteins (PC-1, TRPV4, and P2Y₁₂) were detected using immunofluorescence analysis and Western blotting. In the study group, phlogocytes infiltrated around bile ducts and bile ducts proliferated markedly at 8 weeks. At 16 weeks, the biliary structures were indistinct and some bile ducts disappeared, a large amount of collagen was deposited, numerous phlogocytes infiltrated around ducts, some biliary epithelial cells (BECs) were deformed or dead, and primary cilia disappeared. In the control group, the intrahepatic bile ducts and BECs were nearly intact and the primary cilia were present. In the study group, the expression of α -tubulin, polycystin-1 (PC-1), TRPV4, and P2Y₁₂ in bile ducts disappeared completely after 8 weeks. In the control group, expression of the marker and proteins decreased at 2 weeks and increased slightly after 8 weeks. These results suggest that the study group had dysfunctional primary cilia at the start of OLT and that this dysfunction was irreversible. In the control group, the primary cilia defects and subsequent biliary injury were temporary. Thus, prolonged cold preservation of a donor liver may cause graft cholangiopathy by altering the integrity and functions of cholangiocyte primary cilia.

Keywords: Liver transplantation, cold preservation, primary cilium, graft cholangiopathy

1. Introduction

Graft cholangiopathy (GC) produces non-anastomotic strictures and intrahepatic bile duct dilation in the biliary tree of a graft and may be associated with the

formation of biliary sludge or gallstones. Primary pathological manifestations of GC in the biliary tree are bile duct loss and cholestasis. Major risk factors for GC are ischemia/reperfusion injury, immune response, and cytotoxic injury (1,2).

Biliary epithelial cell (BEC) defects caused by cold preservation are the direct cause of biliary complications after liver transplantation (3). The pathophysiological modification of BECs lining the biliary tree is the pathologic basis of GC. Each intrahepatic BEC contains

*Address correspondence to:

Dr. Jiahong Dong, Department of Hepatobiliary Surgery, Chinese PLA General Hospital, Beijing 100853, China.
E-mail: dongjiahong2001@163.com

a primary cilium (4). The primary cilia that extend from the apical plasma membrane of BECs into the bile duct lumen are ideally positioned to detect changes in bile flow, composition, and osmolality, i.e., to be sensory organelles that may control cholangiocyte functions such as ductal bile formation (5-7). The primary cilia can sense a traumatic physical or chemical stimulus and they participate in the process of repairing injury (8). The primary cilia function as a result of membrane proteins such as polycystin-1 (PC-1), PC-2, TRPV4, P2Y₁₂, and fibrocystin (9,10).

An OLT model was created to verify whether or not prolonged cold preservation would cause GC by damaging the structures and functions of primary cilia.

2. Materials and Methods

2.1. Animal model

Male inbred Wistar rats (6-8 weeks old, 220-250 g, Vital River Laboratory Animal Technology Co. Ltd, Beijing, China) were used as donors or recipients, and care was provided according to the guidelines of the Institutional Animal Care and Use Committee. All animals were kept in a temperature-controlled environment with a 12-h light-dark cycle and were allowed free access to food and water 12 or 4 h before surgery.

Sixty rats were randomly divided into 2 groups. In the study group ($n = 30$), the donor livers were preserved for 12 h. In the control group ($n = 30$), the donor livers were preserved for 1 h. The donor liver was preserved with University of Wisconsin (UW) solution at 4°C after *in situ* perfusion. After hepatectomy of the recipient's liver, the donor liver was implanted in an orthotopic position. The anhepatic time in the recipient was kept to less than 15 min. After completion of the end-to-end anastomosis between the suprahepatic inferior vena cava of the recipient and the donor, the portal vein was reconstructed with the cuff technique, the liver was reperfused, circulation to the intrahepatic inferior vena cava was re-established with another cuff, and the hepatic artery and bile ducts were reconstructed using stents. All samples were collected 2, 8, and 16 weeks after surgery, and 5 samples were collected from each group at each time point.

2.2. Serum biochemical testing

Total bilirubin (TBIL), alkaline phosphatase (ALP), and gamma glutamyl transpeptidase (GGT) are considered to be markers of BEC injury after liver transplantation (11). Serum concentrations of TBIL, ALP, and GGT were measured with an automatic biochemistry analyzer (Glamour 6000, UV-VIS METROLAB S.A., Buenos Aires, Argentina).

2.3. Histopathological observation

Liver tissues were fixed in formaldehyde and embedded in paraffin and then cut into 3-5- μ m sections. After deparaffinization, the tissues were stained with hematoxylin and eosin (HE) for histopathologic evaluation using an optical microscope (Olympus BX41, Tokyo, Japan).

2.4. Scanning electron microscopy (SEM)

Samples for SEM were fixed in 2.5% glutaraldehyde for 24 h, dehydrated with a graded ethanol series, and critical-point dried in CO₂. The dried samples were mounted on aluminum and sputter-coated with gold and they were then examined under a scanning electron microscope (Hitachi S-4300, Tokyo, Japan).

2.5. Immunofluorescence analysis

Immunofluorescence microscopy was performed with a Zeiss LSM 510 confocal microscope with a 100- Pan-Apochromat 1.4-nm oil objective (Carl Zeiss, Inc., Thornwood, NY, USA). Liver samples were frozen at -20°C and cut into 8- μ m sections. Samples were then fixed in acetone for 10 min, washed 3 times in phosphate-buffered saline with 0.05% Triton-X, and incubated in 1% bovine serum albumin for 10 min at room temperature. After samples were washed 3 times in phosphate-buffered saline, they were incubated overnight at 4°C with antibodies against acetylated α -tubulin, PC-1, TRPV4, and P2Y₁₂ (1:50, Santa Cruz Biotechnology, Inc.). Afterwards, they were incubated for 1 hour with secondary antibodies (1:50) (Santa Cruz Biotechnology, Inc.). Nuclei were stained with 4-,6-diamidino-2-phenylindole.

2.6. Western blotting of α -tubulin, PC-1, TRPV4, and P2Y₁₂

Samples of the intrahepatic bile ducts were lysed in 1-mL lysis buffer. Equal amounts of sample were separated using SDS-PAGE. Gels were electroblotted with Sartoblot onto polyvinylidene difluoride membranes. The membranes were blocked in Carnation non-fat milk and probed with a 1:200 dilution of the α -tubulin, PC-1, TRPV4, P2Y₁₂ and β -actin antibodies (Santa Cruz Biotechnology, Inc.) and a 1:1,000 dilution of the second antibody (Rabbit anti-rabbit IgG, Santa Cruz Biotechnology, Inc.). Antigen/antibody complexes were visualized with a chemiluminescence system (Amersham Biosciences, Piscataway, NY, USA) and scanned into images. The relative densities of the bands were analyzed using NIH Image (version 1.61; National Institute of Health, Bethesda, MD, USA). The ratio of target protein to β -actin served as an index for statistical analysis.

2.7. Statistical analysis

Statistical analyses were performed using SPSS version 13.0 system for Windows (SPSS Inc. Chicago, IL, USA). Data are expressed as the mean and standard deviations (SD). Differences were analyzed using analysis of variance (ANOVA). Results were considered significant at $p < 0.05$.

3. Results

3.1. Prolonged cold preservation injured cholangiocytes

The control group exhibited inflammation and swelling in cholangiocytes with an increase in serum TBIL, ALP, and GGT at 2 weeks and a gradual return to normal after 8 weeks. In the study group, the cholangiocytes displayed sloughing and necrosis at 2 weeks, and this was accompanied by increasing levels of TBIL, ALP,

and GGT. These changes worsened over time (Figure 1, Table 1).

3.2. Prolonged cold preservation injured bile ducts

In the control group, the biliary structures in portal area and interlobular ducts were almost normal and bile duct proliferation and phlogocyte infiltration were marked at 2 weeks. These manifestations slowly disappeared prior to 16 weeks. In the study group, numerous phlogocytes infiltrated around bile ducts and bile ducts proliferated markedly at 2 weeks. These manifestations became more marked at 8 weeks. At 16 weeks, the biliary structure was indistinct; some bile ducts in the portal area disappeared and a large amount of collagen was deposited around ducts (Figure 2).

3.3. Prolonged cold preservation injured primary cilia

In the control group, some cholangiocytes lost their primary cilia while other cholangiocytes had shortened cilia. Expression of the ciliary marker (α -tubulin) and membrane proteins (PC-1, TRPV4, and P2Y₁₂) decreased at 2 weeks and increased slightly after 8 weeks. In the study group, the primary cilia were sparse and shorter. Moreover, the primary cilia disappeared

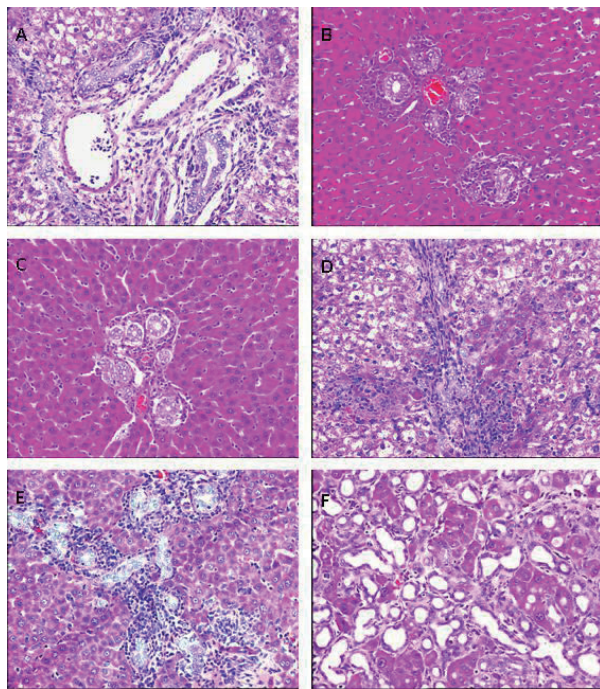


Figure 1. Cholangiocyte expression. Control group: There was marked bile duct edema, bile duct proliferation, and phlogocyte infiltration around ducts at 2 weeks (A). Bile duct edema resolved and phlogocyte infiltration decreased while bile duct proliferation remained the same at 8 (B) and 16 weeks (C). **Study group:** Cholangiocytes swelled and some died, many phlogocytes infiltrated around bile ducts, and bile ducts proliferated at 2 weeks (D). These manifestations became more apparent at 8 weeks (E). Numerous cholangiocytes died, the biliary structure was indistinct, and some bile ducts disappeared at 16 weeks (F).

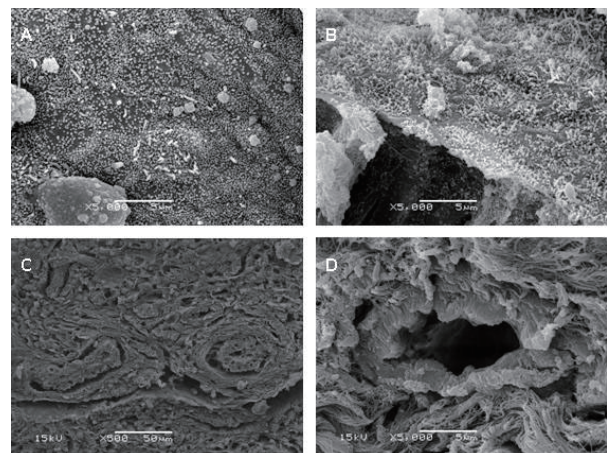


Figure 2. Bile duct expression (scanning electron microscopy). Control group: The primary cilia shortened ($\times 5,000$, A). **Study group:** Most cholangiocytes lost primary cilia. Cholangiocytes with primary cilia had sparse and shorter cilia at 2 weeks ($\times 5,000$, B). Bile ducts proliferated markedly at 8 weeks ($\times 2,000$, C). Cholangiocytes died and were sloughed off and collagen was deposited around ducts at 16 weeks ($\times 5,000$, D).

Table 1. Comparison of biochemical indicators in two groups (mean \pm s)

Items	Control group			Study group		
	2 weeks (n = 5)	8 weeks (n = 5)	16 weeks (n = 5)	2 weeks (n = 5)	8 weeks (n = 5)	16 weeks (n = 5)
TBIL ($\mu\text{mol/L}$)	14.28 \pm 7.9	3.96 \pm 1.13 ^c	2.37 \pm 0.86 ^c	17.75 \pm 8.34 ^{a,b}	24.53 \pm 7.95 ^{a,b}	41.62 \pm 14.95 ^{a,b}
ALP (U/L)	320.64 \pm 36.75	77.35 \pm 15.92 ^c	68.63 \pm 4.02 ^c	383.67 \pm 53.23 ^{a,b}	435.87 \pm 86.34 ^{a,b}	574.56 \pm 106.63 ^{a,b}
GGT (U/L)	34.72 \pm 9.36	5.90 \pm 2.58 ^c	6.73 \pm 1.60 ^c	46.75 \pm 4.93 ^{a,b}	61.45 \pm 10.52 ^{a,b}	78.22 \pm 12.05 ^{a,b}

^a $p < 0.05$, within the same group over time; ^b $p < 0.05$, vs. control group at the same time point; ^c $p < 0.05$, vs. 2 weeks for control group.

and the expression of α -tubulin, PC-1, TRPV4 and P2Y₁₂ was completely absent after 8 weeks (Figures 2, 3, and 4; Table 2).

4. Discussion

The vascular plexus around bile ducts is a unique blood supply for BECs, so they are susceptible to damage as a result of ischemia/reperfusion and immune injury (12,13). That said, BECs are powerful cells because they produce 40% of bile even though they only account for about 4% of all cells in the liver (14,15).

During liver transplantation, BECs inevitably suffer ischemia/reperfusion injury and exhibit immunological

rejection (16,17). Cold ischemia and reperfusion injury (CIRI) is crucial to estimating graft function after cadaveric donor liver transplantation. However, some marginal donor livers that have been preserved in the cold for a prolonged period must be used because of the scarcity of donors. Use of these livers is associated with a number of biliary problems, such as delayed biliary recovery, ischemic bile duct lesions, and biliary strictures after liver transplantation (18). During transplantation, the bile ducts are susceptible to warm ischemia before they are subsequently preserved, rewarmed, and reperfused (19). Cholangiocytes lining the bile duct wall are weakened by depletion of energy stores. Cholangiocytes are susceptible to CIRI because of the following factors: an increase in oxygen free radicals and depletion of glutathione in cellular stores, the toxic effects of hydrophobic bile salts, and the infiltration of inflammatory cells into the basement membrane and release of inflammatory mediators (20). Therefore, the number of cholangiocytes that detach from the underlining basement membrane and enter bile is related to the duration of cold ischemia (21). Sufficient cellular repair or regeneration to replace the lost cells damaged by CIRI is generally considered necessary for bile duct recovery after liver transplantation and the extent of the cholangiocyte regenerative response is considered to correlate with the degree of injury. The primary cilia may, as sensory organelles, participate in bile formation and bile duct recovery after CIRI.

In order to explore the effect of GC on primary cilia

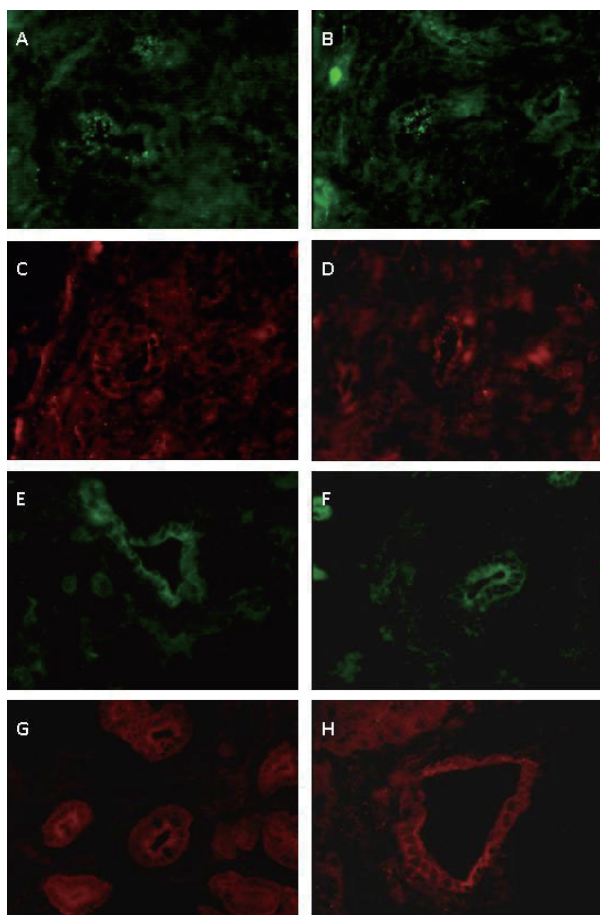


Figure 3. The expression of α -tubulin, PC-1, TRPV4, and P2Y₁₂. **Control group:** The expression of α -tubulin (A), PC-1 (B), TRPV4 (C), and P2Y₁₂ (D) decreased at 8 weeks. **Study group:** Expression of α -tubulin (E), PC-1 (F), TRPV4 (G), and P2Y₁₂ (H) was absent. Immunofluorescence $\times 200$.

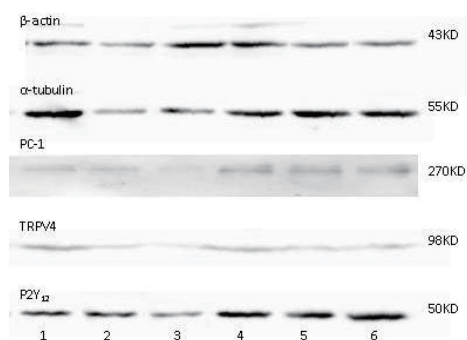


Figure 4. The expression of α -tubulin, PC-1, TRPV4, and P2Y₁₂ in intrahepatic bile ducts. **Study group:** 1 (2 weeks), 2 (8 weeks), 3 (16 weeks); **Control group:** 4 (2 weeks), 5 (8 weeks), 6 (16 weeks).

Table 2. Levels of expression of α -tubulin, PC-1, and TRPV4 in intrahepatic bile ducts (mean \pm s)

Items	Control group			Study group		
	2 weeks (n = 5)	8 weeks (n = 5)	16 weeks (n = 5)	2 weeks (n = 5)	8 weeks (n = 5)	16 weeks (n = 5)
α -tubulin/ β -actin	1.34 \pm 0.58	1.79 \pm 0.47	1.71 \pm 0.62	0.86 \pm 0.62 ^{ab}	1.14 \pm 0.43 ^{ab}	0.69 \pm 0.33 ^{ab}
PC-1/ β -actin	0.87 \pm 0.23	0.73 \pm 0.29	0.95 \pm 0.32	0.42 \pm 0.18 ^{ab}	0.23 \pm 0.11 ^{ab}	0.08 \pm 0.04 ^{ab}
TRPV4/ β -actin	0.48 \pm 0.18	0.53 \pm 0.22	0.64 \pm 0.26	0.33 \pm 0.11 ^{ab}	0.17 \pm 0.09 ^{ab}	0.13 \pm 0.06 ^{ab}
P2Y ₁₂ / β -actin	2.16 \pm 0.74	2.53 \pm 0.46	2.72 \pm 1.14	1.53 \pm 0.59 ^{ab}	0.76 \pm 0.48 ^{ab}	0.64 \pm 0.25 ^{ab}

^a $p < 0.05$, within the same group; ^b $p < 0.05$, vs. control group at the same time.

as a result of prolonged cold preservation, the current study created a rat model of OLT after preserving the donor liver in UW solution at 4°C for 1 or 12 h. This study then observed several indicators over time. The morphology of intrahepatic bile ducts and BECs was markedly altered in the study group in comparison to the control group, although bile duct proliferation did proceed for up to 8 weeks. Cholangiocyte sloughing and necrosis were marked at 16 weeks. These manifestations were accompanied by an increase in serum TBIL, ALP, and GGT. These findings indicated that prolonged cold preservation was responsible for injury to bile ducts and BECs, and this injury was in turn closely associated with GC. However, the question of whether or not powerful organelles like the primary cilia affect GC must be studied further.

In the liver, only BECs have cilia. Liver disease caused by defects in ciliary structures and ciliary dysfunction is known as cholangiociliopathy. Cholangiociliopathy includes cystic and/or fibrotic liver diseases such as autosomal dominant polycystic kidney disease (ADPKD, caused by mutations in either *PKD1* or *PKD2*, genes that encode PC-1 and PC-2, respectively), autosomal recessive PKD (ARPKD, caused by mutations in a single gene, *PKHD1*, that encodes fibrocystin), nephronophthisis (NPHP, caused by mutations in the six *NPH1-6* genes that encode nephrocystins 1-6), Bardet-Biedl syndrome (BBS, caused by mutations in the 12 *BBS* genes that encode BBS1-12), and Meckel-Gruber syndrome (MKS, caused by mutations in three *MKS1-3* genes that encode MKS1 and meckelin) (22,23). In addition, some forms of cholecystopathy such as primary sclerosing cholangitis (PSC) and primary biliary cirrhosis (PBC) may also be forms of cholangiociliopathy. Abnormalities in cilia are involved in the development of some tumors, such as astrocytomas and glioblastomas (24,25). Understanding the key mechanisms that regulate sensation/transduction by cholangiocyte cilia or the phenotypic manifestations of these actions (*i.e.*, the concentrations of intracellular Ca^{2+} and cAMP) should facilitate the development of targeted therapies to prevent or halt these diseases. Indeed, a study recently found that treating PCK rats (an animal model of ARPKD) with octreotide, the synthetic analog of somatostatin, decreased cAMP levels in cholangiocytes, it suppressed hepatic cyst growth, and it reduced hepatic fibrosis (26). Clinical trials are underway to assess this therapeutic approach in humans.

The current results indicated that cholangiocyte primary cilia in the study group were irreversibly damaged after surgery. These cilia were quite sparse at 2 weeks and nearly absent at 8 weeks. At 8 weeks, BECs had a normal morphology for the most part. BECs suffered irreversible injury at 16 weeks. In the study group, levels of α -tubulin, PC-1, TRPV4, and P2Y₁₂ expression in intrahepatic bile ducts decreased

markedly starting at 2 weeks. This finding indicates that the primary cilia were dysfunctional at the start of OLT and that this dysfunction was irreversible. In the control group, primary cilia defects and subsequent biliary injury were temporary, suggesting that ciliary abnormalities are part of the pathophysiology of GC.

Genes and proteins that play a role in the structure or function of primary cilia may represent new targets for treatment of biliary lesions or reconditioning. Levels of biochemical indicators and bile duct morphology in the study group indicated that prolonged cold preservation of a donor liver can cause GC. Moreover, the current results suggested that prolonged cold preservation resulted in reduced expression of α -tubulin, PC-1, TRPV4, and P2Y₁₂ in intrahepatic bile ducts, and this was in turn closely associated with GC. The current results suggest that prolonged cold preservation of a donor liver may cause GC by altering the integrity and functions of cholangiocyte primary cilia.

This study focused on determining whether injury to the primary cilia is the determining factor for GC as a result of prolonged cold preservation. Although logistically difficult, examining abnormalities in primary cilia as a result of GC would prove interesting. There may be association between those abnormalities and GC, and such an approach would facilitate the study of the mechanisms of the disease and therapies to treat it. Nevertheless, whether or not the morphologically and functionally abnormal primary cilia that were observed lead to GC has yet to be determined.

References

1. Chok KSH, Chan SC, Cheung TT, Sharr WW, Chan ACY, Lo CM, Fan ST. Bile duct anastomotic stricture after adult-to-adult right lobe living donor liver transplantation. *Liver Transpl.* 2011; 17:47-52.
2. Verdonk RC, Buis CI, van der Jagt EJ, Gouw ASH, Limburg AJ, Slooff MJH, Kleibeuker JH, Porte RJ, Haagsma EB. Nonanastomotic biliary strictures after liver transplantation, part 2: Management, outcome, and risk factors for disease progression. *Liver Transpl.* 2007; 13:725-732.
3. Vajdova K, Smrekova R, Kukan M, Lutterova M, Wsolova L. Bile analysis as a tool for assessing integrity of biliary epithelial cells after cold ischemia-reperfusion of rat livers. *Cryobiology.* 2000; 41:145-152.
4. Buis CI, Hoekstra H, Verdonk RC, Porte RJ. Causes and consequences of ischemic-type biliary lesions after liver transplantation. *J Hepatobiliary Pancreat Surg.* 2006; 13:517-524.
5. Wojcicki M, Milkiewicz P, Silva M. Biliary tract complications after liver transplantation: A review. *Dig Surg.* 2008; 25:245-257.
6. Praetorius HA, Spring KR. Bending the MDCK cell primary cilium increases intracellular calcium. *J Membr Biol.* 2001; 184:71-79.
7. Liedtke W. Transient receptor potential vanilloid channels functioning in transduction of osmotic stimuli. *J Endocrinol.* 2006; 191:515-523.

8. Masyuk AI, Gradilone SA, Banales JM, Huang BQ, Masyuk TV, Lee SO, Splinter PL, Stroope AJ, Larusso NF. Cholangiocyte primary cilia function as chemosensory organelles that detect biliary nucleotides via P2Y₁₂ purinergic receptors. *Am J Physiol Gastrointest Liver Physiol.* 2008; 295:725-734.
9. Juric-Sekhar G, Adkins J, Doherty D, Hevner RF. Joubert syndrome: Brain and spinal cord malformations in genotyped cases and implications for neurodevelopmental functions of primary cilia. *Acta Neuropathologica.* 2012; 123:695-709.
10. Qian Q. Non-random distribution and sensory functions of primary cilia in vascular, smooth muscle cells. *J Invest Med.* 2008; 56:615-615.
11. Kukan M, Haddad PS. Role of hepatocytes and bile duct cells in preservation-reperfusion injury of liver grafts. *Liver Transpl.* 2001; 7:381-400.
12. Li S, Stratta RJ, Langnas AN, Wood RP, Marujo W, Shaw BW Jr. Diffuse biliary tract injury after orthotopic liver transplantation. *Am J Surg.* 1992; 164:536-540.
13. Strazzabosco M, Fabris L. Functional anatomy of normal bile ducts. *Anat Rec.* 2008; 291:653-660.
14. Esteler E. Physiology of bile secretion. *World J Gastroenterol.* 2008; 14:5641-5649.
15. Glaser S, Francis H, Demorrow S, Lesage G, Fava G, Marzioni M, Venter J, Alpini G. Heterogeneity of the intrahepatic biliary epithelium. *World J Gastroenterol.* 2006; 12:3523-3536.
16. de Rougemont O, Dutkowski P, Clavien PA. Biological modulation of liver ischemia-reperfusion injury. *Curr Opin Organ Transplant.* 2010; 15:183-189.
17. Rosen HR. Transplantation immunology: what the clinician needs to know for immunotherapy. *Gastroenterology.* 2008; 134:1789-1801.
18. Buis CI, Verdonk RC, Van der Jagt EJ, van der Hilst CS, Slooff MJ, Haagsma EB, Porte RJ. Nonanastomotic biliary strictures after liver transplantation, part 1: Radiological features and risk factors for early vs. late presentation. *Liver Transpl.* 2007; 13:708-718.
19. Kukan M, Haddad PS. Role of hepatocytes and bile duct cells in preservation-reperfusion injury of liver grafts. *Liver Transpl.* 2001; 7:381-400.
20. Schmidt A, Tomasdottir H, Bengtsson A. Influence of cold ischemia time on complement activation, neopterin, and cytokine release in liver transplantation. *Transplant Proc.* 2004; 36:2796-2798.
21. Chimalakonda AP, Mehvar R. Effects of methylprednisolone and its liver-targeted dextran prodrug on ischemia reperfusion injury in a rat liver transplantation model. *Pharm Res.* 2007; 24:2231-2238.
22. Fliegauf M, Benzing T, Omran H. When cilia go bad: Cilia defects and ciliopathies. *Nat Rev Mol Cell Biol.* 2007; 8:880-893.
23. Adams M, Smith UM, Logan CV, Johnson CA. Recent advances in the molecular pathology, cell biology and genetics of ciliopathies. *J Med Genet.* 2008; 45:257-267.
24. Moser JJ, Fritzier MJ, Rattner JB. Primary ciliogenesis defects are associated with human astrocytoma/glioblastoma cells. *BMC Cancer.* 2009; 17:448-460.
25. Han YG, Alvarez-Buylla A. Role of primary cilia in brain development and cancer. *Curr Opin Neurobiol.* 2010; 20:737-747.
26. Masyuk TV, Masyuk AI, Torres VE, Harris PC, Larusso NF. Octreotide inhibits hepatic cystogenesis in a rodent model of polycystic liver disease by reducing cholangiocyte adenosine 3',5'-cyclic monophosphate. *Gastroenterology.* 2007; 132:1104-1116.

(Received May 23, 2014; Revised June 3, 2014; Re-revised August 9, 2014; Accepted August 12, 2014)

Migration of breast cancer cells into reconstituted type I collagen gels assessed *via* a combination of frozen sectioning and azan staining

Kyohei Fukuda, Yo Kamoshida, Taisuke Kurokawa, Mito Yoshida, Yoko Fujita-Yamaguchi*, Munehiro Nakata**

Department of Applied Biochemistry, Tokai University, Hiratsuka, Kanagawa, Japan.

Summary This study sought to devise a way to assess the infiltration of cancer cells in model stromal tissues. Human breast carcinoma MDA-MB-231 cells were loaded on the surface of a type I collagen gel in the well of 8-well chamber slide and allowed to migrate into the gel. The gel was then subjected to frozen sectioning and staining. Azan staining facilitated satisfactory microscopic observation of cancer cells migrating into the collagen gel. Cell migration was promoted by the presence of fetal calf serum in the gel. In contrast, the proportion of cells remaining on the gel surface increased in the presence of galardin, a matrix metalloproteinase inhibitor. Moreover, the distance of cell migration from the gel surface was significantly shorter depending on the concentration of galardin. Observation of cancer cell migration into reconstituted type I collagen gel with a combination of frozen sectioning and azan staining is a useful way to assess the ability of individual cancer cells to migrate and to evaluate how effectively pharmaceuticals inhibit the first step of invasion.

Keywords: Cancer cell invasion, type I collagen, frozen section, azan stain, galardin

1. Introduction

Cancer cells that develop in epithelial tissues destroy the basement membrane and invade stromal tissues (1,2). During invasion, some matrix metalloproteinases (MMPs) are involved in the degradation of extracellular matrix components such as type IV collagen in the basement membrane and type I collagen in stromal tissues (3,4). Since cancer cell invasion is an initial stage of metastasis, the ability to observe and control that invasion would benefit cancer research.

A Boyden chamber assay is typically used to assess cancer cell invasion by comparing the number of cells on a gel surface to the number that reach the bottom of the gel (5-7). This method is convenient but it does not allow the detailed observation of the invasive characteristics of individual cancer cells. A previous study used time-lapse

microscopy to dynamically observe the disappearance of cancer cells from the surface of reconstituted type I collagen gel into the gel (8). Results suggested that the migratory behavior of cancer cells varies depending on their malignancy and that their behavior is unique even when they are members of the same cell population. This previously described method is suited to counting cells disappearing from the gel surface and the Boyden chamber assay is suited to counting cells that reach the bottom of the gel, but neither is suited to observing cells that migrate into the gel.

The present study used type I collagen gel as a model of stromal tissue and it prepared frozen sections of that gel in order to microscopically observe cancer cells both on the gel surface and in the gel. Staining to visualize cells in collagen gels and the effects of several pharmaceuticals on cell migration were also investigated.

2. Materials and Methods

2.1. Cells

The human breast carcinoma cell line MDA-MB-231 was obtained from the American Type Culture

*Current address: Beckman Research Institute of City of Hope, Duarte, CA 91010, USA.

**Address correspondence to:

Dr. Munehiro Nakata, Department of Applied Biochemistry, Tokai University, Hiratsuka, Kanagawa 259-1292, Japan.

E-mail: nak@keyaki.cc.u-tokai.ac.jp

Collection (ATCC; Rockville, MD, USA). The cells were maintained in high-glucose Dulbecco's modified Eagle's medium (DMEM; Invitrogen, Carlsbad, CA, USA) containing 10% fetal calf serum (FCS) supplemented with penicillin-streptomycin and 2 mM glutamine. Cells were cultured at 37°C in a 5% CO₂ atmosphere. The cells were harvested after pre-incubation in serum-free medium for 24 h at 37°C and resuspended in the same medium before use.

2.2. Reconstitution of collagen gel

Reconstituted type I collagen gel was prepared as described before with some modifications (8). Briefly, a solution of bovine skin type I collagen (Koken, Tokyo, Japan) was diluted to 1 mg/mL in 0.05 M acetic acid and mixed with 10× DMEM and a reconstitution buffer (1 M HEPES buffer, pH 7.4, containing 10 M NaHCO₃) at a ratio of 8:1:1 (v/v, type I collagen solution/DMEM/reconstitution buffer). Two hundred μL of the solution was added to each well of an 8-well chamber slide (Nalge Nunc, Naperville, IL, USA) and the mixture was then incubated at 37°C for 18-20 h to form mature single-layer gels.

Bilayer type I collagen gels were prepared as follows. A lower gel was first prepared by mixing 100 μL of 0.1% collagen solution with or without 10% FCS, DMEM, and reconstitution buffer (8:1:1, v/v) in an 8-well chamber slide. Two hundred μL of type I collagen gel without FCS (upper gel) formed on the solidified gel containing 8% FCS, as described earlier.

2.3. Incubation of cells on reconstituted type I collagen gel and frozen sectioning

Two hundred and fifty μL of a cell suspension (4×10^5 cells/mL) was loaded onto the reconstituted type I collagen gel in a chamber slide and incubated for 3 h at 37°C in a 5% CO₂ atmosphere. After incubation, the gel surface was rinsed twice with 250 μL of phosphate-buffered saline (PBS) and then DMEM containing 0.1% BSA to remove unbound cells. The gel was subsequently incubated for 18 h at 37°C in a 5% CO₂ atmosphere to allow the cells to migrate into the gel.

To investigate the effects of pharmaceuticals such as the matrix metalloproteinase inhibitor galardin (Cosmo Bio Co., Ltd., Tokyo, Japan), type I collagen gels were prepared in the presence of pharmaceuticals of interest. Cells were pre-incubated with the same concentration of the pharmaceuticals for 30 min at 37°C and then allowed to migrate into the gels.

After removing the medium on the gel surface, the gel was then mounted with an embedding compound (Tissue-Tek O.C.T. Compound; Sakura Finetechnical, Tokyo, Japan) and frozen at -80°C. The frozen gel was sliced perpendicular to the gel surface with a cryostat in sections with a thickness of 20 μm and the sections were placed on glass slides.

2.4. Azan staining of frozen collagen gel sections

Frozen sections of reconstituted type I collagen gel into which cells had migrated were stained using conventional hematoxylin-eosin staining or azan staining that can stain cells and collagen fiber different colors (9,10). For azan staining, the sections were fixed with 20% (v/v) formalin solution for 2 min, soaked in xylene, and then successively immersed in 80% ethanol and 100% ethanol for 3 min each. For metachroming, the sections were immersed in 10% (w/v) potassium dichromate solution containing 10% (w/v) trichloroacetic acid for 10 min and then stained with 0.1% (w/v) azocarmine G (Alfa Aesar, Ward Hill, MA, USA) for 3 h with occasional observation under an optical microscope. After staining with azocarmine G, the sections were soaked in 0.1% (v/v) aniline in 95% (v/v) ethanol for a few seconds and then in 0.1% (v/v) acetic acid in 95% (v/v) ethanol for 1 min. After the sections were rinsed with water, they were immersed in 5% (w/v) phosphotungstic acid solution for 1 h and then stained with aniline blue-orange G solution (Wako Pure Chemical Industries, Osaka, Japan) for 1 h with occasional observation under an optical microscope. The stained sections were mounted and then observed under a microscope (×200 or ×400; BX-51, Olympus, Tokyo, Japan).

2.5. Data processing

The distance each cell migrated from the gel surface was measured using at least 5 photographs of microscopic visual fields (× 200) or at least 150 cells. A Mann-Whitney *U* test was performed with StatMate III software (ATMS, Tokyo, Japan) and a *p* value less than 0.05 was considered significant.

3. Results

3.1. Enhanced visualization of cells in reconstituted type I collagen gel via azan staining

While conventional histochemical staining using hematoxylin-eosin is not suited to identifying the gel surface (Figure 1A), azan staining is often used to distinguish collagen fibers in connective tissues (9,10). Azan staining was thus examined to microscopically observe the cancer cell distribution in frozen sections of reconstituted type I collagen gels. As shown in Figure 1B, azan staining of frozen sections stained cancer cells red and it stained type I collagen fibers blue. This facilitated the microscopic observation of the cancer cell distribution in reconstituted type I collagen gels.

3.2. Promotion of cell migration by FCS

Cell migration into reconstituted collagen gels was promoted by using FCS as a chemoattractant. The

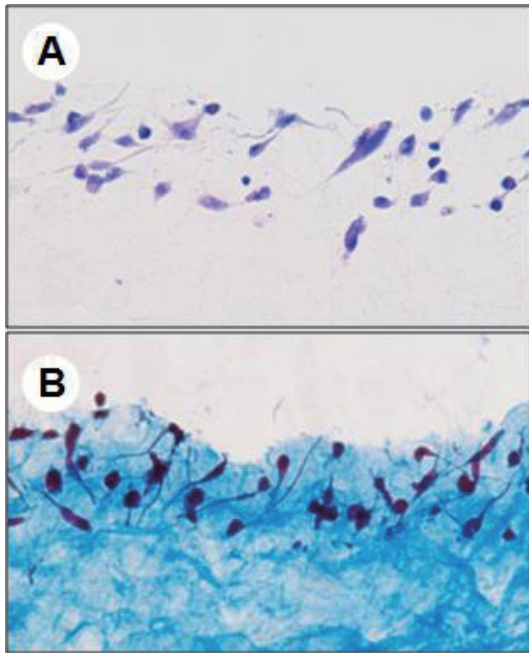


Figure 1. Comparison of microscopic views of gels stained with hematoxylin-eosin and azan staining. MDA-MB-231 cells were allowed to migrate into a type I collagen gel and frozen sections of the gel were stained with hematoxylin-eosin (A) and azan (B) as described in the Materials and Methods. Original magnification: $\times 200$.

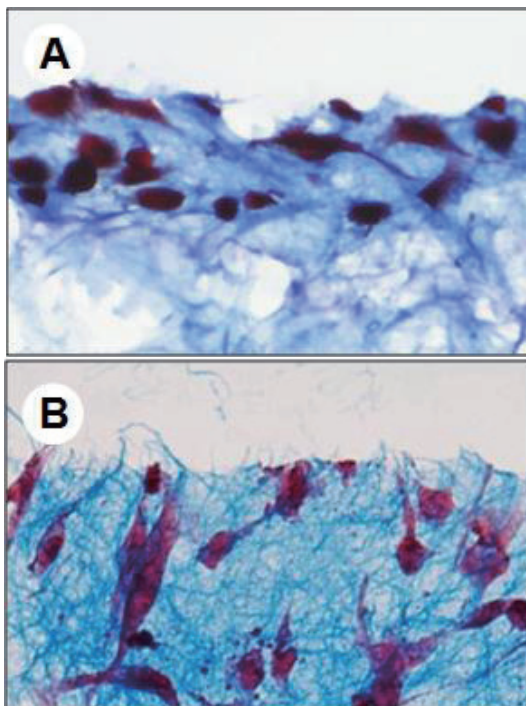


Figure 2. Typical microscopic views of gels where cells were allowed to migrate into the gels in the absence or presence of FCS. MDA-MB-231 cells were allowed to migrate into bilayer type I collagen gels without FCS (A) or with 8% FCS in the lower gel (B). The frozen sections were stained with azan and observed under a microscope. Original magnification: $\times 400$.

following 2 types of gels were examined: *i*) bilayer gels without FCS and *ii*) bilayer gels with 8% FCS in the lower gel. As shown in Figure 2, the cell morphology

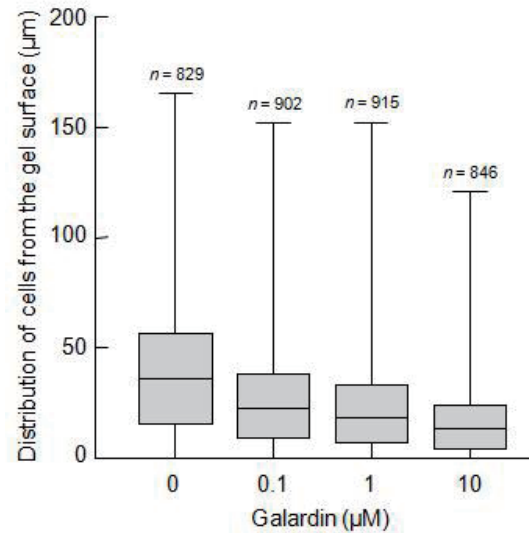


Figure 3. Distribution of cells migrating into type I collagen gels containing various concentrations of galardin. MDA-MB-231 cells were allowed to migrate into bilayer type I collagen gels containing the concentrations of galardin as indicated in the figure and 8% FCS in upper and lower gels, respectively. The frozen sections were stained with azan and then the cell distribution was observed microscopically. For data processing, the distance from the gel surface was taken into account only for cells distributed in the gel but not for cells remaining on the gel surface.

changed dramatically and cell migration was promoted in the latter gel system using FCS. In the absence of FCS, 24.1% of cells remained on the gel surface and cells that migrated into the gel were distributed at a median distance of 17.5 μm (8.9, 21.1; $n = 216$) from the gel surface (data not shown). In contrast, the number of cells remaining on the gel surface decreased (11.9%) in the presence of FCS and the distance of migration from the gel surface increased to a median distance of 26.4 μm (15.8, 40.7; $n = 193$) (data not shown).

3.3. Cell migration in the presence of galardin

During invasion, cancer cells produce MMPs to digest extracellular collagens (4). Galardin is a synthetic MMP inhibitor with a broad spectrum of activity against various MMP species (11,12). Figure 3 shows the distribution of the distance that cells migrated from the gel surface in the presence of lower gel containing 8% FCS for untreated cells and cells treated with various concentrations of galardin. The proportion of cells remaining on the gel surface was $2.9 \pm 0.9\%$ in the absence of galardin. This proportion increased to $6.8 \pm 0.6\%$ in the presence of 0.1 μM of galardin, to $7.7 \pm 1.3\%$ in the presence of 1 μM of galardin, and to $12.4 \pm 2.0\%$ in the presence of 10 μM of galardin (data not shown). Some cells migrated a relatively long distance in the presence of galardin but the median distance that cells migrated from the gel surface was significantly shorter than in the absence of galardin: $63.0 \pm 2.1\%$ in 0.1 μM of galardin, $57.1 \pm 3.7\%$ in 1 μM of galardin, and $45.7 \pm 1.2\%$ in 10 μM of galardin ($p < 0.001$).

4. Discussion

The present study devised a novel approach to assess the invasive ability of cancer cells. Cells of the human breast carcinoma cell line MDA-MB-231 served as model cancer cells and reconstituted type I collagen gel served as a model of stromal tissue. Cancer cells migrating into the gel were satisfactorily observed using a combination of FCS to promote cell migration on the bilayer gel (Figure 2B) and azan staining of frozen sections of the gel (Figure 1B). This approach allows the observation of cells on the gel surface and cells migrating into the gel. Invasive ability can be assessed based on the proportion of cells migrating into the gel and the distance cells have migrated from the gel surface. The distance of migration can also be used to assess the invasive ability of an individual cell. Additionally, this approach is suited to observing the promotion of cell migration by chemoattractants (Figure 2) and to assessing the inhibition of cell migration by pharmaceuticals such as galardin. Galardin is a known as MMP inhibitor (11-13) and is reported to prevent invasion and metastasis (14,15) (Figure 3).

Recently, various quantitative methods of assessing cell migration and invasion have been reported (8,14-19). Some of these methods facilitate the fluorescence-assisted quantification or real-time observation of migrating cells. The present method involves observation of frozen sections, and this approach would facilitate immunocytochemistry to detect molecular species expressed on the cell surface or released around cells.

Cancer cells invading stromal tissues have routes of migration that involves various matrix-degrading metalloproteinases, such as MMPs, and cell adhesion molecules, such as integrins (2,4,20-22). Since most of the previous studies of the migratory ability of cancer cells have mainly dealt with cell populations but not individual cells, a detailed molecular basis for individual characteristics of migratory ability needed to be elucidated. A previous study involving the real-time observation of cancer cell invasion noted that individual cells invaded at different times (8). The present study found that some cells remained on the gel surface while others migrated into the gel a considerable distance from the gel surface (Figure 3), suggesting that migratory ability exhibits individual characteristics. The present approach could be used to examine the individual characteristics of that ability in combination with immunocytochemistry.

Carcinoma cell migration and invasion play a role in the initial phase of metastasis, in which cells migrate from a tumor to invade normal stromal tissues and then the circulatory system. Therefore, cells may migrate a long distance in stromal tissues. The present study using a model of stromal tissues suggested that some cells migrated a relatively long distance (Figure

3). In addition, the MMP inhibitor galardin was not very effective at inhibiting the long distance that cells migrated at the concentrations used in this study. Pharmaceuticals that can inhibit this cell migration step would help to prevent metastasis.

In conclusion, the present study devised an approach to observe cancer cell migration into reconstituted type I collagen gel *via* a combination of frozen sectioning and azan staining. This approach is a useful way to assess the ability of individual cancer cells to migrate and to evaluate how effective certain pharmaceuticals are at inhibiting the first step of invasion process.

Acknowledgements

The authors wish to thank Dr. Keiko Sakai for her valuable input. The authors received a grant-in-aid for research and education from the Tokai University School of Engineering and technical support from the Department of Cell Biology and Histology, Education and Research Support Center, Tokai University School of Medicine.

References

1. Hagedorn EJ, Sherwood DR. Cell invasion through basement membrane: the anchor cell breaches the barrier. *Curr Opin Cell Biol.* 2011; 23:589-596.
2. Valastyan S, Weinberg RA. Tumor metastasis: molecular insights and evolving paradigms. *Cell.* 2011; 147:275-292.
3. Liotta LA, Thorgeirsson UP, Garbisa S. Role of collagenases in tumor cell invasion. *Cancer Metastasis Rev.* 1982; 1:277-288.
4. Ennis BW, Matrisian LM. Matrix degrading metalloproteinases. *J Neurooncol.* 1994; 18:105-109.
5. Boyden SV. The chemotaxis effect of mixtures of antibody and antigen on polymorphonuclear leukocytes. *J Exp Med.* 1962; 115:453-466.
6. Simon N, Noël A, Foidart JM. Evaluation of *in vitro* reconstituted basement membrane assay to assess the invasiveness of tumor cells. *Invasion Metastasis.* 1992; 12:156-167.
7. Albin A, Benelli R, Noonan DM, Brigati C. The "chemoinvasion assay": A tool to study tumor and endothelial cell invasion of basement membranes. *Int J Dev Biol.* 2004; 48:563-571.
8. Sakai K, Kurokawa T, Furui Y, Kuronuma Y, Sekiguchi M, Ando J, Inagaki Y, Tang W, Nakata M, Fujita-Yamaguchi Y. Invasion of carcinoma cells into reconstituted type I collagen gels: Visual real-time analysis by time-lapse microscopy. *BioSci Trends.* 2011; 5:10-16.
9. Fujii T, Hirabayashi Y. Histochemical studies of glycosaminoglycans in developing periodontal ligaments of ICR mice. *Anat Rec.* 1999; 254:465-473.
10. van Griensven M, Zeichen J, Tschernig T, Seekamp A, Pape HC. A modified method to culture human osteoblasts from bone tissue specimens using fibrin glue. *Exp Toxicol Pathol.* 2002; 54:25-29.
11. Grobelny D, Poncz L, Galardy RE. Inhibition of

- human skin fibroblast collagenase, thermolysin, and *Pseudomonas aeruginosa* elastase by peptide hydroxamic acids. *Biochemistry*. 1992; 31:7152-7154
12. Augé F, Hornebeck W, Laronze JY. A novel strategy for designing specific gelatinase A inhibitors: potential use to control tumor progression. *Crit Rev Oncol Hematol*. 2004; 49:277-282.
 13. Zhang J, Li X, Zhu H, Wang Q, Feng J, Mou J, Li Y, Fang H, Xu W. Design, synthesis, and primary activity evaluation of pyrrolidine derivatives as matrix metalloproteinase inhibitors. *Drug Discov Ther*. 2010; 4:5-12.
 14. Almholt K, Juncker-Jensen A, Laerum OD, Danø K, Johnsen M, Lund LR, Rømer J. Metastasis is strongly reduced by the matrix metalloproteinase inhibitor galardin in the MMTV-PyMT transgenic breast cancer model. *Mol Cancer Ther*. 2008; 7:2758-2767.
 15. Blacher S, Jost M, Melen-Lamalle L, Lund LR, Romer J, Foidart JM, Noël A. Quantification of *in vivo* tumor invasion and vascularization by computerized image analysis. *Microvasc Res*. 2008; 75:169-178.
 16. Duong HS, Le AD, Zhang Q, Messadi DV. A novel 3-dimensional culture system as an *in vitro* model for studying oral cancer cell invasion. *Int J Exp Pathol*. 2005; 86:365-374.
 17. Weaver AM. Invadopodia: specialized cell structures for cancer invasion. *Clin Exp Metastasis*. 2006; 23:97-105.
 18. Liu T, Li C, Li H, Zeng S, Qin J, Lin B. A microfluidic device for characterizing the invasion of cancer cells in 3-D matrix. *Electrophoresis*. 2009; 30:4285-4291.
 19. Selvendiran K, Ahmed S, Dayton A, Ravi Y, Kuppasamy ML, Bratasz A, Rivera BK, Kálai T, Hideg K, Kuppasamy P. HO-3867, a synthetic compound, inhibits the migration and invasion of ovarian carcinoma cells through downregulation of fatty acid synthase and focal adhesion kinase. *Mol Cancer Res*. 2010; 8:1188-1197.
 20. Nicolson GL. Tumor and host molecules important in the organ preference of metastasis. *Semin Cancer Biol*. 1991; 2:143-154.
 21. Jacquemet G, Humphries MJ, Caswell PT. Role of adhesion receptor trafficking in 3D cell migration. *Curr Opin Cell Biol*. 2013; 25:627-632.
 22. Canel M, Serrels A, Frame MC, Brunton VG. E-cadherin-integrin crosstalk in cancer invasion and metastasis. *J Cell Sci*. 2013; 126:393-401.

(Received August 20, 2014; Accepted August 25, 2014)

Ferulic acid combined with astragaloside IV protects against vascular endothelial dysfunction in diabetic rats

Yonghui Yin¹, Fanghua Qi², Zhenhua Song³, Bo Zhang⁴, Jialin Teng^{3,*}

¹ Department of Endocrinology, the First Affiliated Hospital of Shandong University of Traditional Chinese Medicine, Ji'nan, Shandong, China;

² Department of Traditional Chinese Medicine, Shandong Provincial Hospital affiliated to Shandong University, Ji'nan, Shandong, China;

³ Shandong University of Traditional Chinese Medicine, Ji'nan, Shandong, China;

⁴ Department of Traditional Chinese Medicine and Traumatology, the Affiliated Hospital of Shandong Academy of Medical Sciences, Ji'nan, Shandong, China.

Summary

Dysfunction of the endothelium is regarded as an important factor in the pathogenesis of vascular disease in diabetes mellitus (DM). Unfortunately, prevention of the progression of vascular complications of DM remains pessimistic. Ferulic acid and astragaloside IV, isolated from traditional Chinese medicine *Angelica sinensis* and *Radix astragali* respectively, exhibit potential cardio-protective and anti-hyperglycemic properties. In the present study, we investigated the protective effects and underlying mechanism of ferulic acid and astragaloside IV against vascular endothelial dysfunction in diabetic rats. After the diabetic rat model was established using streptozotocin, sixty rats were divided into 6 groups (control, model, ferulic acid, astragaloside IV, ferulic acid + astragaloside IV, and metformin) and treated for 10 weeks. Blood samples were collected to measure levels of hemoglobin A1c (HbA1c), triglyceride (TG), total cholesterol (TC), low density lipoprotein cholesterol (LDL-C), low density lipoproteins (Ox-LDL), alanine aminotransferase (ALT), aspartate aminotransferase (AST) and creatinine (Cr), nitric oxide (NO) and endothelial nitric oxide synthase (eNOS), and abdominal aorta tissue samples were collected for observing histological morphology changes of endothelium and detecting gene and protein expression of nuclear factor- κ B (NF- κ B) P65, monocyte chemoattractant protein-1 (MCP-1), and tumor necrosis factor α (TNF- α). We found that ferulic acid combined with astragaloside IV was capable of improving the structure of the aortic endothelium wall, attenuating the increase of HbA1c, TG, TC, LDL-C and Ox-LDL, promoting the release of NO and eNOS, and inhibiting over-activation of MCP-1, TNF- α , and NF- κ B P65, without damage to liver and kidney function. In conclusion, ferulic acid combined with astragaloside IV exhibited significant protective effects against vascular endothelial dysfunction in diabetic rats through the NF- κ B pathway involving decrease of Ox-LDL, increase of NO and eNOS, and activation of NF- κ B P65, MCP-1 and TNF- α .

Keywords: Ferulic acid, astragaloside IV, vascular endothelial dysfunction, diabetes mellitus

1. Introduction

Diabetes mellitus (DM) is a serious and complex chronic disease, which is dramatically increasing throughout the

world. It has reached epidemic proportions worldwide and is associated with a large economic burden. According to a recent report, the number of diabetics is estimated to reach 439 million by 2030 worldwide (1). Diabetics show several complications, especially vascular complications (e.g., coronary insufficiency, cerebrovascular, and peripheral vascular disease), which are the main etiology for a great percentage of morbidity and mortality (2). Patients with DM exhibit complex

*Address correspondence to:

Dr. Jialin Teng, Shandong University of Traditional Chinese Medicine, Ji'nan, Shandong, China.

E-mail: sd.jia@163.com

vascular changes, such as an accelerated atherosclerosis process and hypercoagulability (3). Atherosclerosis is a major factor that accelerates diabetic vascular complications and vascular endothelial dysfunction is considered to be the earliest detectable abnormality in the process of atherosclerosis (4). Thus, improving vascular endothelial dysfunction plays an important role in DM treatment.

It is well-known that hyperglycemia-induced oxidative stress and inflammation play an important role in development of vascular endothelial dysfunction (5). Hyperglycemia stimulates the body to produce a large number of oxygen free radicals and then induces oxidative stress which damages vascular endothelial cells and causes DM vascular complications (6). Low density lipoproteins (Ox-LDL), an important product of oxidative stress, after binding with a specific receptor (Lectin-like OX-LDL receptor-1, LOX-1) on the surface of vascular endothelial cells, activates nuclear factor- κ B (NF- κ B), and mediates expression of some cytokines or inflammatory molecules including tumor necrosis factor α (TNF- α), intercellular adhesion molecule-1 (ICAM-1), vascular cell adhesion molecule-1 (VCAM-1), as well as monocyte chemoattractant protein-1 (MCP-1) (7,8). These cytokines facilitate the adhesion of neutrophils and monocytes to endothelium affecting production of endothelium-derived nitric oxide (NO), impairing endothelial dependent vasodilation function, inducing inflammatory damage of vascular walls, and initiating atherosclerosis (9).

Although drugs and changing life styles have been widely promoted to control the complications of DM, unfortunately, the prevention of the progression of vascular complications in diabetic patients remains pessimistic (3). Therefore, an effective approach to prevent or delay the development and progression of diabetic vascular complications is urgently needed. In recent years, application of traditional Chinese medicines (TCMs) for DM and its related complications has received increasing attention due to their wide availability, low side effects, and proven therapeutic mechanisms and benefits. Many TCMs and their active components have been reported to have anti-hyperglycemic effects, for example *Angelica sinensis*, *Radix astragali*, *Radix rehmanniae*, *Panax ginseng* (10,11).

Angelica sinensis, which is called Dang-Gui in Chinese, has been mostly used to treat gynecological conditions and anemia for more than two thousand years in East Asia (12). In recent studies, *Angelica sinensis* and its active components have been shown to have multiple properties including cardio-protective, immune-modulatory, anti-oxidative, anti-inflammatory and so on (13). Ferulic acid (Figure 1A), as one of the major active components of *Angelica sinensis*, can effectively improve endothelial function in patients with coronary heart disease (14). *Radix astragali*, which is

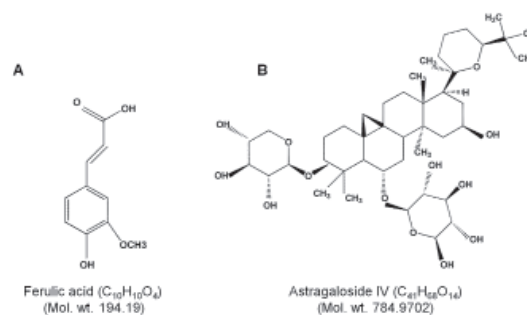


Figure 1. The structure of ferulic acid (A) and astragaloside IV (B).

known as Huang-Qi in Chinese, is traditionally used for treatment of diabetes, cardiovascular diseases, and wound healing, exerting anti-hyperglycemic, anti-oxidant, anti-inflammatory and immune-modulatory effects (15,16). Recently, some active components isolated from *Radix astragali* including astragaloside IV (Figure 1B) have been demonstrated to have effects of alleviating glucose intolerance, insulin resistance, and hypertriglyceridemia in DM (16,17). *Angelica sinensis* combined with *Radix astragali* composes Dang-Gui-Bu-Xue-Tang which is a classical prescription in traditional Chinese medicine for treating inflammation and ischemic diseases (18). Moreover, Dang-Gui-Bu-Xue-Tang is proposed as a potentially useful adjuvant therapy for patients with insulin resistance and/or patients who wish to increase insulin sensitivity (19). In a word, *Angelica sinensis* and *Radix astragali* either used alone or in combination possess effective cardio-protective and anti-hyperglycemic activities. We speculate that ferulic acid combined with astragaloside IV should exhibit effects against vascular complications of DM.

Thus, in the present study, we investigated the protective effects of ferulic acid and astragaloside IV against vascular endothelial dysfunction in diabetic rats. Furthermore, the underlying mechanisms for ferulic acid- and astragaloside IV-induced protective effects were investigated.

2. Materials and Methods

2.1. Chemicals

Ferulic acid and astragaloside IV were purchased from Chengdu Kang Bang Biological Technology Co., Ltd., Chengdu, China. Metformin was purchased from Shanghai Squibb pharmaceutical Co., Ltd., Shanghai, China. They were diluted in 55°C normal saline immediately before each experiment.

2.2. Reagents

High-fat and high-sugar diets were purchased from Shanghai Slac Laboratory Animal Co., Ltd., Shanghai, China. Streptozotocin was purchased from Sigma, St.

Louis, MO, USA. Hemoglobin A1c (HbA1c) detection kit, NO kit and endothelial nitric oxide synthase (eNOS) kits were purchased from Nanjing Jiancheng Bioengineering Institute, Nanjing, China. The anti-TNF- α , anti-MCP-1, anti-NF- κ B P65, anti- β -actin antibodies and second antibodies were purchased from Santa Cruz Biotechnology (Santa Cruz, CA, USA). Diaminobenzidine (DAB) horseradish peroxidase color development kit was purchased from Beyotime Institute of Biotechnology (Shanghai, China). Ox-LDL, TNF- α , and MCP-1 enzyme-linked immune-sorbent assay (ELISA) kits were purchased from Shanghai Dingguo Technology Co., Ltd., Shanghai, China. TRIzol reagent and SuperScript II First-Strand Synthesis System were purchased from Invitrogen (Grand Island, NY, USA). SYBR Premix Ex Taq™ kit was purchased from TaKaRa Bio Inc., Dalian, China.

2.3. Diabetes rat model and drug administrations

Male Wistar rats (Animal experimental center of Shandong University, Ji'nan, China) weighting approximately 180-220 g were used in this study. They were kept in a room with a 12 h/12 h light/dark cycle and appropriate temperature (22-26°C) and humidity (55%), and given food and water *ad libitum*. After adaptive feeding for one week with blood glucose measured in the normal range, 60 rats were randomly divided into control group ($n = 10$) and model group ($n = 50$). The rats in the control group were fed normal chow diets, while the other rats were fed high-fat and high-sugar diets (containing 10.00% lard, 20.00% sucrose, 10.0% yolk powder, 0.50% sodium cholate and 59.50% normal chow) for 6 weeks. After an overnight fast, the rats in the model group were intraperitoneally injected with streptozotocin (40 mg/kg) and the rats in the control group were intraperitoneally injected with vehicle citrate buffer at a dose of 1 mL/kg. Seventy two hours after injection, tail blood samples were taken to test random blood glucose. Rats with random blood glucose levels > 16.70 mmol/L for three measurements were considered diabetic.

Rats proven to be diabetic ($n = 50$) were randomly assigned to five groups with 10 rats in each group: model group, ferulic acid group, astragaloside IV group, ferulic acid + astragaloside IV group, and metformin group. First, the rats were fasted overnight and blood samples were obtained from tails for biochemical determinations including fasting blood glucose (FBG), triglyceride (TG), total cholesterol (TC), low density lipoprotein cholesterol (LDL-C), alanine aminotransferase (ALT), aspartate aminotransferase (AST), creatinine (Cr) and so on. They were administrated with medications as follows: rats were treated with ferulic acid (50 mg/kg•d), or astragaloside IV (50 mg/kg•d), or ferulic acid (50 mg/kg•d) + astragaloside IV (50 mg/kg•d), or metformin (40.5 mg/

kg•d), respectively by intragastric administration (*i.g.*) every day for 10 weeks. Rats in the control group and model group were administered with the same volume of normal saline. Body weight of rats in each group was measured every week and tail blood samples were taken to test FBG every two weeks.

All animal experiments were performed in accordance with the guidelines of Shandong University of Traditional Chinese Medicine for the care and use of laboratory animals and approved by the Animal Ethics Review Committee of Shandong University of Traditional Chinese Medicine.

2.4. Blood and tissue sample collection

After 10 weeks of drug administration, the rats were fasted overnight, then weighed and anesthetized with 10% chloralhydrate (0.3 g/kg, intraperitoneally). After anesthesia, the rats were fixed, the chest opened to expose the heart, and the aorta was isolated. Blood samples were collected from the apex of the heart, and centrifuged at a speed of 3,000 r/min for 5 min. Serum was removed and aliquots for the respective analytical determinations, was stored at -80°C until analysis. The abdominal aorta was dissected carefully, cleaned of fat and adherent connective tissues. A segment of 15 mm in length was cut and fixed with 4% paraformaldehyde for hematoxylin and eosin (HE) staining and immunohistochemical staining, and a segment of 5 mm in length was cut and stored at -80°C for quantitative real-time RT-PCR and Western blot analysis.

2.5. Blood samples detection

According to the manufacture's instructions, the following serum items were detected: First, FPG, TG, TC, LDL-C, ALT, AST and Cr were measured using a fully automatic biochemical analyzer (Olympus, Tokyo, Japan); second, HbA1c was detected to measure long-term blood glucose control; third, concentrations of NO and eNOS in serum were determined by the nitrate reductase method and a colorimetric method respectively.

2.6. HE and immunohistochemistry staining assay

To observe the histological morphology changes of the abdominal aorta, HE staining was performed. First, abdominal aorta tissues were fixed with 10% neutral formaldehyde and dehydrated in graded ethanol (85%, 95%, and 100%). After permeation in xylene, they were embedded in paraffin. The paraffin blocks were cut into 2 μ m slices, mounted onto glass slides and stained by standard techniques of HE staining according to previous studies. The specimens were examined using a Phenom desktop scanning electron microscope (FEI Company, USA).

Immunohistochemistry staining assays were performed to analyze the protein expression of TNF- α , MCP-1, and NF- κ B P65. Paraffin-embedded sections (3-5 μ m thick) were cut from formalin-fixed abdominal aorta and carried out as described previously (20). First, paraffin sections were de-paraffinized, hydrated, and immersed in 0.3% hydrogen peroxide in methanol for 30 min to block the endogenous peroxidase activity. Second, the sections were incubated in primary antibodies (anti-TNF- α or anti-MCP-1 or anti-NF- κ B P65) overnight at 4°C, followed by incubation in anti-mouse secondary antibody for 1 h at room temperature. Third, visualization was carried out using the DAB horseradish peroxidase color development kit, and slides were counter stained in hematoxylin-1. Finally, ten random fields were examined per slice for expression of TNF- α , MCP-1, and NF- κ B P65 using an Olympus BX40 microscope at a magnification of \times 400. Immunohistochemical results of TNF- α , MCP-1, and NF- κ B P65 expression were assessed according to criteria described previously (21). Five fields for each sample were selected randomly for the calculation. The percentage and staining intensity of the positive cells were observed by Image-Pro plus 6.0 to quantify the expression of proteins: (i) Percentage of positive cells was graded on a scale 0-4, indicating 0%, < 10%, 10-50%, 50-80%, and 80-100%, respectively; (ii) Staining intensity of positive cells was graded on a scale of 0-4, indicating colorless, light yellow, brown yellow, and brown, respectively; (iii) The multiplication of percentage scores and staining intensity scores gave the positive rating: 0 means negative (-), 1-4 means weakly positive (+), 5-8 means positive (++), and 9-12 means strongly positive (+++).

2.7. ELISA assay

ELISA assays were performed to determine the levels of OX-LDL in serum, and TNF- α and MCP-1 in abdominal aorta tissue, using commercially available kits according to the manufacturer's instructions. The optical density was measured on a Bio-Rad Model 680 micro plate reader (Bio-Rad Laboratories, Hercules, CA, USA) at 490 nm.

2.8. Quantitative real-time RT-PCR assay

Quantitative real-time RT-PCR was used to detect the mRNA expression of factors related to vascular endothelial dysfunction in the abdominal aorta of diabetic rats. First, total RNA was prepared from the abdominal aorta tissues by using TRIzol reagent according to the manufacturer's instructions. Then, total RNA was reverse-transcribed into cDNA using the SuperScript II First-Strand Synthesis System according to the manufacturer's directions. In the current study, relative mRNA expression levels for the target genes were determined by using glyceraldehyde 3-phosphate dehydrogenase

(GAPDH) as normalization control. The primers for the target genes and GAPDH were shown as follows: TNF- α (198 bp): forward 5'-CTCATTCTGCTCGTGG-3', and reverse 5'-CTCCGCTTGGTGGTTT-3'; MCP-1 (131 bp): forward 5'-CTGTCACGCTTCTGGG-3' and reverse 5'-GCCGACTCATTGGGAT-3'; GAPDH primers (199 bp): forward 5'-ATCGGACGCCTGGTTA-3' and reverse 5'-CGCTCCTGGAAGATGG-3'. Afterwards, according to the protocol of SYBR Premix Ex TaqTM kit, amplification of target genes and GAPDH were conducted in a 20 μ L reaction mixture containing 10 μ L SYBR (2 \times), 0.2 μ L ROX Dye II, 2.5 μ L each forward and reverse primers of each gene, 4 μ L cDNA and 0.8 μ L ddH₂O using ABI Prism 7500 Detection System (Applied Biosystems, Inc., USA). Thermal cycling parameters consisted of a hot-start at 95°C for 3 min followed by 45 cycles of 95°C for 20 s, 55°C for 15 s and extension at 72°C for 20 s. The analysis of relative gene expression was performed by comparative 2^{- $\Delta\Delta$ CT} method (22).

2.9. Western blot analysis

Western blot analysis was performed to determine the expression of proteins-related to vascular endothelial dysfunction in the abdominal aorta of diabetic rats. The abdominal aorta was incubated with 50 μ L RIPA lysis buffer at 4°C for 30 min and then the lysates (30 μ g of protein per lane) were fractionated by SDS-PAGE. The proteins were electro-transferred onto polyvinylidene difluoride (PVDF) membranes. The membranes were first incubated in blocking solution (5% skim milk) for 1 h at room temperature and then incubated overnight at 4°C with the first antibodies: anti-TNF- α or anti-MCP-1 or anti-NF- κ B P65. After they were washed with TBST (10 mM Tris-HCl, 0.15 M NaCl, 8 mM sodium azide, 0.05% Tween-20, pH 8.0) three times, the membranes were incubated with horseradish peroxidase-conjugated secondary antibodies for 1 h and then again washed with TBST three times. Finally, protein bands were visualized with an enhanced chemiluminescence (ECL) detection system. As an internal control, β -actin was detected with anti- β -actin antibodies.

2.10. Statistical analysis

All experiments were performed in triplicate and the results are expressed as mean \pm S.D. Statistical analysis was performed with one-way analysis of variance (ANOVA) and the Student's *t*-test using SPSS.15.0 software (SPSS Inc., USA). *P* < 0.05 was indicative of a significant difference.

3. Results

3.1. The general condition of rats

After treatment for 10 weeks, the rats in the control

Table 1. The effects of ferulic acid and astragaloside IV on biochemical indexes and HbA1c of rats

Group	FPG (mmol/L)	HbA1c (%)	TG (mmol/L)	TC (mmol/L)	LDL-C (mmol/L)
Control	5.43 ± 0.23	5.4 ± 0.2	0.85 ± 0.13	1.88 ± 0.10	0.30 ± 0.06
Model	22.28 ± 2.09	14.5 ± 0.6	2.01 ± 0.09	2.79 ± 0.12	5.20 ± 0.12
Ferulic acid	21.64 ± 1.25	14.6 ± 0.5	1.11 ± 0.18**	2.10 ± 0.19**	0.32 ± 0.10**
Astragaloside IV	12.92 ± 2.94*	9.5 ± 0.4**	1.94 ± 0.11	2.64 ± 0.16	0.65 ± 0.07
Ferulic acid + Astragaloside IV	12.72 ± 2.84**	9.2 ± 0.2**	1.08 ± 0.16**	2.38 ± 0.10**	0.38 ± 0.06**
Metformin	7.64 ± 1.06**	8.9 ± 0.4**	0.85 ± 0.13	1.88 ± 0.10	0.50 ± 0.20

Data are shown as mean ± S.D. ($n = 10$). * $p < 0.05$ and ** $p < 0.01$ versus Model group after treatment for 10 weeks.

group were in good shape, glossy coat color and obesity, while the rats in the model group and drug treatment groups had different degrees of low spirits, matte coat color, and typical characteristics of diabetes mellitus (polydipsia, polyphagia, polyuria, and weakness). In addition, there was a great change in body weight of rats after treatment with ferulic acid and astragaloside IV (Data not shown). After 10 weeks of treatment, body weights in each group increased with the control group increasing the most and the model group increasing the minimum ($p < 0.01$). Body weights in metformin group ($p < 0.01$), astragaloside IV group ($p < 0.05$) and ferulic acid + astragaloside IV group ($p < 0.05$) were higher compared to the model group. However, there was no significant difference between body weights in the ferulic acid group compared to the model group ($p > 0.05$).

3.2. The effects of ferulic acid and astragaloside IV on biochemical indexes and HbA1c of rats

The effects of ferulic acid and astragaloside IV on biochemical indexes (e.g., FPG, TG, TC, and LDL-C) of diabetic rats are presented in Table 1. Compared to model group, levels of FPG in metformin group ($p < 0.01$), astragaloside IV group ($p < 0.05$) and ferulic acid + astragaloside IV group ($p < 0.05$) decreased significantly. However, there was no significant difference between FPG in the ferulic acid group and the model group ($p > 0.05$). Compared to the model group, the levels of HbA1c, TG, TC and LDL-C decreased significantly in the ferulic acid + astragaloside IV group ($p < 0.01$). Compared to the model group, both in the metformin group and astragaloside IV group, levels of HbA1c decreased significantly ($p < 0.01$) but the levels of TG, TC and LDL-C decreased non-significantly ($p > 0.05$). Compared to the model group, in the ferulic acid group, levels of TG, TC and LDL-C decreased significantly ($p < 0.01$) but levels of HbA1c decreased non-significantly ($p > 0.05$). Taken together, ferulic acid combined with astragaloside IV exhibited a significant effect on decreasing the levels of FPG, HbA1c, TG, TC, and LDL-C. In addition, there was no significant difference between ALT, AST, and Cr before and after treatment with ferulic acid and astragaloside IV (data not shown).

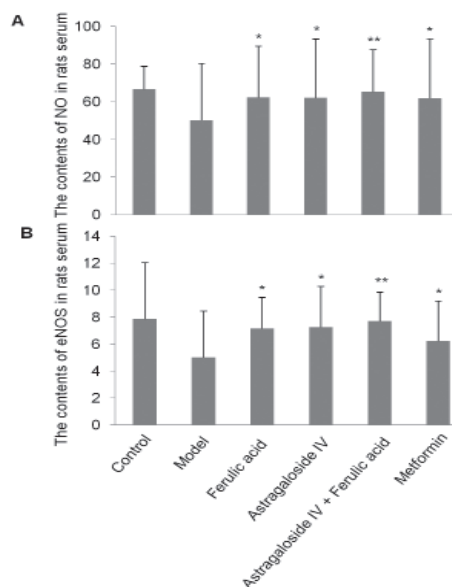


Figure 2. The contents of NO (A) and NOS (B) in the serum of diabetic rats. The data represent mean ± S.D. ($n = 10$). * $p < 0.05$ and ** $p < 0.01$ versus Model group.

3.3. The effects of ferulic acid and astragaloside IV on NO and eNOS of rats

After treatment for 10 weeks, the amount of NO and eNOS in serum were detected. As shown in Figure 2, the amount of NO and eNOS decreased in the model group and drug treatment groups compared to the control group. The amount of NO and eNOS in each drug treatment group ($p < 0.05$) especially ferulic acid + astragaloside IV group ($p < 0.01$) were higher than those in the model group. That is to say, compared to the model group, the amount of NO and eNOS in each drug treatment group increased. Moreover, in the ferulic acid + astragaloside IV group, the amount of NO and eNOS increased significantly compared to other treatment groups ($p < 0.01$).

3.4. The effects of ferulic acid and astragaloside IV on the histological morphology changes of abdominal aorta of rats

As shown in Figure 3A, in the control group, the

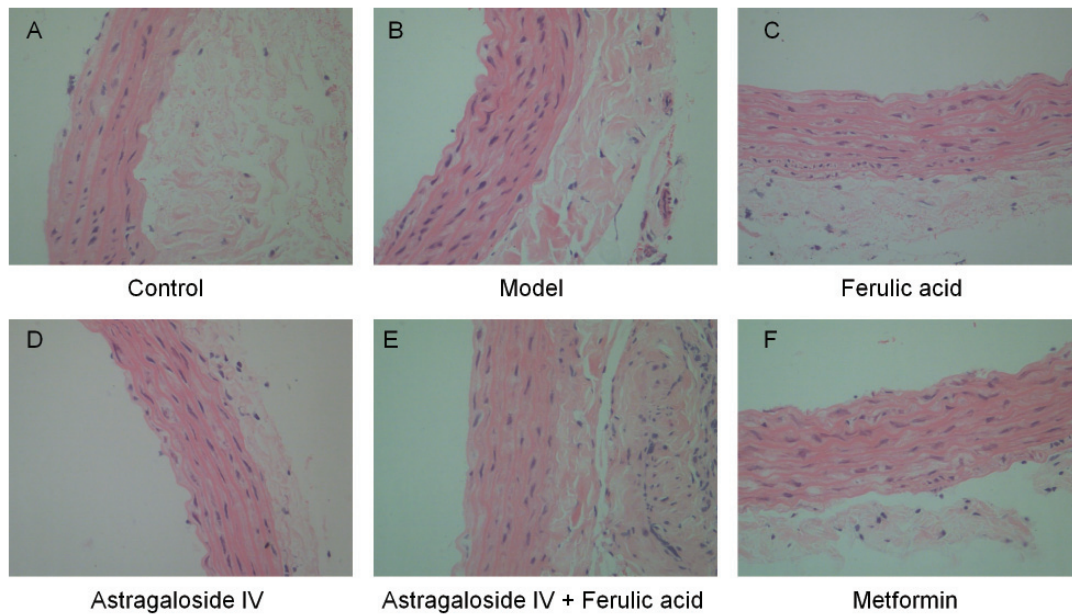


Figure 3. The histological morphology changes of abdominal aorta endothelium of diabetic rats in each group (original magnification ×400). (A) Control group; (B) Model group; (C) Ferulic acid group; (D) Astragaloside IV group; (E) Ferulic acid + Astragaloside IV group; (F) Metformin group.

abdominal aorta intima was smooth, endothelial cell integrity was preserved, the single layer was close to the elastic plate and medial thickness was uniform. However, in the model group (Figure 3B), the typical three-layer structure of the aortic wall was not clear, and intimal thickness increased with irregular intima. In the drug treatment groups especially in ferulic acid combined with astragaloside IV group (Figure 3C-3F), the aortic intima was smooth and intimal thickening was less compared with the model group. Progression of aorta intima and endothelial structure were attenuated by ferulic acid and astragaloside IV therapy. In the ferulic acid + astragaloside IV group, as shown in Figure 3E, intima was smooth with little endothelial cell drop, and media smooth muscle cells proliferated with uniform thickness and regular arrangement.

3.5. The effects of ferulic acid and astragaloside IV on the expression of Ox-LDL, MCP-1, TNF-α and NF-κB P65

The expression of Ox-LDL in serum and the expression of MCP-1 and TNF-α in the abdominal aorta tissue were detected by ELISA assays. As shown in Figure 4, compared to the control group, both the expression of Ox-LDL, MCP-1, and TNF-α in the model group and each drug treatment group increased significantly. Furthermore, compared to the model group, the expression of Ox-LDL were significantly inhibited after treatment with ferulic acid single ($p < 0.01$) or ferulic acid combined with astragaloside IV ($p < 0.01$). Compared to the model group, the expression of MCP-1 and TNF-α were significantly inhibited after treatment with ferulic acid and astragaloside IV especially in

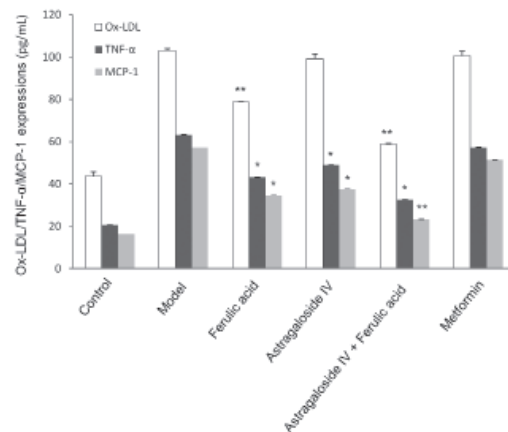


Figure 4. The expressions of Ox-LDL in serum of rats and the expressions of MCP-1 and TNF-α in the abdominal aorta tissue of rats detected by ELISA assay. The data represent mean ± S.D. (n = 10). * $p < 0.05$ and ** $p < 0.01$ versus Model group.

the ferulic acid + astragaloside IV group ($p < 0.01$). However, the expression of Ox-LDL, MCP-1, and TNF-α was inhibited insignificantly in the metformin group compared to the model group. Taken together, ferulic acid combined with astragaloside IV exhibited the greatest effect on inhibiting the expression of Ox-LDL, MCP-1, and TNF-α compared to only treatment with ferulic acid, astragaloside IV or metformin alone.

The mRNA expression of MCP-1 and TNF-α in the abdominal aorta of diabetic rats were detected by quantitative real-time RT-PCR assays. As shown in Figure 5, compared to the control group, the mRNA expression of MCP-1 and TNF-α in the model group and each drug treatment group increased significantly. Furthermore, compared to the model group, the

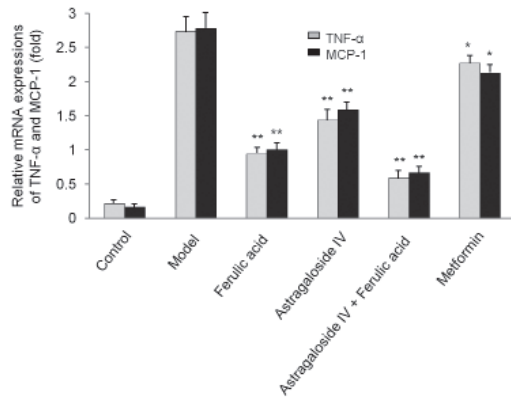


Figure 5. The mRNA expressions of MCP-1 and TNF- α in the abdominal aorta of diabetic rats detected by quantitative real-time RT-PCR assay. The data represent mean \pm S.D. ($n = 10$). * $p < 0.05$ and ** $p < 0.01$ versus Model group.

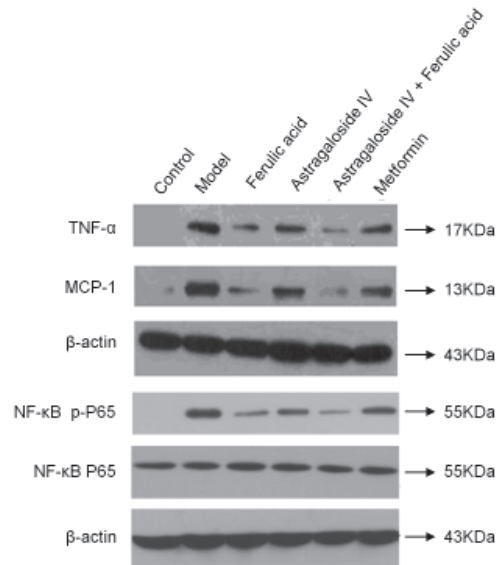


Figure 7. The protein expression of TNF- α , MCP-1, and NF- κ B P65 in the abdominal aorta of diabetic rats in each group detected by Western blot analysis.

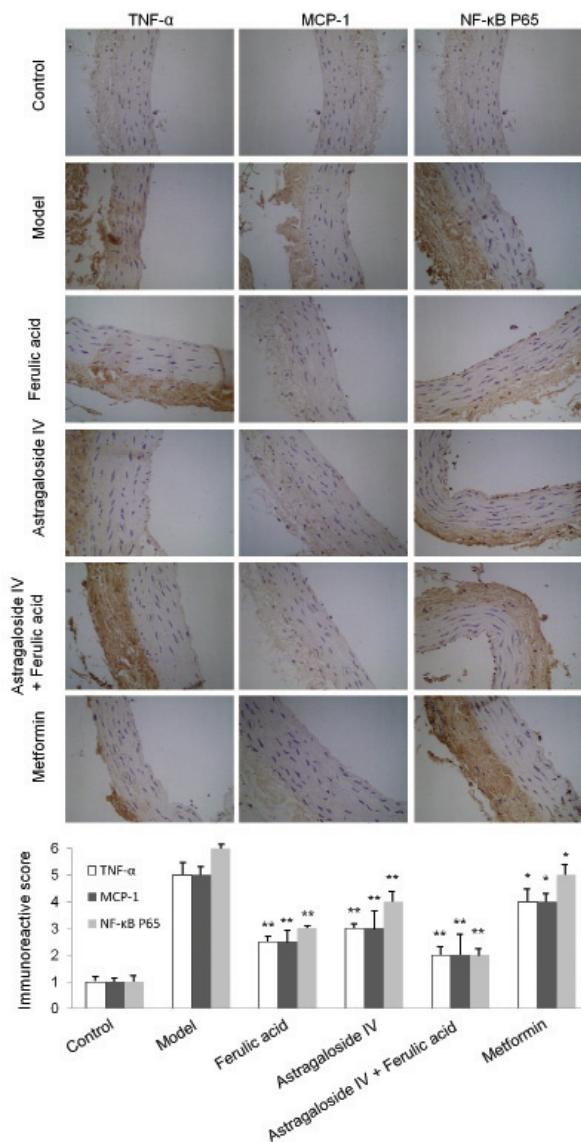


Figure 6. The protein expression of TNF- α , MCP-1 and NF- κ B P65 in the abdominal aorta of diabetic rats in each group detected by immunohistochemistry staining assay (original magnification $\times 400$).

expression of MCP-1 and TNF- α were significantly inhibited in each drug treatment group especially in the ferulic acid + astragaloside IV group ($p < 0.01$). Ferulic acid combined with astragaloside IV exhibited the greatest effect on inhibiting the mRNA expression of MCP-1 and TNF- α compared to only treatment with ferulic acid, astragaloside IV or metformin alone.

The protein expression of TNF- α , MCP-1, and NF- κ B P65 were detected by immunohistochemistry staining and Western blot analysis. As shown in Figure 6 and Figure 7, compared to the control group, the expression of TNF- α , MCP-1, and NF- κ B P65 increased significantly. Furthermore, compared to the model group, the levels of TNF- α , MCP-1, and NF- κ B P65 were significantly down-regulated in each drug treatment group especially in the ferulic acid + astragaloside IV group. Ferulic acid combined with astragaloside IV exhibited the greatest effect on inhibiting the mRNA expression of MCP-1 and TNF- α compared to other treatment.

4. Discussion

Dysfunction of the endothelium is regarded as an important factor in the pathogenesis of vascular disease in DM. In this work, we evaluated the protective effect of ferulic acid and astragaloside IV against vascular endothelial dysfunction in streptozotocin-induced diabetic rats. The major finding of this study was that ferulic acid combined with astragaloside IV was capable of improving the structure of the aortic endothelium wall (Figure 3), attenuating the increase of FPG, HbA1c, TG, TC, LDL-C (Table 1) and Ox-LDL (Figure 4), promoting the release of NO (Figure 2), and inhibiting over-activation of MCP-1, TNF- α , and NF-

κ B P65 (Figures 4-7). Moreover, there was no damage to liver and kidney function after treatment with ferulic acid and astragaloside IV for 10 weeks. In a word, our data contribute in part to elucidate the molecular mechanisms involved in the protective effect of ferulic acid and astragaloside IV against vascular endothelial dysfunction in DM with little side effects. Ferulic acid combined with astragaloside IV might exhibit a significant protective effect against vascular endothelial dysfunction in DM *via* inhibiting the NF- κ B pathway involving a decrease of Ox-LDL, an increase of NO and eNOS, and activation of NF- κ B P65, MCP-1, and TNF- α .

Hyperglycemia is generally considered as a harmful factor in vascular dysfunction, and the focus has been on tight blood glucose control as a treatment for diabetic patients (3). In the current study, we found that ferulic acid combined with astragaloside IV could effectively reduce the levels of FPG and HbA1c. Dyslipidemia is a major risk factor for atherosclerosis. Reducing high levels of TC, particularly LDL-C, decreases the risk for developing atherosclerosis (23). We found that ferulic acid combined with astragaloside IV could effectively reduce the levels of TG, TC, and LDL-C, and decrease the risk for vascular dysfunction in DM.

DM has been known as an oxidative stress disorder which is caused by imbalance between free radical formation and the ability of the body's natural antioxidants in hyperglycemia (24). Many studies have suggested that oxidative stress plays a key role in the pathogenesis of endothelial dysfunction, insulin resistance, and pancreatic β cell damage and so on in development and progression of DM as well as in complications (25). As a major product of oxidative stress, Ox-LDL induces apoptosis, monocyte adhesion, and reactive oxygen species generation *via* up-regulating and binding to its receptor LOX-1, and then causes toxicity to the vascular endothelial cells and causes endothelial dysfunction, which is considered to be a driving force in the initiation and development of atherosclerosis. Notably, the toxicity of Ox-LDL is not only damage of vascular endothelial structure, but more important is that Ox-LDL affects the secretion of endothelium-derived vasomotor factors and adhesion factors which leads to endothelial dysfunction (23). NO is an important vasomotor factor and endothelin (ET) is a stronger vasoconstrictor factor, which are secreted by vascular endothelial cells. Keeping balance between the levels of NO and ET is important in the maintenance of vascular endothelium diastolic function (26). Moreover, the production of NO in endothelial cells is mainly regulated by eNOS which is a nitric oxide synthase that generates NO in blood vessels and is involved with regulating vascular tone by inhibiting smooth muscle contraction and platelet aggregation (27). However, the production or activation of eNOS and NO could be reduced in endothelial cells attributed

to oxidative stress and the increase of Ox-LDL in DM patients. Thus, regulating the activity of eNOS and promoting NO production might be key targets for prevention of endothelial dysfunction in DM. In the current study, we found that the levels of Ox-LDL were significantly decreased by ferulic acid and astragaloside IV (Figure 4). Furthermore, the activity of eNOS and the amount of NO in serum of diabetic rats were effectively improved after treatment with ferulic acid and astragaloside IV (Figure 2). That is to say, ferulic acid combined with astragaloside IV exhibited a significant protective effect against vascular endothelial dysfunction in DM *via* decreasing Ox-LDL and increasing NO.

Some studies demonstrated that enhanced NF- κ B activity is an important factor involved in macro- and microvascular dysfunction in diabetes. It is closely related to DM-associated oxidative stress and inflammation (28). In the state of hyperglycemia-induced oxidative stress, the elevation of free radicals could impair Ca^{2+} translocation and then trigger NF- κ B activation, reducing vascular contractibility and modifying some gene expression including cytokines (*e.g.*, IL-6, TNF- α), angiotensin-II and adhesion molecules (*e.g.*, ICAM-1, VCAM-1, and E-selectin) and chemokines (*e.g.*, MCP-1, IL-8) released from vascular endothelial cells and causing endothelial dysfunction (29). Importantly, as well as hyperglycemia, cytokine stimulation (*e.g.*, TNF- α , IL-1 β , MCP-1, and ICAM-1) also could activate NF- κ B *via* reactive oxygen species formation. In addition, NF- κ B is one of the most important regulators of pro-inflammatory gene expression. In DM models, activation of NF- κ B is correlated with an increased of some cytokine pro-inflammatory molecules. NF- κ B could lead to or enhance expression of host genes, such as cytokine TNF- α and chemokine MCP-1, inducing inflammatory damage of vascular wall, and then initiating atherosclerosis (30). Thus, NF- κ B plays critical roles in the pathophysiology of several process of vascular endothelial dysfunction in DM, and it is plausible that exogenous modulation of NF- κ B activation may be effective in developing new therapeutic strategies. In the current study, we found that gene and protein expression of MCP-1, TNF- α , and NF- κ B P65 were significantly inhibited by ferulic acid and astragaloside IV (Figures 4-7). That is to say, ferulic acid combined with astragaloside IV exhibited a significant protective effect against vascular endothelial dysfunction in DM *via* inhibiting the NF- κ B pathway.

In conclusion, the current study demonstrated that ferulic acid combined with astragaloside IV could effectively reduce the levels of FPG, HbA1c, TG, TC, and LDL-C. The current study also demonstrated that ferulic acid combined with astragaloside IV exhibited a significant protective effect against vascular endothelial dysfunction in diabetic rats through the NF- κ B pathway

involving decrease of Ox-LDL, an increase of NO and eNOS, and activation of NF- κ B P65, MCP-1, and TNF- α . We hope the current study provides a direction of new therapy for treating vascular complications of DM.

Acknowledgements

This project was supported by the science and technology development plan of traditional Chinese medicine in Shandong Province, China (No. 2013057).

References

- Shaw JE, Sicree RA, Zimmet PZ. Global estimates of the prevalence of diabetes for 2010 and 2030. *Diabetes Res Clin Pract.* 2010; 87:4-14.
- Saxena B. Anti-hyperlipidemic activity of *Withania coagulans* in streptozotocin-induced diabetes: A potent anti-atherosclerotic agent. *Drug Discov Ther.* 2010; 4:334-340.
- Goff DC Jr, Gerstein HC, Ginsberg HN, Cushman WC, Margolis KL, Byington RP, Buse JB, Genuth S, Probstfield JL, Simons-Morton DG; ACCORD Study Group. Prevention of cardiovascular disease in persons with type 2 diabetes mellitus: Current knowledge and rationale for the Action to Control Cardiovascular Risk in Diabetes (ACCORD) trial. *Am J Cardiol.* 2007; 99:4i-20i.
- Beckman JA, Creager MA, Libby P. Diabetes and atherosclerosis: epidemiology, pathophysiology, and management. *JAMA.* 2002; 287:2570-2581.
- Capellini VK, Celotto AC, Baldo CF, Olivon VC, Viaro F, Rodrigues AJ, Evora PR. Diabetes and vascular disease: Basic concepts of nitric oxide physiology, endothelial dysfunction, oxidative stress and therapeutic possibilities. *Curr Vasc Pharmacol.* 2010; 8:526-544.
- Tabak O, Gelisgen R, Erman H, Erdenen F, Muderrisoglu C, Aral H, Uzun H. Oxidative lipid, protein, and DNA damage as oxidative stress markers in vascular complications of diabetes mellitus. *Clin Invest Med.* 2011; 34:E163-E171.
- Tousoulis D, Papageorgiou N, Androulakis E, Siasos G, Latsios G, Tentolouris K, Stefanadis C. Diabetes mellitus-associated vascular impairment: Novel circulating biomarkers and therapeutic approaches. *J Am Coll Cardiol.* 2013; 62:667-676.
- Rochette L, Lorin J, Zeller M, Guillard JC, Lorgis L, Cottin Y, Vergely C. Nitric oxide synthase inhibition and oxidative stress in cardiovascular diseases: Possible therapeutic targets? *Pharmacol Ther.* 2013; 140:239-257.
- Polovina MM, Potpara TS. Endothelial dysfunction in metabolic and vascular disorders. *Postgrad Med.* 2014; 126:38-53.
- Tzeng TF, Liou SS, Liu IM. The selected traditional Chinese medicinal formulas for treating diabetic nephropathy: perspective of modern science. *J Tradit Complement Med.* 2013; 3:152-158.
- Xie W, Du L. Diabetes is an inflammatory disease: Evidence from traditional Chinese medicines. *Diabetes Obes Metab.* 2011; 13:289-301.
- Zhang WL, Zheng KY, Zhu KY, Zhan JY, Bi CW, Chen JP, Dong TT, Choi RC, Lau DT, Tsim KW. Chemical and biological assessment of angelica roots from different cultivated regions in a Chinese herbal decoction danggui buxue tang. *Evid Based Complement Alternat Med.* 2013; 2013:483286.
- Chao WW, Lin BF. Bioactivities of major constituents isolated from *Angelica sinensis* (Danggui). *Chin Med.* 2011; 6:29.
- Lekakis J, Rallidis LS, Andreadou I, Vamvakou G, Kazantzoglou G, Magiatis P, Skaltsounis AL, Kremastinos DT. Polyphenolic compounds from red grapes acutely improve endothelial function in patients with coronary heart disease. *Eur J Cardiovasc Prev Rehabil.* 2005; 12:596-600.
- Yuan W, Zhang Y, Ge Y, Yan M, Kuang R, Zheng X. Astragaloside IV inhibits proliferation and promotes apoptosis in rat vascular smooth muscle cells under high glucose concentration in vitro. *Planta Med.* 2008; 74:1259-1264.
- Hoo RL, Wong JY, Qiao C, Xu A, Xu H, Lam KS. The effective fraction isolated from *Radix Astragali* alleviates glucose intolerance, insulin resistance and hypertriglyceridemia in db/db diabetic mice through its anti-inflammatory activity. *Nutr Metab (Lond).* 2010; 7:67.
- Ren S, Zhang H, Mu Y, Sun M, Liu P. Pharmacological effects of astragaloside IV: A literature review. *J Tradit Chin Med.* 2013; 33:413-416.
- Gao D, Guo Y, Li X, Li X, Li Z, Xue M, Ou Z, Liu M, Yang M, Liu S, Yang S. An aqueous extract of *Radix astragali*, *Angelica sinensis*, and *Panax notoginseng* is effective in preventing diabetic retinopathy. *Evid Based Complement Alternat Med.* 2013; 2013:578165.
- Liu IM, Tzeng TF, Liou SS. A Chinese herbal decoction, Dang Gui Bu Xue Tang, prepared from *Radix astragali* and *Radix angelicae sinensis*, ameliorates insulin resistance induced by a high-fructose diet in Rats. *Evid Based Complement Alternat Med.* 2011; 2011:248231.
- Hu L, Xue F, Shao MH, Deng AM, Wei GT. Aberrant expression of Notch3 predicts poor survival for hepatocellular carcinomas. *Biosci Trends.* 2013; 7:152-156.
- Soslow RA, Dannenberg AJ, Rush D, Woerner BM, Khan KN, Masferrer J, Koki AT. Cox-2 is expressed in human pulmonary, colonic, and mammary tumors. *Cancer.* 2000; 89:2637-2645.
- Livak KJ, Schmittgen TD. Analysis of relative gene expression data using real-time quantitative PCR and the $2^{-\Delta\Delta C_T}$ method. *Methods.* 2001; 25:402-408.
- Kita T, Kume N, Minami M, Hayashida K, Murayama T, Sano H, Moriwaki H, Kataoka H, Nishi E, Horiuchi H, Arai H, Yokode M. Role of oxidized LDL in atherosclerosis. *Ann N Y Acad Sci.* 2001; 947:199-206.
- Zatalia SR, Sanusi H. The role of antioxidants in the pathophysiology, complications, and management of diabetes mellitus. *Acta Med Indones.* 2013; 45:141-147.
- Pitocco D, Tesauro M, Alessandro R, Ghirlanda G, Cardillo C. Oxidative stress in diabetes: Implications for vascular and other complications. *Int J Mol Sci.* 2013; 14:21525-21550.
- Pitocco D, Tesauro M, Alessandro R, Ghirlanda G, Cardillo C. Oxidative stress in diabetes: Implications for vascular and other complications. *Int J Mol Sci.* 2013; 14:21525-21550.
- Lu YL, Hu SJ, Shen ZJ, Shao YC. Changes of macrovascular endothelial ultrastructure and gene

- expression of endothelial nitric oxide synthase in diabetic rats. *Chin Med J (Engl)*. 2004; 117:1165-1169.
28. Lorenzo O, Picatoste B, Ares-Carrasco S, Ramírez E, Egido J, Tuñón J. Potential role of nuclear factor κ B in diabetic cardiomyopathy. *Mediators Inflamm*. 2011; 2011:652097.
29. de Winther MP, Kanters E, Kraal G, Hofker MH. Nuclear factor kappaB signaling in atherogenesis. *Arterioscler Thromb Vasc Biol*. 2005; 25:904-914.
30. Palomer X, Salvadó L, Barroso E, Vázquez-Carrera M. An overview of the crosstalk between inflammatory processes and metabolic dysregulation during diabetic cardiomyopathy. *Int J Cardiol*. 2013; 168:3160-3172.

(Received July 22, 2014; Revised August 4, 2014; Accepted August 5, 2014)

A simple, rapid, economical, and practical method for the determination of efavirenz in plasma of Chinese AIDS patients by reverse phase high-performance liquid chromatography with ultraviolet detector

Kang Yin^{1,*}, Xianmin Meng^{2,3,*}, Ping Dong², Tianran Ding², Li Shen², Li Zhang², Renfang Zhang¹, Weimin Cai³, Hongzhou Lu^{1,**}

¹ Department of Infectious Diseases, Shanghai Public Health Clinical Center, Shanghai, China;

² Department of Pharmacy, Shanghai Public Health Clinical Center, Shanghai, China;

³ Department of Clinical Pharmacy and Pharmaceutical Administration, School of Pharmacy, Fudan University, Shanghai, China.

Summary

This study aimed to develop a reverse phase high-performance liquid chromatographic (RP-HPLC) method for the determination of efavirenz in human plasma and to use it for determining the concentrations of efavirenz in Chinese AIDS patient. A simple mobile phase consisting of 0.01 mol/L NaH₂PO₄ solution and acetonitrile (38:62, V/V) was pumped at a flow rate of 1.0 mL/min through a reverse phase Diamonsil C₁₈ column maintained at 30°C. Diazepam was used as an internal standard and monitored with efavirenz at 247 nm. The protein of 100 µL plasma sample was precipitated before 20 µL of the supernatant was directly injected into the column. The linear response over the concentration ranges 0.10-20.0 µg/mL was obtained and the linear regression equations was $Y = 2.2873X - 0.1449$ ($r = 0.9999$). The intra-day and inter-day precisions (1.9-2.6%, 2.2-7.2%, respectively), the relative and absolute recovery (99.3-106.3%, 75.6-80.3%, respectively) met the international standards. Stability of plasma samples were evaluated for short-term (ambient temperature for 16 h) and long-term (-20°C for 30 days) storage conditions and were found to be stable. The mean plasma concentration of efavirenz of the 406 patients was 2.21 ± 1.95 µg/mL, 77.3% of which were within the therapeutic window (1-4 µg/mL), 15.1% were below the window, and 7.6% were over it. In conclusion, the method had advantages of convenience, rapidity, necessary accuracy and precision, high practicality and met the needs for therapeutic drug monitoring and the pharmacokinetic study of efavirenz, especially in underdeveloped countries. For Chinese AIDS patients, it was beneficial to use efavirenz under the guidance of therapeutic drug monitoring.

Keywords: Efavirenz, RP-HPLC, plasma concentration, AIDS

1. Introduction

Efavirenz, a non-nucleoside reverse transcriptase inhibitor for the treatment of HIV infection, is recommended by WHO as a first-line drug with its

excellent therapeutic effect. It has been widely used over the world, especially in underdeveloped countries, such as China and some African countries (1). Efavirenz is mainly metabolized by CYP2B6 enzyme. However, cytochrome P450 2B6 gene exhibits highly degrees of polymorphism (2), which has a great difference in allele frequency among races, thus leading to obvious differences in efavirenz plasma concentration, either among individuals or among races (3-6). In addition, rifampicin and voriconazole, etc., which is often simultaneously used in HIV-infected patients for concurrent diseases, have interactions with efavirenz

*These authors contributed equally to this works.

**Address correspondence to:

Dr. Hongzhou Lu, Department of Infectious Diseases, Shanghai Public Health Clinical Center, 2901 Caolang Road, Jinshan, Shanghai, 201508, China.

E-mail: luhongzhou@fudan.edu.cn

and affect efavirenz plasma concentration. Nowadays, many studies have shown that both the therapeutic effect and side effects of efavirenz are related to its plasma concentration (3,4,7-11). The generally accepted therapeutic window of efavirenz is 1-4 µg/mL (steady state trough concentration). A long-time exposure to a lower efavirenz trough concentration may easily lead to virologic failure or virus resistance to efavirenz, while a higher trough concentration may result in a higher risk of side effects and toxicities (7,11,12). A previous research shows that 28.6% of Chinese HIV-infected patients may have efavirenz plasma concentration above 4 µg/mL after taking a standard dose of efavirenz (600 mg, *po*, qd) (13). If we can monitor the plasma efavirenz concentration of the patients with efavirenz-containing antiretroviral treatment (ART) and adjust the dosage according to the results, a better therapeutic effect as well as a decline of side effects may be achieved (14-16), especially for patients taking rifampicin or voriconazole at the same time. Therefore, we need to develop a method for the quantitative determination of efavirenz in human plasma. Considering the actual situation in under-developed countries, the method must be simple, rapid, economical, and practical, with good accuracy and precision, selectivity, and sensitivity.

Up to now, several methods for the determination of efavirenz in plasma using LC-MS (17,18), LC-MS-MS (19,20), MALDI-TOF/IOF (21), HPLC-PAD (22-25), *etc.*, have been published. These methods may not be widely used in underdeveloped countries because of the inaccessibility and high costs of laboratory equipments. On the contrary, reverse phase high-performance liquid chromatographic with ultraviolet detector (RP-HPLC-UV) method is feasible due to its easy accessibility and low cost. Also, many HPLC-UV methods for determination of plasma efavirenz (23,26-31) or simultaneous determination with other drugs such as anti-tuberculosis (anti-TB) agents or other antiretroviral agents (24,32-50) have been reported. In most of these methods, the volumes of plasma used range from 200 to 900 µL (23,26-28,33,34,44-46), which were inapplicable for children due to the scarcity of sample. High-cost, complicated and time-consuming plasma sample pre-treatments such as solid-phase extraction (26,33,34,44-46), liquid-liquid extraction (23,24,27,28,32,35) appeared in some methods. A few of reported methods were difficult to repeat because of the lack of internal standard (26). Moreover, some methods had complicated mobile phase (34,37) or gradient elution (35,40,50), and some had a longer system run time (32,50). Therefore, none of the reported methods met all the requirements mentioned above. In our study we developed a method for plasma efavirenz determination by RP-HPLC with UV detector. In this method, 100 µL sample plasma was precipitated by 200 µL acetonitrile (including internal standard: diazepam) and the supernatant was directly injected into HPLC

system without dilution after mixing and centrifugation. Isocratic elution was applied and the detection time was 7.5 min. The reliability and repeatability of this method was further verified by using it to determine efavirenz plasma concentrations in large samples. In a word, our method is simple, rapid, cost-effective, and can be applied in the therapeutic drug monitoring and pharmacokinetics researches on efavirenz, especially in underdeveloped countries.

2. Materials and Methods

2.1. Chemicals

Efavirenz standard (99.8% purity) and efavirenz tablet (Stocrin[®]) were purchased from the Toronto Research Chemicals Inc. (North York, Canada, batch number 5-ABY-15-1) and Merck Sharp & Dohme (South Granville, New South Wales, Australia), respectively. Diazepam (99.5% purity, internal standard) was from the Sigma company (Shanghai, China, batch number 34H0556). Acetonitrile and methanol (HPLC grade) were obtained from Merck KGaA (Darmstadt, Germany), triethylamine and phosphoric acid (HPLC grade) from Tedia Company Inc (Fairfield, USA). NaH₂PO₄ was from Shanghai Clinical Research Center (Shanghai, China). Deionized water was processed through a water purification system (Yiyang Enterprise Development Company, Chongqing, China).

2.2. Chromatographic system

The HPLC system, Shimadzu LC-20A (Kyoto Japan), was consisted of column compartment CTO-20A, degasser DGU-20A5, pump CBM-20A, auto-sampler SIL-20AC, and SPD-20AV UV detector. The eluent was monitored at 247 nm. Chromatographic separation was achieved at 30°C using a reverse phase YMC-Pack ODS-A C18 column (C18, 150 mm × 4.6 mm, 5 µm) with a guard column (ZORBAX Eclipse Plus-C18, 150 mm × 4.6 mm, 5 µm, Agilent Technologies, Santa Clara, USA). The mobile phase was consisted of 0.01 mol/L NaH₂PO₄ (containing 0.01 mol/L triethylamine, pH 5.2) and acetonitrile (32:62, V/V), and pumped at a flow rate of 1.0 mL/min. The injection volume was 20 µL (26,28,31,32).

2.3. Selection of study subjects, sample collection, and data collection

Chinese AIDS outpatients, aging from 18 to 75 years, with no obvious hepatic or renal dysfunction, receiving efavirenz-containing ART at Shanghai Public Health Clinical Center from January 2012 to January 2013, were recruited to this study. Peripheral bloods (3-5 mL) were drawn 16 h after the last dose, and were put into heparin anticoagulant tubes (51). Plasma samples

were heat-inactivated (56°C water bath for 60 min) and stored at -80°C before they were analyzed. Correlated information of the patients was collected, including gender, age, weight, height, hepatic and renal functions, antiretroviral regimen, efavirenz dosage, time of taking medicine, time of blood sample collection, drug combinations and adverse drug reactions (ADR). The study followed the Declaration of Helsinki and ethics approval was granted by the Ethics Committee of Shanghai Public Health Clinical Center. Written informed consent was obtained from each patient.

2.4. Preparation of various solutions

NaH₂PO₄ buffer solution was prepared by dissolving accurately weighed NaH₂PO₄ (3.1202 g) and triethylamine (2.0238 g) in 2 L ultrapure water and blended well by ultrasonic. The pH value was adjusted to 5.2 using 20% phosphoric acid. The solution was degassed by ultrasonic for 20 min after vacuum filtration before using. Two hundred µg/mL efavirenz stock solution was prepared by dissolving accurately weighed efavirenz standard (10 mg) into a 50 mL mixture of methanol and water (1:1, V/V), and stored at 4°C before using. Working solutions of efavirenz in concentrations of 1, 2, 5, 10, 20, 30, 40, 80, 100, and 160 µg/mL were prepared by diluting stock solution of efavirenz with the mixture of methanol and water (1:1, V/V). The diazepam stock solution (100 µg/mL) was prepared by dissolving accurately weighed diazepam (10 mg) in 100 mL acetonitrile and stored at 4°C. Before sample preparation, 1 µg/mL diazepam working solution was prepared by diluting stock solution with acetonitrile.

2.5. Sample preparation

One hundred µL plasma sample was transferred to 2 mL centrifuge tubes and 200 µL of diazepam working solution (acetonitrile with 1 µg/mL diazepam) was added. The mixture was blended for 2 min and was laid aside for 10 min at room temperature, then centrifuged at 15,000 rpm/min for 6 min. Twenty µL of the supernatant was directly injected into HPLC system under the condition described in 2.2. The chromatograms were recorded and concentrations of efavirenz were calculated.

2.6. Statistical methods

Descriptive analysis was performed to determine the mean and the standard deviation (mean ± S.D.) for continuous variables such as age, height, body mass index (BMI), and the percentages for categorical variables such as sex. Plasma efavirenz concentrations were showed as mean ± S.D. Statistical analysis was carried out by SPSS 18.0. Normality test of the plasma efavirenz concentrations of different groups

was assessed by Kolmogorov-Smirnov method before comparing. Levene's test was applied to determine variance homogeneity. Plasma efavirenz concentrations of multiple groups were compared with single factor analysis of variance. The comparison between two groups was performed with *t*-test if the data comply with the normal distribution. If not, difference tests were done using Mann-Whitney test or Kruskal-Wallis test. Analyses were done two-sided, and the result was considered as significance when the p value was below 0.05.

3. Results

3.1. Chromatographic behavior

Figure 1 showed the typical Chromatograms of blank plasma (C), blank plasma spiked with efavirenz and diazepam (B), and plasma sample from a patient following the oral administration of 600 mg efavirenz tablet above two weeks (A). The retention times of efavirenz and diazepam were 6.475 min and 4.535 min, respectively. The peaks of the two components were well separated, whilst no endogenous compounds peak was found beside the peaks of efavirenz and diazepam in blank plasma. The retention times of efavirenz and diazepam from patient's plasma sample are the same as those from standard substances, with good peak shapes and no interference peaks.

3.2. Drug combination test

In clinical practice, efavirenz is often used simultaneously with other drugs such as fluconazole, voriconazole, zidovudine, lamivudine, stavudine, tenofovir, ritonavir, and rifampin, *etc.* In order to evaluate the effect of these drugs on chromatographic peaks of efavirenz and diazepam, 2 µg/mL standard solutions of above drug were prepared and 20 µL was injected into the HPLC system, respectively. The chromatograms showed that

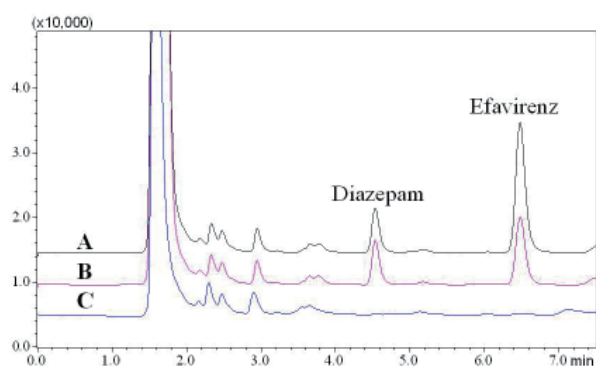


Figure 1. Chromatograms of efavirenz (retention time 6.475 min) and diazepam (retention time 4.535 min) from extracted plasma sample from patient (A); Chromatograms of spiked plasma sample containing efavirenz and diazepam standard (B); Chromatogram of extracted blank plasma (C).

the drugs above had no interference on the peak of efavirenz and diazepam.

3.3. Linearity

Different concentrations of efavirenz (0.10, 0.50, 1.0, 2.0, 4.0, 8.0, 16 µg/mL) were prepared using blank plasma and standard substance. 0.1 mL sample plasma of each concentration was processed according to the sample preparation method and was quantified. According to the chromatography, the concentration of efavirenz (Y) between 0.10 and 16.0 µg/mL had a good linear correlation with the ratio of peak areas of efavirenz and diazepam, and a regression equation was established: $Y = 2.2873X - 0.1449$ ($r = 0.9999$). The lowest detection limit was 0.027 µg/mL (S/N = 3), while limit of quantification was 0.089 µg/mL (S/N = 10).

3.4. Recovery

Varying concentrations of efavirenz quality control samples (0.3, 3.0, and 10.0 µg/mL) were prepared in blank human plasma and extracted as described above. Relative recovery was calculated by comparing the measured concentration according to regression equation with added concentration. Absolute recovery of the efavirenz was determined by comparing the peak area ratio after extraction with those of un-extracted solutions containing same concentrations of efavirenz as in plasma (Table 1). The relative recovery was 99.3-106.3% with RSD ranging from 3.2% to 4.5%, and the absolute recovery was 75.6-80.3% with RSD ranged from 2.8% to 4.8%.

3.5. Accuracy and precision

In order to evaluate the accuracy and precision of the method, three different concentrations quality control samples of efavirenz (0.2, 3.0, 10.0 µg/mL) were prepared in blank human plasma and extracted as described above. Intra-day assay accuracy and precision was determined from the analysis of five replicate

samples at each of the low, mid and high quality control standards, whereas, inter-day accuracy and precision involved the calculation of the mean values of fifteen samples at each of the low, mid and high quality control standards over three different days (Table 2). The intra-day and inter-day precision was 1.9-2.6% and 2.2-7.2%, respectively.

3.6. Stability

3.6.1. Stability of stock solution

Stock solution of efavirenz (200 µg/mL) was taken out at day 1, 15, 30, 45, and 60, and then dissolved in methanol-water (1:1, V/V) at a concentration of 2 µg/mL, while stock solution of diazepam was dissolved in acetonitrile at a concentration of 1 µg/mL, 20 µL of each of which was injected into the HPLC system and determined under the chromatographic condition described in 2.2. The RSD of efavirenz and diazepam was 1.3% and 1.4%, proving the stability of stock solution of efavirenz and that of diazepam within 60 days.

3.6.2. Stability of plasma samples at ambient temperature

Three different concentrations samples of efavirenz (0.2, 3.0, 10.0 µg/mL) were prepared in blank human plasma and were laid aside at room temperature. Samples of each concentration were extracted at 0, 2, 4, 8, 16 h and quantified by the HPLC system. The RSD of efavirenz at concentrations of 0.2, 3.0 and 10.0 µg/mL were 6.0%, 3.1% and 2.5%, respectively, proving the stability of plasma samples at ambient temperature in at least 16 h.

3.6.3. Stability at freezing state

Three different concentrations samples of efavirenz (0.2, 3.0, 10.0 µg/mL) were prepared in blank human plasma and stored at -20°C. The frozen samples were taken out at day 0, 3, 6, 15, and 30, and processed. The efavirenz concentrations of these samples were determined. The RSD of efavirenz at concentrations of 0.2, 3.0, and

Table 1. Results of recovery test of efavirenz

Expected (µg/mL)	Relative recovery			Absolute recovery		
	Mean ± S.D., n = 5	Recovery	RSD	Mean ± S.D., n = 5	Recovery	RSD
0.30	0.319 ± 0.014	106.3%	4.5%	0.756 ± 0.021	75.6%	2.8%
3.00	2.978 ± 0.095	99.3%	3.2%	0.777 ± 0.033	77.7%	4.2%
10.00	10.316 ± 0.384	103.2%	3.7%	0.803 ± 0.038	80.3%	4.8%

Table 2. Results of intra-day and inter-day accuracy and precision test of efavirenz

Expected (µg/mL)	Intra-day (n = 5)			Inter-day (n = 15)		
	Mean ± S.D., µg/mL	Accuracy	Precision	Mean ± S.D., µg/mL	Accuracy	Precision
0.30	0.311 ± 0.006	3.7%	1.9%	0.318 ± 0.023	6.0%	7.2%
3.00	3.070 ± 0.075	2.3%	2.4%	3.009 ± 0.066	0.3%	2.2%
10.00	10.473 ± 0.267	4.7%	2.6%	10.337 ± 0.229	3.4%	2.2%

Table 3. Demographic data and ART regimens, and influence on the efavirenz plasma concentrations

Factors	Categories	n	Percentage (%)	Mean \pm S.D. ($\mu\text{g/mL}$)	p
Gender	Male	364	89.7	2.18 \pm 1.89	0.646
	Female	42	10.3	2.46 \pm 2.40	
Age	< 60	374	92.1	2.20 \pm 1.96	0.641
	\geq 60	32	7.9	2.31 \pm 1.89	
BMI	< 25	105	25.7	2.23 \pm 2.32	0.529
	\geq 25	301	74.1	2.20 \pm 1.80	
ART regimens	Zidovudine + Lamivudine + Efavirenz	224	55.2	2.24 \pm 2.05	0.206
	Stavudine + Lamivudine + Efavirenz	109	26.8	2.27 \pm 2.07	
	Tenofovir + Lamivudine + Efavirenz	65	16.0	1.95 \pm 1.39	
	Others	8	2.0	2.53 \pm 1.16	

10.0 $\mu\text{g/mL}$ were 4.3%, 5.2%, and 3.6%, respectively, proving the stability of plasma samples at -20°C in at least 30 days.

3.6.4. Stability of freezing and thawing cycles

Three different concentrations samples of efavirenz (0.2, 3.0, 10.0 $\mu\text{g/mL}$) were prepared in blank human plasma and extracted after three times freezing and thawing cycles. The RSD of efavirenz at concentrations of 0.3, 3.0, and 10.0 $\mu\text{g/mL}$ were 7.7%, 4.1%, and 1.3%, respectively, proving the stability of plasma samples after exposing to three freeze-thaw cycles.

3.6.5. Stability of re-dissolved supernatants at ambient temperature

Efavirenz with blank plasma at concentrations of 0.2, 3.0, and 10.0 $\mu\text{g/mL}$ were dealt with according to the method described above. The supernatants were assessed for stability at ambient temperature at hour 0, 3, 6, and 12. The RSD of efavirenz concentration were 5.2%, 4.3%, and 2.0%, respectively, which proved the stability of re-dissolved supernatants in 12 h at ambient temperature.

3.7. Clinical application

Four hundred and six plasma samples of Chinese AIDS patients were dealt with and determined. The mean steady state trough concentration of the 406 patients was $2.21 \pm 1.95 \mu\text{g/mL}$, 77.3% of which were within the therapeutic window (1-4 $\mu\text{g/mL}$), 15.1% were below the window, and 7.6% were over it. The highest concentration was 14.89 $\mu\text{g/mL}$, 36 folds as the lowest concentration (0.41 $\mu\text{g/mL}$). Plasma efavirenz concentrations had no significant difference among the groups ($p > 0.05$) divided by the patients' gender, age, BMI and therapeutic regimen (Table 3).

4. Discussion

As mentioned above, although there are many methods

for determination of efavirenz in plasma, most of them have high requirements for equipments and technologies, hardly repeated in undeveloped countries. The method established in this paper, by RP-HPLC with UV detector, has a lower requirement for equipments compared to reported methods (17-25). In our method, diazepam was used as internal standard because of its cheapness, accessibility, and well-separated with efavirenz. But patients who take diazepam had to be excluded so as to avoid the interference on the results. For sample pretreatment, 100 μL plasma was mixed with 200 μL acetonitrile (with 1 $\mu\text{g/mL}$ diazepam) to precipitate protein, and the mixture was centrifuged and then the supernatant was directly injected into the HPLC system. In contrast to solid-phase extraction, liquid-liquid extraction (23,24,26-28,32-35,38,44-46), this method has advantages of simplicity, rapidity, economical and low requirement for plasma volume, suitable for pediatric patients. As shown in Figure 1, endogenous substances have no interference on the peak of efavirenz and diazepam, and the column pressure have no obvious rise after the determination of over 400 plasma samples, which indicated that plasma proteins could be precipitated completely in this method. The detection wavelength of 245, 246, 247, 250 nm were used in different methods (26,28,31,33). In our study, 100 $\mu\text{g/mL}$ solution of efavirenz standard were scanned by ultraviolet spectrophotometer ranging from 190-500 nm, and a maximum absorption was achieved at 247 nm with no interference, so 247 nm was chosen as detective wavelength.

As to mobile phase, complicated mobile phase and time-wasting gradient elution were reported. In this paper, we finally took 0.01 mol/L NaH_2PO_4 (containing 0.01 mol/L triethylamine, pH 5.2)-acetonitrile (38:62, V/V) as mobile phase after repeated attempts with reference to other reports (26,28,31,32). The addition of diluted phosphoric acid and triethylamine adjusted the pH of the mobile phase, improved the peak shapes of the efavirenz and diazepam. Under the chromatographic conditions described above, the system run time was 7.5 min and efavirenz was well-separated from internal standard

diazepam with good peak shapes. The retention times of efavirenz and diazepam were 6.475 min and 4.535 min, respectively. Figure 1 showed that blank plasma samples had no peak near the retention time of efavirenz and diazepam. No endogenous substances or other co-administered drugs such as zidovudine, lamivudine, stavudine, tenofovir, ritonavir, lopinavir, fluconazole, voriconazole, and rifampicin interfered with the chromatogram of efavirenz and diazepam. The standard curve parameters of efavirenz concentrations ranging from 0.10 to 16.0 µg/mL showed a linear relationship between peak area and concentrations. The absolute recoveries of efavirenz at a concentration of 0.3, 3.0, and 10.0 were 75.6%, 77.7%, and 80.3%, while the relative recovery were 106%, 99.3%, and 103%, respectively. The intra-day and inter-day RSD for standards at a concentration of 0.3, 3.0, and 10.0 µg/mL ranged from 1.9 to 2.6% and 2.2 to 7.2%. The lowest detection limit and limit of quantification estimated mathematically from the standard curve equation were 27 ng/mL and 89 ng/mL, respectively. Via the tests on the repetitiveness, accuracy and the stability, supposed this method was reliable.

The mean efavirenz concentration of 406 Chinese AIDS patients was 2.21 ± 1.95 µg/mL, which was in accordance with two other published papers related to Chinese patients (13,52), but a little lower than that of Spanish (2.27 µg/mL) (53). Of all the plasma samples, 77.3% were within the therapeutic window of 1-4 µg/mL, 15.1% below 1 µg/mL, and 7.6% over 4 µg/mL, which showed that a considerable proportion of Chinese patients might have a higher risk of treatment failure or ADR. There was no significant difference of plasma efavirenz concentrations among the groups divided according to gender, age, BMI, and ART regimens, which indicated that efavirenz concentrations would not be influenced by demographic backgrounds or regimens in Chinese patients. It had been reported that the main reason leading to wide intra- and inter-individual variability of plasma efavirenz concentrations was the polymorphism of *CYP2B6* gene. For example, *CYP2B6* 516 G>T, a SNP highly related to the concentration of efavirenz, has a high mutation frequency. In Chinese, the mutation frequency of the SNP was at a higher level, 18-35% from different reports (52,54-56). This may well explain part of the difference in plasma efavirenz concentrations in Chinese AIDS patients. Therefore, in virtue of the great difference in pharmacodynamics and pharmacokinetics of efavirenz among races and individuals, the close relationship between therapeutic effects or side effects and its plasma concentration, and the higher prices of efavirenz, the dose of efavirenz should be individualized on the basis of therapeutic drug monitoring for patients with high frequency of *CYP2B6*, so as to improve therapeutic efficacy, to reduce the incidence of ADR, and to cut public health expenditure.

In conclusion, with its simplicity, fastness, accuracy

and reliability, the method introduced above is suitable for therapeutic drug monitoring and pharmacokinetic study of efavirenz, especially in economically challenged countries. Chinese AIDS patients, with the great inter-individual difference of plasma efavirenz concentrations, need therapeutic drug monitoring when taking efavirenz.

Acknowledgements

This work was supported by the 12th Five-year Plan, the People's Republic of China (NO: 2012ZX10001003); the 12th Five-Year Major New Drug Discovery Science and Technology: Technology Platform Construction of anti-HIV drugs clinical evaluation (NO: 2012ZX09303013), the People's Republic of China; and Shanghai municipal natural science foundation (14ZR1434900). We thank all the patients and research assistants for their cooperation.

References

1. Bock P, Fatti G, Grimwood A. Comparing the effectiveness of efavirenz and nevirapine for first-line antiretroviral therapy in a South African multicentre cohort. *Int Health*. 2013; 5:132-138.
2. Ward BA, Gorski JC, Jones DR, Hall SD, Flockhart DA, Desta Z, Gorski JC, Jones DR. The cytochrome P4502B6 (*CYP2B6*) is the main catalyst of efavirenz primary and secondary metabolism: Implication for HIV/AIDS therapy and utility of efavirenz as a substrate marker of *CYP2B6* catalytic activity. *J Pharmacol Exp Ther*. 2003; 306:287-300.
3. Stahle L, Moberg L, Svensson JO, Sonnerborg A. Efavirenz plasma concentrations in HIV-infected patients - Inter- and intraindividual variability and clinical effects. *Ther Drug Monit*. 2004; 26:267-270.
4. Aurpibul L, Chotirosniramit N, Sugandhavesa P, Kosashunhanan N, Thetket S, Supindham T, Piyamongkol W, Supparatpinyo K. Correlation of *CYP2B6*-516 G>T Polymorphism with Plasma Efavirenz Concentration and Depression in HIV-Infected Adults in Northern Thailand. *Curr HIV Res*. 2012; 10:653-660.
5. Desta Z, Saussele T, Ward B, Blievernicht J, Li L, Klein K, Flockhart D, Zanger UM. Impact of *CYP2B6* polymorphism on hepatic efavirenz metabolism *in vitro*. *Pharmacogenomics*. 2007; 8:547-558.
6. Nyakutira C, Roshammar D, Chigutsa E, Chonzi P, Ashton M, Nhachi C, Masimirembwa C. High prevalence of the *CYP2B6* 516G -> T(*6) variant and effect on the population pharmacokinetics of efavirenz in HIV/AIDS outpatients in Zimbabwe. *Eur J Clin Pharmacol*. 2008; 64:357-365.
7. Marzolini C, Telenti A, Decosterd LA, Greub G, Biollaz J, Buclin T. Efavirenz plasma levels can predict treatment failure and central nervous system side effects in HIV-1-infected patients. *Aids*. 2001; 15:71-75.
8. Gutierrez F, Navarro A, Padilla S, Anton R, Masia M, Borrás J, Martín-Hidalgo A. Prediction of neuropsychiatric adverse events associated with long-term efavirenz therapy, using plasma drug level monitoring. *Clin Infect Dis*. 2005; 41:1648-1653.
9. Yimer G, Amogne W, Habtewold A, Makonnen E, Ueda N, Suda A, Worku A, Haefeli WE, Burhenne J, Aderaye

- G, Lindquist L, Aklillu E. High plasma efavirenz level and *CYP2B6*(*)6 are associated with efavirenz-based HAART-induced liver injury in the treatment of naive HIV patients from Ethiopia: a prospective cohort study. *Pharmacogenomics J*. 2012; 12:499-506.
10. Langmann P, Weissbrich B, Desch S, Vath T, Schirmer D, Zilly M, Klinker H. Efavirenz plasma levels for the prediction of treatment failure in heavily pretreated HIV-1 infected patients. *Eur J Med Res*. 2002; 7:309-314.
 11. Kappelhoff BS, van Leth F, Robinson PA, MacGregor TR, Baraldi E, Montella F, Uip DE, Thompson MA, Russell DB, Lange JMA, Beijnen JH, Huitema ADR, 2NN Study Group. Are adverse events of nevirapine and efavirenz related to plasma concentrations? *Antivir Ther (Lond)*. 2005; 10:489-498.
 12. Mukonzo JK, Okwera A, Nakasujja N, Luzze H, Sebuwufu D, Ogwal-Okeng J, Waako P, Gustafsson LL, Aklillu E. Influence of efavirenz pharmacokinetics and pharmacogenetics on neuropsychological disorders in Ugandan HIV-positive patients with or without tuberculosis: a prospective cohort study. *BMC Infect Dis*. 2013; 13:261.
 13. Sun J, Chen J, Yao Y, Zhang R, Zheng Y, Liu L, Zhang L, Shen Y, Lu H. Minimum effective plasma concentration of efavirenz in treatment-naive Chinese HIV-infected patients. *Int J STD AIDS*. 2010; 21:810-813.
 14. Johnson DH, Gebretsadik T, Shintani A, Mayo G, Acosta EP, Stein CM, Haas DW. Neuropsychometric correlates of efavirenz pharmacokinetics and pharmacogenetics following a single oral dose. *Br J Clin Pharmacol*. 2013; 75:997-1006.
 15. Solas C, Gagnieu MC. Evidence-based therapeutic drug monitoring for efavirenz. *Therapie*. 2011; 66:197-205.
 16. Rotger M, Telenti A. Optimizing efavirenz treatment: *CYP2B6* genotyping or therapeutic drug monitoring? *Eur J Clin Pharmacol*. 2008; 64:335-336.
 17. Rouzes A, Berthoin K, Xuereb F, Djabarouti S, Pellegrin I, Pellegrin JL, Coupet AC, Augagneur S, Budzinski H, Saux MC, Breilh D. Simultaneous determination of the antiretroviral agents: amprenavir, lopinavir, ritonavir, saquinavir and efavirenz in human peripheral blood mononuclear cells by high-performance liquid chromatography-mass spectrometry. *J Chromatogr B Analyt Technol Biomed Life Sci*. 2004; 813:209-216.
 18. Martin J, Deslandes G, Dailly E, Renaud C, Reliquet V, Raffi F, Jolliet P. A liquid chromatography-tandem mass spectrometry assay for quantification of nevirapine, indinavir, atazanavir, amprenavir, saquinavir, ritonavir, lopinavir, efavirenz, tipranavir, darunavir and maraviroc in the plasma of patients infected with HIV. *J Chromatogr B Analyt Technol Biomed Life Sci*. 2009; 877:3072-3082.
 19. Avery LB, Parsons TL, Meyers DJ, Hubbard WC. A highly sensitive ultra performance liquid chromatography-tandem mass spectrometric (UPLC-MS/MS) technique for quantitation of protein free and bound efavirenz (EFV) in human seminal and blood plasma. *J Chromatogr B Analyt Technol Biomed Life Sci*. 2010; 878:3217-3224.
 20. Kim KB, Kim H, Jiang F, Yeo C-W, Bae SK, Desta Z, Shin JG, Liu KH. Rapid and simultaneous determination of efavirenz, 8-hydroxyefavirenz, and 8,14-dihydroxyefavirenz using LC-MS-MS in human plasma and application to pharmacokinetics in healthy volunteers. *Chromatographia*. 2011; 73:263-271.
 21. Notari S, Mancone C, Alonzi T, Tripodi M, Narciso P, Ascenzi P. Determination of abacavir, amprenavir, didanosine, efavirenz, nevirapine, and stavudine concentration in human plasma by MALDI-TOF/TOF. *J Chromatogr B Analyt Technol Biomed Life Sci*. 2008; 863:249-257.
 22. Matthews CZ, Woolf EJ, Mazenko RS, Haddix-Wiener H, Chavez-Eng CM, Constanzer ML, Doss GA, Matuszewski BK. Determination of efavirenz, a selective non-nucleoside reverse transcriptase inhibitor, in human plasma using HPLC with post-column photochemical derivatization and fluorescence detection. *J Pharm Biomed Anal*. 2002; 28:925-934.
 23. Langmann P, Schirmer D, Vath T, Zilly M, Klinker H. High-performance liquid chromatographic method for the determination of HIV-1 non-nucleoside reverse transcriptase inhibitor efavirenz in plasma of patients during highly active antiretroviral therapy. *J Chromatogr B Biomed Sci Appl*. 2001; 755:151-156.
 24. Poirier J-M, Robidou P, Jaillon P. Simple and simultaneous determination of the hiv-protease inhibitors amprenavir, atazanavir, indinavir, lopinavir, nelfinavir, ritonavir and saquinavir plus M8 nelfinavir metabolite and the nonnucleoside reverse transcriptase inhibitors efavirenz and nevirapine in human plasma by reversed-phase liquid chromatography. *Ther Drug Monit*. 2005; 27:186-192.
 25. Dogan-Topal B, Ozkan SA, Uslu B. Simultaneous determination of abacavir, efavirenz and valganciclovir in human serum samples by isocratic HPLC-DAD detection. *Chromatographia*. 2007; 66:S25-S30.
 26. Saras-Nacenta M, López-Púa Y, López-Cortés LF, Mallolas J, Gatell JM, Carné X. Determination of efavirenz in human plasma by high-performance liquid chromatography with ultraviolet detection. *J Chromatogr B Biomed Sci Appl*. 2001; 763:53-59.
 27. Sailaja AL, Kumar KK, Kumar DVRR, Kumar CM, Yugandhar NM, Srinubabu G. Development and validation of a liquid chromatographic method for determination of efavirenz in human plasma. *Chromatographia*. 2007; 65:359-361.
 28. Ramachandran G, Kumar AKH, Swaminathan S, Venkatesan P, Kumaraswami V, Greenblatt DJ. Simple and rapid liquid chromatography method for determination of efavirenz in plasma. *J Chromatogr B Analyt Technol Biomed Life Sci*. 2006; 835:131-135.
 29. Veldkamp AI, van Heeswijk RP, Meenhorst PL, Mulder JW, Lange JM, Beijnen JH, Hoetelmans RM. Quantitative determination of efavirenz (DMP 266), a novel non-nucleoside reverse transcriptase inhibitor, in human plasma using isocratic reversed-phase high-performance liquid chromatography with ultraviolet detection. *J Chromatogr B Biomed Sci Appl*. 1999; 734:55-61.
 30. Villani P, Pregolato M, Banfo S, Rettani M, Burrioni D, Seminari E, Maserati R, Regazzi MB. High-performance liquid chromatography method for analyzing the antiretroviral agent efavirenz in human plasma. *Ther Drug Monit*. 1999; 21:346-350.
 31. Mogatle S, Kanfer I. Rapid method for the quantitative determination of efavirenz in human plasma. *J Pharm Biomed Anal*. 2009; 49:1308-1312.
 32. Takahashi M, Yoshida M, Oki T, Okumura N, Suzuki T, Kaneda T. Conventional HPLC method used for simultaneous determination of the seven HIV protease inhibitors and nonnucleoside reverse transcription inhibitor efavirenz in human plasma. *Biol Pharm Bull*. 2005; 28:1286-1290.

33. Fox D, O'Connor R, Mallon P, McMahon G. Simultaneous determination of efavirenz, rifampicin and its metabolite desacetyl rifampicin levels in human plasma. *J Pharm Biomed Anal.* 2011; 56:785-791.
34. Aymard G, Legrand M, Trichereau N, Diquet B. Determination of twelve antiretroviral agents in human plasma sample using reversed-phase high-performance liquid chromatography. *J Chromatogr B Biomed Sci Appl.* 2000; 744:227-240.
35. Titier K, Lagrange E, Pehourcq F, Edno-Mcheik L, Moore N, Molimard M. Simultaneous assay of antiretroviral drugs in human plasma by high performance liquid chromatography. *Therapie.* 2002; 57:169-174.
36. Boffito M, Tija J, Reynolds HE, Hoggard PG, Bonora S, Di Perri G, Back DJ. Simultaneous determination of rifampicin and efavirenz in plasma. *Ther Drug Monit.* 2002; 24:670-674.
37. Cociglio M, Hillaire-Buys D, Peyrière H, Alric R. Performance analysis of a rapid HPLC determination with the solvent demixing extraction of HIV antiproteases and efavirenz in plasma. *J Chromatogr Sci.* 2003; 41:80-86.
38. Kappelhoff BS, Rosing H, Huitema ADR, Beijnen JH. Simple and rapid method for the simultaneous determination of the non-nucleoside reverse transcriptase inhibitors efavirenz and nevirapine in human plasma using liquid chromatography. *J Chromatogr B Analyt Technol Biomed Life Sci.* 2003; 792:353-362.
39. Keil K, Frerichs VA, DiFrancesco R, Morse G. Reverse phase high-performance liquid chromatography method for the analysis of amprenavir, efavirenz, indinavir, lopinavir, nelfinavir and its active metabolite (M8), ritonavir, and saquinavir in heparinized human plasma. *Ther Drug Monit.* 2003; 25:340-346.
40. Dailly E, Raffi F, Jolliet P. Determination of atazanavir and other antiretroviral drugs (indinavir, amprenavir, nelfinavir and its active metabolite M8, saquinavir, ritonavir, lopinavir, nevirapine and efavirenz) plasma levels by high performance liquid chromatography with UV detection. *J Chromatogr B Analyt Technol Biomed Life Sci.* 2004; 813:353-358.
41. Choi SO, Rezk NL, Kashuba ADM. High-performance liquid chromatography assay for the determination of the HIV-protease inhibitor tipranavir in human plasma in combination with nine other antiretroviral medications. *J Pharm Biomed Anal.* 2007; 43:1562-1567.
42. Marzolini C, Telenti A, Buclin T, Biollaz J, Decosterd LA. Simultaneous determination of the HIV protease inhibitors indinavir, amprenavir, saquinavir, ritonavir, nelfinavir and the non-nucleoside reverse transcriptase inhibitor efavirenz by high-performance liquid chromatography after solid-phase extraction. *J Chromatogr B Biomed Sci Appl.* 2000; 740:43-58.
43. Notari S, Bocedi A, Ippolito G, Narciso P, Pucillo LP, Tossini G, Donnorso RP, Gasparrini F, Ascenzi P. Simultaneous determination of 16 anti-HIV drugs in human plasma by high-performance liquid chromatography. *J Chromatogr B Analyt Technol Biomed Life Sci.* 2006; 831:258-266.
44. Rezk NL, Tidwell RR, Kashuba ADM. High-performance liquid chromatography assay for the quantification of HIV protease inhibitors and non-nucleoside reverse transcriptase inhibitors in human plasma. *J Chromatogr B Analyt Technol Biomed Life Sci.* 2004; 805:241-247.
45. Simon VA, Thiam MD, Lipford LC. Determination of serum levels of thirteen human immunodeficiency virus-suppressing drugs by high-performance liquid chromatography. *J Chromatogr A.* 2001; 913:447-453.
46. Titier K, Lagrange F, Péhourcq F, Edno-Mcheik L, Moore N, Molimard M. High-performance liquid chromatographic method for the simultaneous determination of the six HIV-protease inhibitors and two non-nucleoside reverse transcriptase inhibitors in human plasma. *Ther Drug Monit.* 2002; 24:417-424.
47. Turner ML, Reed-Walker K, King JR, Acosta EP. Simultaneous determination of nine antiretroviral compounds in human plasma using liquid chromatography. *J Chromatogr B Analyt Technol Biomed Life Sci.* 2003; 784:331-341.
48. Usami Y, Oki T, Nakai M, Sagisaka M, Kaneda T. A simple HPLC method for simultaneous determination of lopinavir, ritonavir and efavirenz. *Chem Pharm Bull.* 2003; 51:715-718.
49. Weller DR, Brundage RC, Balfour HH Jr, Vezina HE. An isocratic liquid chromatography method for determining HIV non-nucleoside reverse transcriptase inhibitor and protease inhibitor concentrations in human plasma. *J Chromatogr B Analyt Technol Biomed Life Sci.* 2007; 848:369-373.
50. Hirabayashi Y, Tsuchiya K, Kimura S, Oka S. Simultaneous determination of six HIV protease inhibitors (amprenavir, indinavir, lopinavir, nelfinavir, ritonavir and saquinavir), the active metabolite of nelfinavir (M8) and non-nucleoside reverse transcriptase inhibitor (efavirenz) in human plasma by high-performance liquid chromatography. *Biomed Chromatogr.* 2006; 20:28-36.
51. Donnerer J, Kronawetter M, Kapper A, Haas I, Kessler HH. Therapeutic drug monitoring of the HIV/AIDS drugs abacavir, zidovudine, efavirenz, nevirapine, indinavir, lopinavir, and nelfinavir. *Pharmacology.* 2003; 69:197-204.
52. To KW, Liu ST, Cheung SW, Chan DPC, Chan RCY, Lee SS. Pharmacokinetics of plasma efavirenz and *CYP2B6* polymorphism in southern Chinese. *Ther Drug Monit.* 2009; 31:527-530.
53. Rodriguez-Novoa S, Barreiro P, Rendón A, Jiménez-Nacher I, González-Lahoz J, Soriano V. Influence of 516G>T polymorphisms at the gene encoding the *CYP450-2B6* isoenzyme on efavirenz plasma concentrations in HIV-infected subjects. *Clin Infect Dis.* 2005; 40:1358-1361.
54. Xu BY, Guo LP, Lee SS, Dong QM, Tan Y, Yao H, Li LH, Lin CK, Kung HF, He ML. Genetic variability of *CYP2B6* polymorphisms in four southern Chinese populations. *World J Gastroenterol.* 2007; 13:2100-2103.
55. Guan S, Huang M, Li X, Chen X, Chan E, Zhou SF. Intra- and inter-ethnic differences in the allele frequencies of cytochrome P450 2B6 gene in Chinese. *Pharm Res.* 2006; 23:1983-1990.
56. Guan S, Huang M, Chan E, Chen X, Duan W, Zhou SF. Genetic polymorphisms of cytochrome P4502B6 gene in Han Chinese. *Eur J Pharm Sci.* 2006; 29:14-21.

(Received January 9, 2014; Revised July 29, 2014; Accepted August 1, 2014)

A case of advanced lung cancer with malignant pericardial effusion treated by intrapericardial Cinobufacini injection instillation

Tao Sun, Yuhua Zhang, Yang Shen, Kaiwen Hu*, Minghuan Zuo*

Oncology Department, Dongfang Hospital, Beijing University of Chinese Medicine, Beijing, China.

Summary

Malignant pericardial effusion is one of the severe complications in advanced lung cancer patients, seriously affecting the patient's cardiopulmonary function and even life. Pericardial drainage and instillation of anti-neoplastic drugs in the pericardial cavity seems to offer the best chance of controlling pericardial effusion. We reported a case concerning treatment of a 63-year-old man in advanced lung cancer with a large amount of pericardial effusion. We utilized pericardium puncture and drainage combined with instillation of Cinobufacini injection in the pericardial cavity to treat pericardial effusion. After treatment with Cinobufacini injection for two weeks, the patient was followed up in one month to assess effectiveness, quality of life, and safety. We found that the cardiac tamponade symptoms such as difficult breathing, chest distress, and palpitations were significantly relieved. The patient's quality of life was effectively improved with KPS scores increased. We also found that the levels of tumor marker CA-125 in the pericardial effusion decreased (from 340.80 U/mL to 34.85 U/mL) and pericardium B ultrasound showed that the quantity of pericardial effusion reduced significantly (from 2.5 cm to 0.6 cm). Furthermore, there were little gastrointestinal adverse reactions and myelosuppression in the patient after instillation of the Cinobufacini injection. Taken together, this provides a new way for treating cancerous pericardial effusion, especially for patients who cannot tolerate instillation of chemotherapy drugs, and is worthwhile to carry out more standardized studies in the future.

Keywords: Cinobufacini injection, malignant pericardial effusion, advanced lung cancer, intrapericardial instillation

1. Introduction

Lung cancer is the leading cause of cancer-related mortality in men and women throughout the world and contributes approximately 1.37 million deaths per year worldwide (1). A series of complications occurs in advanced lung cancer, including malignant pleural effusion, pericardial effusion, central airway

obstruction, and superior vena cava syndrome, which threatens life and necessitates urgent palliation (2). As one of the most common complications of advanced lung cancer, malignant pericardial effusion often leads to chronic cardiac tamponade and obstinate cardiac insufficiency, seriously affecting the patients' cardiopulmonary function and even life (3). Recently, various approaches have been proposed to prevent occurrence of pericardial effusion: extended drainage, pericardial window, sclerosing local therapy, local and/or systemic chemotherapy, and radiation therapy (4). For advanced lung cancer with pericardial effusion, pericardial drainage and the use of local anti-neoplastic therapy seems to offer the best chance of controlling effusion. Local instillation of anti-neoplastic agents (e.g., cisplatin) is used to cure the metastases rather than simply prevent effusion by drainage with short-term effective rates at 76-100% (5,6). Although local

Released online in J-STAGE as advance publication July 20, 2014.

*Address correspondence to:

Oncology Department, Dongfang Hospital, Beijing University of Chinese Medicine, Beijing, China. No. 6, District 1, Fangxingyuan, Fangzhuang, Fengtai District, Beijing 100078, China.

E-mail: kaiwenh@163.com (Dr. Hu KW)

zuomh@263.net (Dr. Zuo MH)

instillation of chemotherapy is extremely effective, there are different levels of digestive tract, liver and kidney damage and blood toxicity reactions and other adverse reactions (6). Thus, it is urgent to look for novel anti-neoplastic agents to treat pericardial effusion. Recently, traditional Chinese medicines have attracted attention as candidates for treating malignant pericardial effusion opening a new research direction.

Cinobufacini injection or Huachansu injection, an aqueous extract from the skin and parotid venom glands of the toad (*Bufo bufo gargarizans* Cantor) that contains Chansu, is a Chinese medicine preparation widely used in clinical cancer therapy in China (7). Cinobufacini injection used alone or in combination with other chemotherapeutic agents (e.g., gemcitabine and oxaliplatin) have significant anticancer activity against many human cancers, such as non-small-cell lung cancer. It can improve the patients' quality of life and even effectively reduce tumor shrinkage with little toxicity (8). However, there are few reports about treating malignant pericardial effusion by instillation of Cinobufacini injection. In our department, pericardium puncture and pericardial cavity instillation of Cinobufacini injection using indwelling catheter drainage were performed for treating one advanced lung cancer patient with malignant pericardial effusion. The effect was satisfactory with good safety. Now the case report is presented as follows.

2. Case report

The patient was a 63-year-old man. Three years ago, he underwent a right lower pulmonary lobectomy because of lung space-occupying lesions according to CT examination results. The post-operative course was uneventful and pathology showed squamous carcinoma. After the operation, the patient received radiotherapy 30 times and six cycles of chemotherapy with regimens of gemcitabine with cisplatin, and the process of radiotherapy and chemotherapy went smoothly. Two years ago, the patient went to Cancer Institute & Hospital, Chinese Academy of Medical Sciences re-checking with chest CT examination and the results showed right side pleural effusion with a new and small amount of pericardial effusion. Since the symptoms including dyspnea, cough, and being flustered was not evident at that time, the patient didn't accept any systematic therapy for pericardial effusion. A month later, the patient felt that symptoms such as dyspnea, cough, and being flustered became more serious than before, so he came to our hospital for a re-check. We found that the patient had no history of heart failure but was associated with different levels of cardiac tamponade symptoms and signs such as difficulty in breathing, being flustered, coughing repeatedly, orthopnea, distension of the jugular vein, heart enlargement, etc. Chest CT examination showed right

side pleural effusion with a large amount of pericardial effusion and the heart B-ultrasound showed that the effusion had a length-diameter more than 2.0 cm (Note: the effusion quantity detected by echocardiography is commonly classified based on the method proposed by Dr. Weitzman (9), a small amount of effusion is defined as the maximum diastole dark space in the pericardial cavity < 1.0 cm while 1.0-1.9 cm for the medium amount of effusion, > 2.0 cm for a large amount of effusion). Furthermore, the level of CA-125 (340.80 U/mL) was extremely increased in the pericardial effusion. At the same time, no acid fast bacilli or toxic symptoms of TB were detected in pericardial effusion. Taken together, according to the patient's symptoms and signs and auxiliary examinations such as chest CT or pericardium B ultrasound, the diagnosis was clear: the patient showed phase IV advanced lung cancer with a large amount of pericardial effusion.

After being diagnosed, the patient was hospitalized in our department many times to improve pericardial effusion. First, the pericardium puncture was guided by ultrasonic probe positioning and a central venous catheter was indwelled for drainage. Briefly, after the puncture point was located by B ultrasound, the needle was inserted into the patient until the effusion was taken out and a guide wire was implanted slowly from the end of the needle puncture, and then the central venous catheter was entered into the pericardial cavity within 10 to 15 cm along with the guide wire, and finally the guide wire was pulled out and the central venous catheter was fixed for continuous drainage. Second, after drainage, the pericardium B ultrasound was performed to confirm if the pericardial effusion had completely drained out (the residual effusion in the pericardial cavity ≤ 0.2 cm), and then 40 mL of Cinobufacini injection was injected into the pericardial cavity. Finally, the catheter was closed and fastened, and the patient was advised repeatedly to change positions in order to ensure a maximum contact area between the drug and the inner pericardial cavity. Treatment took place twice per week with a course every two weeks. After treatment with a Cinobufacini injection course and one month later, the patient was followed up to assess effectiveness, quality of life, and safety. Furthermore, routine physical examinations, lab tests including blood routines, tumor markers in the pericardial effusion such as CA-125 and CEA, and morphologic imaging tests were performed during each follow-up. The response to Cinobufacini injection in treatment of malignant serous membrane cavity effusion was assessed using the WHO criteria (1979) as follows: (i) Complete response (CR): It was defined as effusion disappears entirely maintaining for at least 4 weeks according to clinical examination, chest radiography, CT or echocardiogram; (ii) Partial response (PR): It was defined as effusion reduced by more than 50% maintaining for at least 4 weeks; (iii) No remission (NR): It was defined as effusion beyond control or the effusion

Table 1. The results of intrapericardial instillation of Cinobufacini injection for malignant pericardial effusion

Items	Before Cinobufacini injection instillation	After Cinobufacini injection instillation one month later
Symptoms	Difficult breathing, chest distress, and palpitations	Difficult breathing relieved, no chest distress and palpitations
KPS scores	50 points	80 points
Blood routine	WBC: $7.36 \times 10^9/L$ (N); RBC: $1.63 \times T/L$ (L); HGB: 55 g/L (L)	WBC: $6.51 \times 10^9/L$ (N); RBC: $2.33 \times T/L$ (L); HGB: 85 g/L (L)
Tumor markers	CA-125: 340.80 U/mL (H); CEA: 2.07 ng/mL (N); NSE: 1.65 ng/mL (N)	CA-125: 34.85 U/mL (N); CEA: 2.25 ng/mL (N); NSE: 8.35 ng/mL (N)
Pericardium B ultrasound	Quantity of pericardial effusion: 2.5 cm	Quantity of pericardial effusion: 0.6 cm

Note: N means normal, L means low, and H means high.

quantity reduced less than 50% (10). The effective rate was worked out by CR + PR. Quality of life was assessed using Karnofsky performance scale (KPS) scores with a score from 0 to 100, where 0 is dead and 100 is completely normal (11). The safety profile was assessed by recording: adverse events, physical examinations, and lab and imaging tests.

The process of pericardium puncture was successful and the patient did not experience any adverse effects including complications of drainage insertion, or infection with indwelling pericardial catheters after puncture. Furthermore, the patient was steady without any discomfort in the process of continuous drainage. After Cinobufacini injection instillation, adverse reactions such as pain, gastrointestinal reactions, shock, infection, hemorrhage, arrhythmia and pulse pause, acute pulmonary edema and heart failure did not occur.

After treatment with Cinobufacini injection for two weeks, the patient was followed up one month to assess effectiveness, quality of life, and safety. The treatment outcomes of the patient are summarized in Table 1. The cardiac tamponade symptoms were significantly relieved and symptoms such as difficult breathing, chest distress, and palpitations were eased with KPS scores increased to 80 points. Blood routine examinations showed that there was no myelosuppression with hemoglobin (HGB) increased from 55 g/L to 85 g/L. The levels of tumor marker CA-125 in pericardial effusion decreased from 340.80 U/mL to 34.85 U/mL and the levels of tumor marker CEA were normal. Pericardium B ultrasound showed that the quantity of pericardial effusion was significantly reduced. The maximum diastole dark space in the pericardial cavity decreased from 2.5 cm to 0.6 cm (Figure 1). That is to say, that pericardial effusion was reduced by more than 50% maintaining more than 4 weeks. The clinical response to treatment was PR.

3. Discussion

Malignant pericardial effusion is one of the severe

complications in advanced lung cancer patients. It often affects circulatory and respiratory functions rapidly causing difficulty in breathing, fluttering, shortness of breath, chest distress, cough, inability to be supine, heart failure and even death. It seriously affects the patient's survival and quality of life (3). Thus, the immediate control of pericardial effusions is mandatory for both survival and an improvement in the performance status and the quality of life of patients. Pericardium puncture and drainage could effectively relieve the above symptoms, however, if only simple pericardial drainage is performed, effusion recurrences can be observed in up to 40% of cases (12). Instillation of cytotoxic chemotherapy drugs in the pericardial cavity is most commonly used, which can kill tumor cells directly and eliminate the effusion. However, because of the limited efficacy of existing chemotherapy drugs, obvious toxicity, and easily relapsed malignant pericardial effusion, patient's quality of life, treatment and prognosis are significantly affected (13). Therefore, it is a big issue or challenge to control the malignant pericardial effusion clinically and an urgent need is to actively seek new efficient low-toxicity drugs.

In recent years, many traditional Chinese medicines have been shown to have potent anti-cancer effects and have attracted considerable interest as potential candidates for the development of novel cancer therapeutics. Chansu is a traditional Chinese medicine obtained from the post-auricular and skin glands of *Bufo bufo gargarizans* Cantor, which has been used to treat conditions like swelling, pain, and heart failure for thousands of years in China and has recently been used for treatment of cancer because of its anti-cancer effects (14). Cinobufacini, a traditional Chinese medicine containing the water-soluble components of Chansu, exhibits a variety of biological activities, such as anesthetic, anodyne, antimicrobial, cardioactive, and antineoplastic properties (15). Currently, Cinobufacini has been developed into a variety of dosage forms such as tablets, oral solutions, and injections which

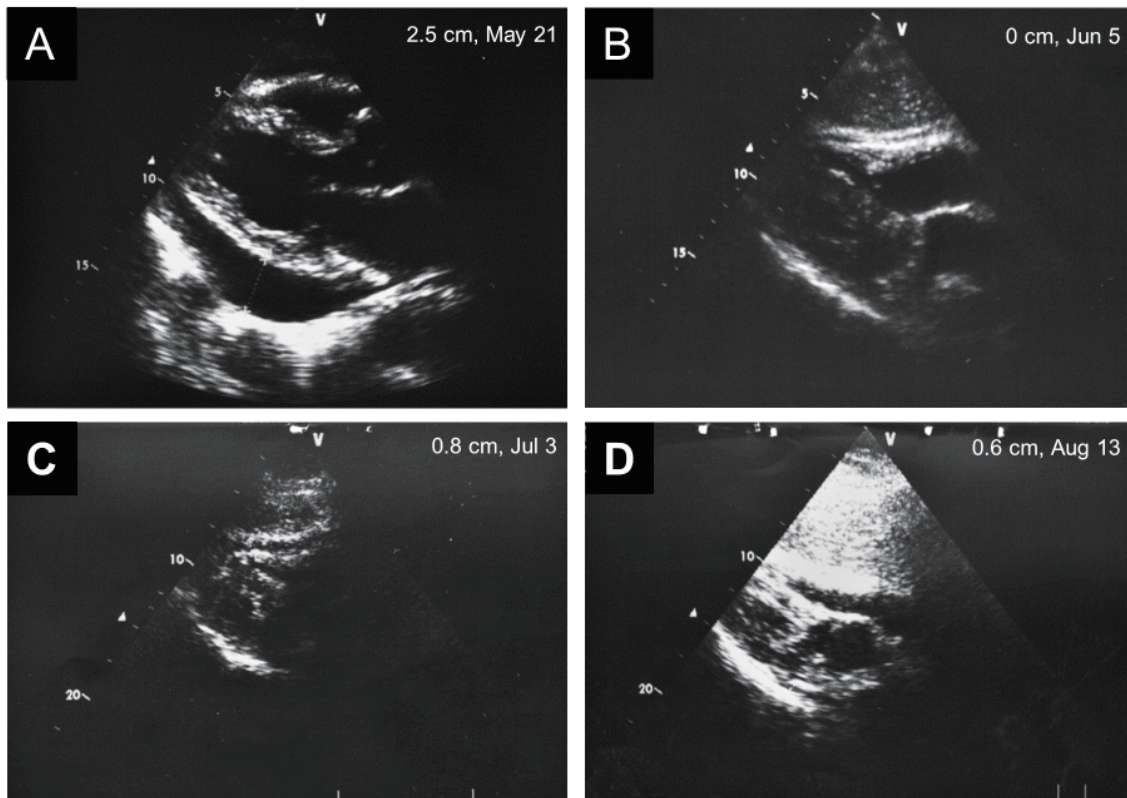


Figure 1. Quantitative assessment of pericardial effusion size in the patient was detected by pericardium B ultrasound, which was usually defined as the maximum diastole dark space in the pericardial cavity. (A) The quantity of pericardial effusion before pericardium puncture (2.5 cm); **(B)** The quantity of pericardial effusion after drainage (0 cm); **(C)** The quantity of pericardial effusion after instillation of Cinobufacini injections two weeks later (0.8 cm); **(D)** The quantity of pericardial effusion after instillation of Cinobufacini injections one month later (0.6 cm).

are approved by the Chinese State Food and Drug Administration (SFDA) and widely used to treat patients with lung, liver, colon, and pancreatic cancers at oncology clinics in China (7,8). It could effectively inhibit cell proliferation, induction of cell differentiation and apoptosis, disruption of the cell cycle, inhibition of cancer angiogenesis, reversal of multi-drug resistance, and regulation of the immune response in cancer cells (14). It also could effectively enhance physical immunity and improve the quality of life with little toxicity in cancer patients.

Recently, Cinobufacini injection has been reported to be effective for treating malignant pleural effusions and ascites. Zhang *et al.* found that symptoms such as cough, chest pain, difficult breathing, and chest distress were significantly relieved and the cancer patients' quality of life was improved after intrapleural instillation of Cinobufacini injection with little gastrointestinal adverse reactions, myelosuppression and nephrotoxicity (16). Furthermore, Cinobufacini injection in combination with Cisplatin treating malignant pleural effusions by intrapleural instillation exhibited great synergistic action while improving efficiency and reducing the toxicity of Cisplatin (17). Ran reported that Cinobufacini injection in combination with BCG-polysaccharide nucleic acid treating malignant pleural effusions and ascites was effective for improving

KPS scores with little adverse reaction (18). Taken together, instillation of Cinobufacini injection might be an effective therapy for malignant pleural effusions and ascites, especially for the patients who could not tolerate instillation of chemotherapy drugs. However, there are few reports on instillation of Cinobufacini injection treating malignant pericardial effusion. In the current study, we utilized pericardium puncture and drainage combined with instillation of Cinobufacini injection in the pericardial cavity to treat one advanced lung cancer patient with malignant pericardial effusion. The effect was satisfactory with good safety. We found that the cardiac tamponade symptoms such as difficult breathing, chest distress, and palpitations were significantly relieved after treatment with Cinobufacini injection. The patient's quality of life was effectively improved with KPS scores increased. We also found that the levels of tumor marker CA-125 in pericardial effusion decreased and pericardium B ultrasound showed that the quantity of pericardial effusion was significantly reduced. Furthermore, there were little gastrointestinal adverse reactions and myelosuppression in the patient after instillation of Cinobufacini injection in the pericardial cavity.

To sum up, the current case report indicates that Cinobufacini injection instillation therapy is likely to become a new option for advanced lung cancer patients

with malignant pericardial effusion. It is easy to perform with little adverse reactions. It can relieve the patient's suffering and improve quality of life. It provides a new way for treatment of cancerous pericardial effusion, especially for patients who cannot tolerate instillation of chemotherapy drugs, and it is worthwhile to carry out clinical observations using a larger group of patients and further standardized studies in the future.

Acknowledgements

This project was supported by the National Natural Science Fund of China (No. 81373832).

References

- World Health Organization. Cancer, 2013. <http://www.who.int/mediacentre/factsheets/fs297/en/> (Accessed May 23, 2014).
- Gompelmann D, Eberhardt R, Herth FJ. Advanced malignant lung disease: What the specialist can offer. *Respiration*. 2011; 82:111-123.
- Jiang QA, Zhou YD, Cheng GE, Gong FY, Zhang SY, Lang FP, Zhao MH. Clinical observation on pericardial effusion in patients with lung cancer treated by intrapericardial catheterization and infusion of highly agglutinative staphylococin and cisplatin. *Chin Ger J Clin Oncol*. 2006; 5:316-318.
- Lestuzzi C. Neoplastic pericardial disease: Old and current strategies for diagnosis and management. *World J Cardiol*. 2010; 2:270-279.
- Imazio M, Adler Y. Management of pericardial effusion. *Eur Heart J*. 2013; 34:1186-1197.
- Wu YF, Yu Lei, Wang JW. Advances in medical treatment of malignant pericardial effusion. *Oncology Progress*. 2007; 5:352-354.
- Qi F, Li A, Inagaki Y, Gao J, Li J, Kokudo N, Li XK, Tang W. Chinese herbal medicines as adjuvant treatment during chemo- or radio-therapy for cancer. *Biosci Trends*. 2010; 4:297-307.
- Meng Z, Yang P, Shen Y, Bei W, Zhang Y, Ge Y, Newman RA, Cohen L, Liu L, Thornton B, Chang DZ, Liao Z, Kurzrock R. Pilot study of huachansu in patients with hepatocellular carcinoma, non-small-cell lung cancer, or pancreatic cancer. *Cancer*. 2009; 115:5309-5318.
- Weitzman LB, Tinker WP, Kronzon I, Cohen ML, Glassman E, Spencer FC. The incidence and natural history of pericardial effusion after cardiac surgery – an echocardiographic study. *Circulation*. 1984; 69:506-511.
- Zhang X, Hu Y, Wang J, Zhang S, Tao H, Jing S, Wu B. Efficacy of recombinant adenoviral human p53 gene in treatment of malignant pleural or peritoneal effusions. *Zhongguo Fei Ai Za Zhi*. 2013; 16:153-156.
- Leppert W, Majkovicz M, Forycka M, Mess E, Zdun-Ryzewska A. Quality of life assessment in advanced cancer patients treated at home, an inpatient unit, and a day care center. *Onco Targets Ther*. 2014; 7:687-695.
- Martinoni A, Cipolla CM, Civelli M, Cardinale D, Lamantia G, Colleoni M, DeBraud F, Susini G, Martinelli G, Goldhirsh A, Fiorentini C. Intrapericardial treatment of neoplastic pericardial effusions. *Herz*. 2000; 25:787-793.
- Prados J, Alvarez PJ, Melguizo C, Rodriguez-Serrano F, Carrillo E, Boulaiz H, Vélez C, Marchal JA, Caba O, Ortiz R, Rama A, Aranega A. How is gene transfection able to improve current chemotherapy? The role of combined therapy in cancer treatment. *Curr Med Chem*. 2012; 19:1870-1888.
- Qi F, Li A, Inagaki Y, Kokudo N, Tamura S, Nakata M, Tang W. Antitumor activity of extracts and compounds from the skin of the toad *Bufo bufo gargarizans* Cantor. *Int Immunopharmacol*. 2011; 11:342-349.
- Qi F, Li A, Inagaki Y, Xu H, Wang D, Cui X, Zhang L, Kokudo N, Du G, Tang W. Induction of apoptosis by cinobufacini preparation through mitochondria- and Fas-mediated caspase-dependent pathway. *Food Chem Toxicol*. 2012; 50:295-302.
- Zhang LP, Jin J, Zhao YY, Wang M. The curative effect on intrapleural hyperthermic perfusion of Cinobufacini injection plan in the treatment of malignant pleural effusion. *Asia-Pacific Traditional Medicine*. 2013; 9:174-175. (in Chinese)
- Chen WM. The clinical observation on Cinobufacini injection in combination with Cisplatin treating malignant pleural effusions by intrapleural instillation. *Journal of Clinical Medicine in Practice*. 2013; 17:115-116. (in Chinese)
- Ran ZR. Intracavitary infusion of Cinobufacini injection combined with BCG-polysaccharide nucleic acid or cisplatin in the treatment of malignant pleural and peritoneal effusions. *Tumor*. 2008; 28:517-519. (in Chinese)

(Received April 14, 2014; Revised June 20, 2014; Accepted July 2, 2014)

Japan's emerging challenge for child abuse: System coordination for early prevention of child abuse is needed

Kenzo Takahashi^{1,*}, Hideyuki Kanda², Nagisa Sugaya²

¹ Graduate School of Public Health, Teikyo University, Tokyo, Japan;

² Department of Epidemiology and Public Health, Graduate School of Medicine, Yokohama City University, Kanagawa, Japan.

Summary

At the end of 2013, a Japanese newspaper reported that 4,173 children were unidentified or missing in Japan. The article concluded that child abuse was a matter of national concern. In examining the strengths and weaknesses of Japan's welfare system in regard to child abuse, it would seem that a weakness exists with regard to its ambiguity on the roles of different officers who contact suspected cases. Although three types of officer (health, welfare, and police officers) can take charge, child abuse cases might be missed because the division of labor varies between the different types of officer. However, a strength exists in the periodical pediatric health check system that is in place in each of Japan's 1,742 municipalities. To efficiently implement early intervention for child abuse, it is necessary to rearrange the division of labor among the three types of officers to clarify who should intervene in suspected cases.

Keywords: Child abuse, Japan, pediatric health checks

Child abuse is a national concern in Japan. The number of child abuse notification cases is increasing (1). The Japanese police report that 32 children were killed by abuse in 2012. Of the 59,919 cases that resulted in notification in 2011, physical abuse accounted for 36.6%, followed by neglect (31.5%), psychological abuse (29.5%), and sexual abuse (2.4%) (2). Worldwide, the estimated number of homicide deaths in children under 15 amounts is approximately 34,000 (3). Gilbert *et al.* report that about 4-16% of children experience physical abuse and that one in ten is neglected or psychologically abused. As for sexual abuse, between 5% and 10% of girls and up to 5% of boys are exposed to penetrative sexual abuse during childhood (4).

The difficulty in early detection of child abuse is that it usually occurs behind closed doors in a home environment, and that the main players in the abuse, usually parents, may be unaware that they are committing abuse. In Japan, this is further complicated by the fact that people nearby who suspect child abuse

may be reluctant to notify authorities because it tends to be viewed as a family affair. Thus, the true situation of child abuse is likely to be hidden. Those who engage in the management of child abuse view it as a difficult challenge (5).

On December 31, 2013, *The Yomiuri Shimbun* (a Japanese newspaper) reported that 4,173 infants were unidentified or missing in Japan, and concluded that child abuse was a matter of concern (6). The article reported that the newspaper had conducted a questionnaire survey targeting all of Japan's 1,742 municipalities in November 2013. Each municipality notes instances of non-attendance at periodical pediatric health checks; 334 municipalities showed the probable existence of missing infants. Some municipality officers were reported to have conducted home visits to check if the children were brought up in a safe environment. Others reported that they only performed a phone or mail survey and simply asked whether the infants in question were being nurtured properly. The article concluded that Japan has no surveillance system for identifying missing children with regard to cases of possible child abuse.

From the above-mentioned article, we see the strengths and weaknesses of Japan's welfare system for children and gain a clue as to how the early prevention

*Address correspondence to:

Dr. Kenzo Takahashi, Graduate School of Public Health, Teikyo University, 2-11-1 Kaga, Itabashi-ku, Tokyo 173-8605, Japan.

E-mail: kenzo.takahashi.chgh@med.teikyo-u.ac.jp

of child abuse might be achieved. With regard to early detection, the weakness of Japan's system is in the ambiguity of the roles of the different types of officer who make contact with suspected child abuse cases. Throughout Japan, three types of officer (police, welfare, and health officers) can, in principle, take charge in cases of child abuse.

While health officers take charge in the health service (including through consultation of parents suspected of abuse), welfare officers are generally in charge of managing child abuse cases. Welfare officers collect information on notifications of abuse from neighbors of the families in which child abuse is suspected and hospital staff, including medical doctors. Aside from these points of contact, police officers receive notification in cases where law enforcement might be necessary.

The roles for identifying child abuse seem to be deliberate because there is an overlap in the roles of the three types of officer. However, child abuse cases might be missed due to the lack of clear definition. In fact, while the number of notifications has increased year by year, there has not been a corresponding decrease in the number of confirmed child abuse cases. In the Netherlands, pediatricians are trying to detect child abuse among children who present to the emergency department (7). Learning from these practices, Japanese pediatricians are also trying to identify abuse cases at the emergency department and several manuals have been published and circulated (5). However, the efficacy of this type of medical approach has a limitation in that its basic focus is on the detection of physical abuse. We believe that a population-focused approach would be more effective in the early detection of child abuse.

A possible avenue for a population-focused approach to child abuse prevention in Japan exists in the periodical pediatric health check system, which is in place in every municipality of Japan. Health checks are provided, free of charge, for children aged 3-4 months, 1.5 years and 3 years (8,9). All of the target children are registered and health officers at their corresponding municipalities have contact with parents. Thus, it would

seem to be relatively easy to monitor attendance of pediatric health checks.

Properly utilized, pediatric health checks could provide an innovative and functional avenue for facilitating the early prevention of child abuse. For that purpose, it is necessary to redefine the mandate of the pediatric health check system and to rearrange the division of labor among health officers, welfare officers and police, in order to clarify who should intervene in cases where child abuse is suspected.

References

1. Ministry of Health, Labour and Welfare, Japan. Child Abuse Prevention Measures. Ministry of Health, Labour and Welfare, Tokyo, Japan, 2011.
2. Cabinet Office, Japan. White Paper on Children and Young People, 2013. Cabinet Office, Tokyo, Japan, 2013.
3. World Health Organization. Fact Sheet: Child Maltreatment. World Health Organization, Geneva, Switzerland, 2014.
4. Gilbert R, Widom CS, Browne K, Fergusson D, Webb E, Janson S. Burden and consequences of child maltreatment in high-income countries. *The Lancet*. 2009; 373:68-81.
5. Japan Pediatric Society. The Manual for Child Abuse Management (2nd ed.). Japan Pediatric Society, Tokyo, Japan, 2014.
6. Whereabouts of 4,200 kids in Japan unknown. *The Yomiuri Shimbun/Asia News Network*. Tokyo, Japan, Dec 31, 2013 (in Japanese).
7. Teeuw AH, Derkx BHF, Koster WA, van Rijn RR. Educational paper: Detection of child abuse and neglect at the emergency room. *Eur J Pediatr*. 2012; 171:877-885.
8. Nakamura Y. Maternal and Child Health Handbook in Japan. *Japan Medical Association Journal*. 2010; 53:259-265 (in Japanese).
9. Yoda T, Takahashi K, Yamauchi Y. Japanese trends in breastfeeding rate in baby-friendly hospitals between 2007 and 2010: A retrospective hospital-based surveillance study. *BMC Pregnancy Childbirth*. 2013; 13:207.

(Received June 9, 2014; Revised August 1, 2014; Accepted August 2, 2014)

Guide for Authors

1. Scope of Articles

BioScience Trends is an international peer-reviewed journal. BioScience Trends devotes to publishing the latest and most exciting advances in scientific research. Articles cover fields of life science such as biochemistry, molecular biology, clinical research, public health, medical care system, and social science in order to encourage cooperation and exchange among scientists and clinical researchers.

2. Submission Types

Original Articles should be well-documented, novel, and significant to the field as a whole. An Original Article should be arranged into the following sections: Title page, Abstract, Introduction, Materials and Methods, Results, Discussion, Acknowledgments, and References. Original articles should not exceed 5,000 words in length (excluding references) and should be limited to a maximum of 50 references. Articles may contain a maximum of 10 figures and/or tables.

Brief Reports definitively documenting either experimental results or informative clinical observations will be considered for publication in this category. Brief Reports are not intended for publication of incomplete or preliminary findings. Brief Reports should not exceed 3,000 words in length (excluding references) and should be limited to a maximum of 4 figures and/or tables and 30 references. A Brief Report contains the same sections as an Original Article, but the Results and Discussion sections should be combined.

Reviews should present a full and up-to-date account of recent developments within an area of research. Normally, reviews should not exceed 8,000 words in length (excluding references) and should be limited to a maximum of 100 references. Mini reviews are also accepted.

Policy Forum articles discuss research and policy issues in areas related to life science such as public health, the medical care system, and social science and may address governmental issues at district, national, and international levels of discourse. Policy Forum articles should not exceed 2,000 words in length (excluding references).

Case Reports should be detailed reports of the symptoms, signs, diagnosis, treatment, and follow-up of an individual patient. Case reports may contain a demographic profile of the patient but usually describe an unusual or novel occurrence. Unreported or unusual

side effects or adverse interactions involving medications will also be considered. Case Reports should not exceed 3,000 words in length (excluding references).

News articles should report the latest events in health sciences and medical research from around the world. News should not exceed 500 words in length.

Letters should present considered opinions in response to articles published in BioScience Trends in the last 6 months or issues of general interest. Letters should not exceed 800 words in length and may contain a maximum of 10 references.

3. Editorial Policies

Ethics: BioScience Trends requires that authors of reports of investigations in humans or animals indicate that those studies were formally approved by a relevant ethics committee or review board.

Conflict of Interest: All authors are required to disclose any actual or potential conflict of interest including financial interests or relationships with other people or organizations that might raise questions of bias in the work reported. If no conflict of interest exists for each author, please state "There is no conflict of interest to disclose".

Submission Declaration: When a manuscript is considered for submission to BioScience Trends, the authors should confirm that 1) no part of this manuscript is currently under consideration for publication elsewhere; 2) this manuscript does not contain the same information in whole or in part as manuscripts that have been published, accepted, or are under review elsewhere, except in the form of an abstract, a letter to the editor, or part of a published lecture or academic thesis; 3) authorization for publication has been obtained from the authors' employer or institution; and 4) all contributing authors have agreed to submit this manuscript.

Cover Letter: The manuscript must be accompanied by a cover letter signed by the corresponding author on behalf of all authors. The letter should indicate the basic findings of the work and their significance. The letter should also include a statement affirming that all authors concur with the submission and that the material submitted for publication has not been published previously or is not under consideration for publication elsewhere. The cover letter should be submitted in PDF format. For example of Cover Letter, please visit <http://www.biosciencetrends.com/downcentre.php> (Download Centre).

Copyright: A signed JOURNAL PUBLISHING AGREEMENT (JPA) form must be provided by post, fax, or as a scanned file before acceptance of the article. Only forms with a hand-written signature are accepted. This copyright will ensure the widest possible dissemination of information. A form facilitating transfer of copyright can be downloaded by clicking the

appropriate link and can be returned to the e-mail address or fax number noted on the form (Please visit [Download Centre](#)). Please note that your manuscript will not proceed to the next step in publication until the JPA Form is received. In addition, if excerpts from other copyrighted works are included, the author(s) must obtain written permission from the copyright owners and credit the source(s) in the article.

Suggested Reviewers: A list of up to 3 reviewers who are qualified to assess the scientific merit of the study is welcomed. Reviewer information including names, affiliations, addresses, and e-mail should be provided at the same time the manuscript is submitted online. Please do not suggest reviewers with known conflicts of interest, including participants or anyone with a stake in the proposed research; anyone from the same institution; former students, advisors, or research collaborators (within the last three years); or close personal contacts. Please note that the Editor-in-Chief may accept one or more of the proposed reviewers or may request a review by other qualified persons.

Language Editing: Manuscripts prepared by authors whose native language is not English should have their work proofread by a native English speaker before submission. If not, this might delay the publication of your manuscript in BioScience Trends.

The Editing Support Organization can provide English proofreading, Japanese-English translation, and Chinese-English translation services to authors who want to publish in BioScience Trends and need assistance before submitting a manuscript. Authors can visit this organization directly at <http://www.iacmhr.com/iac-eso/support.php?lang=en>. IAC-ESO was established to facilitate manuscript preparation by researchers whose native language is not English and to help edit works intended for international academic journals.

4. Manuscript Preparation

Manuscripts should be written in clear, grammatically correct English and submitted as a Microsoft Word file in a single-column format. Manuscripts must be paginated and typed in 12-point Times New Roman font with 24-point line spacing. Please do not embed figures in the text. Abbreviations should be used as little as possible and should be explained at first mention unless the term is a well-known abbreviation (e.g. DNA). Single words should not be abbreviated.

Title Page: The title page must include 1) the title of the paper (Please note the title should be short, informative, and contain the major key words); 2) full name(s) and affiliation(s) of the author(s), 3) abbreviated names of the author(s), 4) full name, mailing address, telephone/fax numbers, and e-mail address of the corresponding author; and 5) conflicts of interest (if you have an actual or potential conflict of interest to disclose, it must be included as a footnote on the title page of the manuscript; if no conflict of

interest exists for each author, please state "There is no conflict of interest to disclose"). Please visit [Download Centre](#) and refer to the title page of the manuscript sample.

Abstract: The abstract should briefly state the purpose of the study, methods, main findings, and conclusions. For article types including Original Article, Brief Report, Review, Policy Forum, and Case Report, a one-paragraph abstract consisting of no more than 250 words must be included in the manuscript. For News and Letters, a brief summary of main content in 150 words or fewer should be included in the manuscript. Abbreviations must be kept to a minimum and non-standard abbreviations explained in brackets at first mention. References should be avoided in the abstract. Key words or phrases that do not occur in the title should be included in the Abstract page.

Introduction: The introduction should be a concise statement of the basis for the study and its scientific context.

Materials and Methods: The description should be brief but with sufficient detail to enable others to reproduce the experiments. Procedures that have been published previously should not be described in detail but appropriate references should simply be cited. Only new and significant modifications of previously published procedures require complete description. Names of products and manufacturers with their locations (city and state/country) should be given and sources of animals and cell lines should always be indicated. All clinical investigations must have been conducted in accordance with Declaration of Helsinki principles. All human and animal studies must have been approved by the appropriate institutional review board(s) and a specific declaration of approval must be made within this section.

Results: The description of the experimental results should be succinct but in sufficient detail to allow the experiments to be analyzed and interpreted by an independent reader. If necessary, subheadings may be used for an orderly presentation. All figures and tables must be referred to in the text.

Discussion: The data should be interpreted concisely without repeating material already presented in the Results section. Speculation is permissible, but it must be well-founded, and discussion of the wider implications of the findings is encouraged. Conclusions derived from the study should be included in this section.

Acknowledgments: All funding sources should be credited in the Acknowledgments section. In addition, people who contributed to the work but who do not meet the criteria for authors should be listed along with their contributions.

References: References should be numbered in the order in which they appear in the text. Citing of unpublished results, personal communications, conference abstracts, and theses in the reference list is not recommended but these sources may be mentioned in the text. In the reference list,

cite the names of all authors when there are fifteen or fewer authors; if there are sixteen or more authors, list the first three followed by *et al.* Names of journals should be abbreviated in the style used in PubMed. Authors are responsible for the accuracy of the references. Examples are given below:

Example 1 (Sample journal reference): Inagaki Y, Tang W, Zhang L, Du GH, Xu WF, Kokudo N. Novel aminopeptidase N (APN/CD13) inhibitor 24F can suppress invasion of hepatocellular carcinoma cells as well as angiogenesis. *Biosci Trends*. 2010; 4:56-60.

Example 2 (Sample journal reference with more than 15 authors): Darby S, Hill D, Auvinen A, *et al.* Radon in homes and risk of lung cancer: Collaborative analysis of individual data from 13 European case-control studies. *BMJ*. 2005; 330:223.

Example 3 (Sample book reference): Shalev AY. Post-traumatic stress disorder: diagnosis, history and life course. In: Post-traumatic Stress Disorder, Diagnosis, Management and Treatment (Nutt DJ, Davidson JR, Zohar J, eds.). Martin Dunitz, London, UK, 2000; pp. 1-15.

Example 4 (Sample web page reference): Ministry of Health, Labour and Welfare of Japan. Dietary reference intakes for Japanese. <http://www.mhlw.go.jp/houdou/2004/11/h1122-2a.html> (accessed June 14, 2010).

Tables: All tables should be prepared in Microsoft Word or Excel and should be arranged at the end of the manuscript after the References section. Please note that tables should not be image format. All tables should have a concise title and should be numbered consecutively with Arabic numerals. If necessary, additional information should be given below the table.

Figure Legend: The figure legend should be typed on a separate page of the main manuscript and should include a short title and explanation. The legend should be concise but comprehensive and should be understood without referring to the text. Symbols used in figures must be explained.

Figure Preparation: All figures should be clear and cited in numerical order in the text. Figures must fit a one- or two-column format on the journal page: 8.3 cm (3.3 in.) wide for a single column, 17.3 cm (6.8 in.) wide for a double column; maximum height: 24.0 cm (9.5 in.). Please make sure that the symbols and numbers appeared in the figures should be clear. Please make sure that artwork files are in an acceptable format (TIFF or JPEG) at minimum resolution (600 dpi for illustrations, graphs, and annotated artwork, and 300 dpi for micrographs and photographs). Please provide all figures as separate files. Please note that low-resolution images are one of the leading causes of article resubmission and schedule delays. All color figures will be reproduced in full color in the online edition of the journal at no cost to authors.

Units and Symbols: Units and symbols

conforming to the International System of Units (SI) should be used for physicochemical quantities. Solidus notation (*e.g.* mg/kg, mg/mL, mol/mm²/min) should be used. Please refer to the SI Guide www.bipm.org/en/si/ for standard units.

Supplemental data: Supplemental data might be useful for supporting and enhancing your scientific research and BioScience Trends accepts the submission of these materials which will be only published online alongside the electronic version of your article. Supplemental files (figures, tables, and other text materials) should be prepared according to the above guidelines, numbered in Arabic numerals (*e.g.*, Figure S1, Figure S2, and Table S1, Table S2) and referred to in the text. All figures and tables should have titles and legends. All figure legends, tables and supplemental text materials should be placed at the end of the paper. Please note all of these supplemental data should be provided at the time of initial submission and note that the editors reserve the right to limit the size and length of Supplemental Data.

5. Submission Checklist

The Submission Checklist will be useful during the final checking of a manuscript prior to sending it to BioScience Trends for review. Please visit [Download Centre](#) and download the Submission Checklist file.

6. Online Submission

Manuscripts should be submitted to BioScience Trends online at <http://www.biosciencetrends.com>. The manuscript file should be smaller than 5 MB in size. If for any reason you are unable to submit a file online, please contact the Editorial Office by e-mail at office@biosciencetrends.com.

7. Accepted Manuscripts

Proofs: Galley proofs in PDF format will be sent to the corresponding author via e-mail. Corrections must be returned to the editor (proof-editing@biosciencetrends.com) within 3 working days.

Offprints: Authors will be provided with electronic offprints of their article. Paper offprints can be ordered at prices quoted on the order form that accompanies the proofs.

Page Charge: Page charges will be levied on all manuscripts accepted for publication in BioScience Trends (\$140 per page for black white pages; \$340 per page for color pages). Under exceptional circumstances, the author(s) may apply to the editorial office for a waiver of the publication charges at the time of submission.

(Revised February 2013)

Editorial and Head Office:

Pearl City Koishikawa 603
2-4-5 Kasuga, Bunkyo-ku
Tokyo 112-0003 Japan
Tel: +81-3-5840-8764
Fax: +81-3-5840-8765
E-mail: office@biosciencetrends.com

JOURNAL PUBLISHING AGREEMENT (JPA)

Manuscript No.:

Title:

Corresponding Author:

The International Advancement Center for Medicine & Health Research Co., Ltd. (IACMHR Co., Ltd.) is pleased to accept the above article for publication in BioScience Trends. The International Research and Cooperation Association for Bio & Socio-Sciences Advancement (IRCA-BSSA) reserves all rights to the published article. Your written acceptance of this JOURNAL PUBLISHING AGREEMENT is required before the article can be published. Please read this form carefully and sign it if you agree to its terms. The signed JOURNAL PUBLISHING AGREEMENT should be sent to the BioScience Trends office (Pearl City Koishikawa 603, 2-4-5 Kasuga, Bunkyo-ku, Tokyo 112-0003, Japan; E-mail: office@biosciencetrends.com; Tel: +81-3-5840-8764; Fax: +81-3-5840-8765).

1. Authorship Criteria

As the corresponding author, I certify on behalf of all of the authors that:

- 1) The article is an original work and does not involve fraud, fabrication, or plagiarism.
- 2) The article has not been published previously and is not currently under consideration for publication elsewhere. If accepted by BioScience Trends, the article will not be submitted for publication to any other journal.
- 3) The article contains no libelous or other unlawful statements and does not contain any materials that infringes upon individual privacy or proprietary rights or any statutory copyright.
- 4) I have obtained written permission from copyright owners for any excerpts from copyrighted works that are included and have credited the sources in my article.
- 5) All authors have made significant contributions to the study including the conception and design of this work, the analysis of the data, and the writing of the manuscript.
- 6) All authors have reviewed this manuscript and take responsibility for its content and approve its publication.
- 7) I have informed all of the authors of the terms of this publishing agreement and I am signing on their behalf as their agent.

2. Copyright Transfer Agreement

I hereby assign and transfer to IACMHR Co., Ltd. all exclusive rights of copyright ownership to the above work in the journal BioScience Trends, including but not limited to the right 1) to publish, republish, derivate, distribute, transmit, sell, and otherwise use the work and other related material worldwide, in whole or in part, in all languages, in electronic, printed, or any other forms of media now known or hereafter developed and the right 2) to authorize or license third parties to do any of the above.

I understand that these exclusive rights will become the property of IACMHR Co., Ltd., from the date the article is accepted for publication in the journal BioScience Trends. I also understand that IACMHR Co., Ltd. as a copyright owner has sole authority to license and permit reproductions of the article.

I understand that except for copyright, other proprietary rights related to the Work (e.g. patent or other rights to any process or procedure) shall be retained by the authors. To reproduce any text, figures, tables, or illustrations from this Work in future works of their own, the authors must obtain written permission from IACMHR Co., Ltd.; such permission cannot be unreasonably withheld by IACMHR Co., Ltd.

3. Conflict of Interest Disclosure

I confirm that all funding sources supporting the work and all institutions or people who contributed to the work but who do not meet the criteria for authors are acknowledged. I also confirm that all commercial affiliations, stock ownership, equity interests, or patent-licensing arrangements that could be considered to pose a financial conflict of interest in connection with the article have been disclosed.

Corresponding Author's Name (Signature):

Date:

